JULY 2018

Ph.D in Mechanical Engineering

KAAN EMRE ENGİN

UNIVERSITY OF GAZİANTEP

GRADUATE SCHOOL OF

NATURAL&APPLIED SCIENCES

EVALUATION OF CUTTING SURFACE QUALITY IN HIGH SPEED BLANKING PROCESS

Ph.D THESIS

IN

MECHANICAL ENGINEERING

BY

KAAN EMRE ENGİN

JULY 2018

Evaluation of Cutting Surface Quality in High Speed Blanking Process

Ph.D Thesis

in

Mechanical Engineering

University of Gaziantep

Supervisor

Prof. Dr. Ömer EYERCİOĞLU

by

Kaan Emre ENGİN

JULY 2018

REPUBLIC OF TURKEY
UNIVERSITY OF GAZIANTEP
GRADUATE SCHOOL OF NATURAL & APPLIED SCIENCES
MECHANICAL ENGINEERING

Name of the Thesis: Evaluation of Cutting Surface Quality in High Speed Blanking Process

Name and Surname of the Student: Kaan Emre ENGİN

Exam Date: 19.07.2018

Approval of the Graduate School of Natural and Applied Sciences

Prof. Dr. A. Necmeddin YAZICI
Director

I certify that this thesis satisfies all the requirements as a thesis for the degree of Doctor of Philosophy

Prof. Dr. Mehmet Sait SÖYLEMEZ
Head of Department

This is to certify that we have read this thesis and that in our opinion it is fully adequate, in scope and quality, as a thesis for the degree of Doctor of Philosophy.

Prof. Dr. Ömer EYERCİOĞLU
Supervisor

Examining Committee Members:	Signature
Prof. Dr. Ömer EYERCİOĞLU	....
Prof. Dr. Turhan KOYUNCU	....
Prof. Dr. Abdulkadir EKŞİ	....
Prof. Dr. Metin KÖK	....
Assoc. Prof. Dr. Necip Fazıl YILMAZ	....

I hereby declare that all information in this document has been obtained and presented in accordance with academic rules and ethical conduct. I also declare that, as required by these rules and conduct, I have fully cited and referenced all materials and results that are not original to this work.

Kaan Emre ENGİN

ABSTRACT

EVALUATION OF CUTTING SURFACE QUALITY IN HIGH SPEED BLANKING PROCESS

ENGİN, Kaan Emre

Ph.D. in Mechanical Engineering

Supervisor(s): Prof. Dr. Ömer EYERCİOĞLU

July 2018

116 pages

Blanking process holds a crucial point in metal forming industry. The main goal in blanking is to achieve the best surface quality on the blanked parts while spending minimum energy. In this study the surface quality, cutting load and cutting energy of the workpieces were investigated under three different speeds (0.1 m/s, 1 m/s and 10 m/s) with respect to the clearance, material thickness and thickness to die diameter ratios. Five different clearances (1%, 3%, 5.%, 10.0% and 20.0%) were used to blank 2 mm, 3 mm and 4 mm thick workpieces made of AISI 304 stainless steel under four different ratios (t/D_m=1/5, t/D_m=1/10, t/D_m=1/30, t/D_m=1/50). Both experimental and FEM studies were accomplished.

Results showed that increasing punch speed improves the surface quality and best surface quality was achieved at 10 m/s by reaching lowest surface roughness values. Another important contribution is the thickness to die diameter ratio and found out that energy, surface quality and related clearance values change according to the workpiece diameters that are neglected in the literature which only considers the thickness of workpiece. The total energy increases due to increasing punch speed, thickness and thickness to die diameter ratios. Clearance between 3% and 5% is found to be optimal value range for AISI 304 stainless steel when considered all investigated parameters.

Key Words: Punch speed, surface roughness, clearance, cutting energy

ÖZET

YÜKSEK HIZLI KESME PROSESİNDE KESME YÜZEY KALİTESİNİN BELİRLENMESİ

ENGİN, Kaan Emre

Doktora Tezi, Makine Müh. Bölümü

Tez Yöneticisi: Prof. Dr. Ömer EYERCİOĞLU

Temmuz 2018

116 sayfa

Kesme prosesi, metal şekillendirme endüstrisinde çok önemli bir yer tutmaktadır ve ana hedef, minimum enerji harcarken, kesilen iş parçalarında en iyi yüzey kalitesini elde etmektir. Bu çalışmada; 3 farklı hız (0.1 m/s, 1 m/s and 10 m/s) altında iş parçası yüzey kalitesi, kesme yükü ve kesme enerjisini; kalıp arası boşluğu, malzeme kalınlığı ve kalınlık- kalıp çapı oranı çerçevesinde incelenmiştir. AISI 304 paslanmaz çelikten levhadan yapılmış 2 mm, 3 mm ve 4 mm kalınlığında iş parçalarının kesilmesi için beş farklı kalıp boşluğu (% 1, % 3, % 5,% 10 ve % 20) ve dört farklı kalınlık- kalıp çapı oranı (t/D_m=1/5, t/D_m=1/10, t/D_m=1/30, t/D_m=1/50) kullanılmıştır. Hem deneysel hem de Sonlu Elemanlar Yöntemi ile çalışmalar gerçekleştirilmiştir.

Sonuçlar, artan zımba hızının yüzey kalitesini iyileştirdiğini ve en iyi yüzey kalitesinin, yüzey pürüzlülüğü değerlerinin düşmesi vasıtasıyla 10 m/s zımba hızında elde edildiğini göstermiştir. Diğer bir önemli katkı kalınlık- kalıp çapı oranıdır ve enerji, yüzey kalitesi ve kalıp boşluğu değerlerinin, sadece iş parçasının kalınlığını dikkate alarak literatürde ihmal edilen iş parçası çaplarına göre değiştiği tespit edilmiştir. Toplam enerjinin, artan zımba hızına, kalınlığa ve kalınlık- kalıp çapı oranına göre arttığı bulunmuştur. Tüm parametreler açısından ele alındığında, %3 ve %5 arası kalıp boşluğunun AISI 304 paslanmaz çelik için optimal değer aralığı olduğu belirlenmiştir.

Anahtar Kelimeler: Zımba hızı, yüzey pürüzlülüğü, kalıp boşluğu, kesme enerjisi

To my precious wife, my daughters and my family…

ACKNOWLEDGEMENTS

I wish to submit my deepest gratitude and thanks to my supervisor Prof. Dr. Ömer EYERCİOĞLU, who does not refrain from sharing all his knowledge with me during this work, does not hesitate to give any kind of support to me, makes a great effort in my thesis and adds a lot to my personal life and academic career.

I would also like to thank Prof. Dr. İ. Hüseyin FİLİZ and Prof. Dr. Turhan KOYUNCU for serving in my thesis committee and providing valuable contributions to the study.

This study would have never been completed without the moral support of my precious wife Selin ENGİN, who helps me in all circumstances and every time, my family for their trust, patience, understanding and my lovely daughters Serra and Hira, whom I have stolen from their own times.

TABLE OF CONTENTS

Page

LIST OF TABLES

Page

LIST OF FIGURES

Page

CHAPTER 1

INTRODUCTION

1.1. Purpose of the Study

In today's sheet metal forming industry, two trends can be observed clearly. Firstly, time-to-market needs to be shortened in order to introduce new products competitively. Secondly, energy conservation concerns and decrease in raw material stocks are getting more pressing. As a result of these trends; to sustain the production rate and competitiveness, efficiency of the production has to be at the highest level as possible. So, minimizing the cost and increasing the efficiency by means of fewer manufacturing processes, fewer final finishing processes and as a result using less natural resources and labor become the main goals in the production cycle.

Sheet metal forming processes differ into several branches [1], and all of them have their own kind of importance but amongst these processes, blanking process has an utmost importance in manufacturing industry. It can easily be mentioned from research and experience that majority of manufacturing industry produce and form sheet metal parts directly by blanking or use blanking within their production steps.

Blanking is simply the shearing of the workpiece into the desired shape (blank) by the usage of a punch and a die. Blanking is also a near net shape manufacturing process which means that the manufactured parts have dimensions and shape so close to the predetermined and desired parts after the process. Although the process seems simple, parameters governing the process are many and all of them have their own effect on the surface quality of the blank and the energy consumption of the process. Punch-die clearance, punch speed, material properties and thickness, tooling material and shape of the punch can be counted as the main parameters in blanking.

The main issue in blanking is; generally, a subsequent deburring is required after blanking so that the processing time and labor cost are increased. Elimination of burr formation may eliminate the final finishing process totally and therefore the cost. Also there has to be a balance between surface quality and energy efficiency. The adjustments on parameters can change the scale on either good surface quality but more energy consumption side or less energy consumption but low surface quality side. So, the overall goal is to improve the blanking process in such a way that the produced part does not need to be reworked and also ensure energy efficiency.

Unfortunately, analyses of blanking are mainly based on phenomenological knowledge. For manufacturers, since requirements concerning finished product quality have become more severe, approaches to the situation result in lengthier trial and error procedures that cause excessive spending of time, labor, energy, source and money. For researchers, the angle of view to the situation are divided into two that one approach follows experimental studies to investigate the effects of parameters as manufacturers do, and the other approach follows Finite Element Method (FEM) and modelling studies to foresee the final quality of the blanks and try to optimize the parameters in that regard. However, the optimization results vary on a big scale and there are only few researches that combine both of these approaches.

As a result of these studies, it is understood that amongst the other blanking parameters, punch-die clearance, punch speed, material properties and thickness show the most dominant effects on the overall process. Punch speed is relatively a new parameter due to the time interval between the first usage of traditional blanking and the newer and faster version called high speed blanking.

Apart from the traditional blanking, high speed blanking introduced a new augmented approach to the process. In particular, when blanking with high punch velocities, it may be possible to manufacture near net-shape parts with improved part edge quality and lower energy values. There had been some investigations regarding the effect of blanking speed but they were restricted to specific parameters like the change in cutting load, burr formation on the blanked surface and also tool wear characteristics. But taking only one parameter and its relevancy to other parameters is not a proper approach to come to a conclusion about the process. Because all parameters have their own share and interaction with each other and this is the main reason why optimization in blanking is a difficult goal to accomplish. Also in many studies the necessary blanking speeds were not reached to obtain the advantages of high speed blanking.

On the other hand, it is a common situation when industrial applications and processes require blanking of parts with different sizes and different thicknesses. General treatment is to use parameter values specific to the given thickness and apply it to every size. However, parameters governing the process should not be same for all kind of sizes and carry a probability to deviate. Furthermore, there are nearly no investigations or studies about the ratio of the workpiece thickness to the size (diameter) of the blank on other parameters which can simply be named "the effect of thickness to die diameter ratio". This lack of information also creates a gap in the literature of the blanking process.

Therefore, the main purpose of this study is to investigate the effect of high speed blanking. However, only taking speed value is not enough to reach a conclusion for the whole process. Therefore, the effect of clearance, material thickness, thickness to die diameter ratio and punch speed on cutting load, cutting energy and blank's surface quality will be investigated combined. After that, it will become possible to reach a conclusion and determine the optimal values. These combined investigations and implications will contribute in the comprehension of blanking process and inhibit the deficient conclusions due to single (one parameter based) investigations and researches not providing the necessary blanking speeds for high speed blanking.

1.2. Scope and Work Plan of the Study

The scope of the thesis is to take up blanking process comprehensively by experimental and FE methods. Blanking speed, clearance, material thickness and first-time introduced thickness to die diameter ratio and their relation between each other and their effect on cutting load, cutting energy and surface quality covers a large scale. To investigate the relations and results by experimental and FE methods properly, determined work plan were given below;

- Investigation of the change in cutting load, cutting energy and surface quality of blanks under three different blanking speeds (0.1 m/s, 1m/s and 10 m/s), five different clearances (1%, 3%, 5%, 10% and 20% of the thickness), three different workpiece thicknesses (2 mm, 3 mm and 4 mm) and four different thickness to die diameter ratios t/D_m=1/5, t/D_m=1/10, t/D_m=1/30 and t/D_m=1/50 by using FEA (Finite Element Analysis) analysis.

- The validation of results gathered from FE analysis through manufacturing of die/punch sets and execute blanking by using a hydraulic, an eccentric presses and a specially designed and constructed high speed blanking set.

- Evaluation of the effects of mentioned blanking parameters and try to find an optimal point to achieve both good surface quality and low energy consumption for the given material.

1.3. Organization of the Thesis

This thesis is comprised of 7 chapters which were explained below;

Chapter 2 covers the literature review of blanking. Studies accomplished by other researchers were given in terms of the effects of different aspects like clearance, punch speed, thickness and mechanical properties of the workpiece.

In Chapter 3, the fundamentals of the blanking process were explicated. Blanking parameters governing the process, input and output parameters and their possible effects were explained. Further, quality parameters and mechanical aspects of the material and theoretical background were described.

Chapter 4 deals with the experimental part of the study. The presses used to execute blanking, related die and punch setups and equipment to evaluate the surface features and the mechanical properties of the workpiece were given.

The simulation environment; the program used to execute simulations, the virtual blanking setup, related meshes and mesh windows, fracture criterions, hardening rules and die diameters were presented in Chapter 5.

In Chapter 6, the gathered results were investigated and evaluated. The results gathered from the blanking of AISI 304 stainless steel under five different clearances, three thicknesses, four thickness to die diameter ratios and three different punch speeds were determined and their effects on cutting load, cutting energy and surface quality were evaluated.

Chapter 7 includes the conclusion and the summary of achievements and findings so far. Additionally, recommendations were presented for future studies in this Chapter.

CHAPTER 2

LITERATURE REVIEW

2.1. Blanking Process and Related Literature

Blanking is an important and a commonly used sheet metal forming process in the industry. An extensive understanding of the process parameters is crucial to achieve a good surface quality on the blanked parts while maintaining energy efficiency. The general aspects of the process seem quite simple. The sheet metal workpiece is placed between a punch and die and perforated into desired shapes with the downward movement of the punch. But the parameters effecting the overall system and outcomes during the shearing are many. And the relations between them are quite complex. These conditions make blanking process unpredictable and difficult to foresee the outcomes before.

The parameters governing the process are many but the major input parameters which drastically changes the outcomes can be simplified into; punch-die clearance, punch speed, material properties and thickness, tooling material and shape of the punch. The outcome parameters are cutting load, cutting energy, stroke depth and surface quality of the blanks. All these input parameters, single or combined, have different effects on the outcome parameters. For an example; increase in clearance lowers the cutting load which is a desired situation. On the other hand, surface quality radically gets reduced due to the unmatched crack propagations because of the excessive length between die and the punch. Also stroke depth increases and it effects the total energy consumption in a bad way. This intricate nature of the process is the exact reason of its unpredictability. The adjustments of the input parameters have to be precise to overcome the negative effects and acquire the best surface quality with least energy consumption.

From industrial and non-academic perspective, the main courses of actions to optimize the blanking parameters for the desired results are generally rely on lengthy trial and error procedures which cost money, labor and precious manufacturing time spent only to observe the outcomes and adjust the parameters.

This problem can be solved by the usage of computer modelling. Usage of FEM (**F**inite **E**lement **M**ethod) based programs to simulate blanking to obtain numerical results and observe the effect of different parameters is a cheap and a detailed way for industrial applications. They are especially very useful to observe the exact cutting moment in step by step style visualization. Also there is no need for various sets with different traits designed specifically to observe the effects of parameters. FEM modeling presents the opportunity to change and adjust the parameters according to practitioner's choice and evaluate the effects and outcomes. A model can contain single or multiple parameters to be adjusted and the effects of them to the outcomes can be evaluated in a rapid way. By the usage of FEM modelling; one can easily save time, labor and cost instead of long trial and error procedure which is a consumer in every aspect.

For many years researchers have been trying to assess the effects of blanking parameters. These studies generally cover the main input parameters like clearance, workpiece material, punch speed, punch material/coating and outcome parameters like cutting load, tool wear and surface quality of the blanks. Many of these studies combine FEM modelling and experiments at the same time whereas some follow only experimental methods or FEM analysis.

Tekiner et al. [2] carried out an experimental study to see the effect of clearance on the shear depth, burr height and cutting load. The workpiece material was an aluminum sheet with 0.8, 1, and 1.5 mm thicknesses. They used blanking dies with different diameters (6, 8, 10, and 12 mm diameters) and six different clearances (0.009, 0.064, 0.12, 0.175, 0.231 and 0.287 mm) for every material and diameter. A mechanical press having a capacity of 60 tones and speed of 250 rpm were used in the experiment. They found out that the change in clearance effects the distribution of the shear depth and cutting load. With tight clearance, shear depth increases while increasing cutting load. Surface quality in terms of smooth sheared surface depth decreases with increasing clearance. They suggested that burr formation is same for all diameters for the same clearances.

Greban et al. [3] observed the zone distribution on the blanked surface of 8 different copper alloys with different compositions experimentally. The workpiece thicknesses were 0.254 mm and the clearance was 10 µm. They used rectangular punches with 0.5mm×10.5mm dimensions and the blanking speed was 550 rpm. They stated that the different chemical compositions that can alter the strength of the material also change the formation of the zones. The more potential for sheet metal to work harden, the longer the crack zone is. Also they mentioned that chemical compositions hence the material properties change the formation of burrs. They showed that there is 25% reduction in burr height between two alloys which have different compositions.

Breitling and Altan [4] investigated the influence of clearance on the sheared edge quality of rectangular punches with different radiuses at the edges. They employed a high speed blanking press with stroke rates of up to 1.200 strokes per minute at 60 Tons capacity. They executed two tests. In the first test they used uniform clearance at all the edges. They found out that the part edge was not uniform around the circumference. They saw deviations especially at the sharp corners. In the second test, first they halved the clearance then doubled compared to the straight cutting-edge. They stated that the change in clearance had the same effects as in the round punches. When the clearance increases, rollover and burr height increases where shear zone decreases. For the second tests, they found out that by reducing the clearance, the shear zone increases but sharp corners still had different sheared edges in slug and skeleton.

Lubis and Mahardika [5] carried out experiments to observe the effect of clearance and punch speed on the surface quality of the blanks. They used pure copper workpiece to execute blanking experiments under 2.5%, 5%, 7.5% and 10% clearance values. They employed a mechanical press that can work between 0.1 m/s and 1.6 m/s punching speeds. The investigations were made to observe the distribution of the zones and the height of the burr formation. The claimed that they achieved the best results in terms of maximum shear zone length and minimum burr height at 2.5% clearance and at 1.6 m/s punch speed.

Wu and Bahmanpour [6] studied the sheared edge characteristics of three different dual phase steels DP600, DP780 and DP980 (Dual phase steels contain fine-grained martensite particles embedded within a ferrite matrix by experimental work. They have high ductility and strength). The workpiece thickness was 1.6 mm and the clearances used for experiments were 5%, 7.5%, 10% and 15% of the workpiece thickness. They reported that the mixed nature of the double phase steels with significantly different properties play very important role in edge shear fracture process. Depending on the martensite distribution feature, multiple cracks may develop along the martensite cluster boundaries, initiate at different locations and time, and develop at different stages. The best results were achieved with more narrow clearances and but the achievement of four zones showed random occurrence on the sheared edge in contrast with regular steels.

Akyürek et al [7] experimentally investigated the effect of punch-die clearance and punch hardness on the wear characteristics of the edge and the cutting surface of the punch in blanking. In their work, they used AISI D2 cold work steel with 50, 55 and 60 HRC-hardness as punches and S235JR as the workpiece sheet material with 2 mm thickness. They used three different clearances as 0.06 (3%), 0.10 (5%) and 0.16 (8%) mm. The sheet material was subjected to 2000, 4000, 6000 and 8000 presses by using combinations of three different die clearances and three different hardened punches. Lubrications were applied at every 1000 strokes. They used an eccentric press with 15-ton and 180 cycles per minute capacity. The results showed that the increase in punch hardness directly improves the wear of the punch and there became a decrease on the wear of the edge and cutting surface of the punch. Also lower clearances gave more smooth sheared edge characteristics and they stated that the distribution of smooth edge is strongly dependent on the clearance.

Mucha [8] studied on the effects of punch-die clearance, tool materials, and tool coatings on the wear of blanking tools during the blanking of the stator and rotor parts. In their experimental work, they used high-speed steel M2, sintered steel M3:2, and tungsten carbide as the tool materials for punches. The tool materials were coated to reduce direct metal to metal contact between the tool and workpiece and to reduce friction. M3:2 sintered steel and M2 high-speed steels were coated with TiN (Titanide). TiN coating thickness was in the range of 3.5-4 µm which had the hardness level of 2300 HV5 on a single layer coating. Sheet material was industrial silicon steel sheet (Si=1.43%) plate M530-50A (old designation EP530-50A) with a thickness of 0.5 mm. The sheet used in the experiments had the AISI C6 isolation coating with ~7 µm at each side. The experiments were performed under 0%, 4% and 8% clearances. The results showed that the material and coating of the punch played a significant role on the wearing characteristics. M3:2 sintered steel had featured a higher durability than high-speed steel M2 and tungsten carbide in terms of burr height with their uncoated states. Mucha stated that the durability was changed when the punches coated with TiN. M3:2 sintered steel showed good durability but the main durability was achieved for high-speed steel M2 which doubled the wear resistance. But tungsten carbide gave the best results in terms of wear and burr formation creation. When the blanking clearance decreased to 0%, the flank face of M2+TiN punch had been worn more. The blanks made under the clearance of 8% for M2+TiN punch resulted in reduced wear of the flank face. But the cutting edge wear increased. Deep grooves were created at the cutting edge that got rounded with a greater width at the cutting edge. For M3:2+TiN punch, reducing the blanking clearance to 0% caused increased wear on the flank face which is greater than for blanking clearance of 8%.

Çöl et al. [9] studied experimentally on the wear characteristics of AlCrN coated punches during blanking. They used DIN-1.2379 (X155CrVMo 12-1) cold-work tool steel as the punch material and DIN-1.0037 (S235JR) low-carbon steel with 1 mm thickness as the workpiece material. The punches were hardened and then tempered to get a core hardness of 60 HRC. They used an eccentric press with 250 kN capacity and 70 rpm punch speed. The clearance was constant for all studies and its value was 5%. The wear performances were taken into consideration for coated and uncoated punches. They measured the tool wear volume of the punch and the burr height of the blanked strip every 5000 and 1000 strokes, respectively. They showed by using SEM observations that wear at the edge and flank zones of uncoated punches were much more severe than coated punches, although the uncoated punches did only the half of the strokes that coated punches did. The burr formation due to the wearing of the punch is also lesser for coated punches. But for high numbers of strokes, burr formations have a tendency to increase linearly for both punches.

A similar study was performed using the same materials and the conditions of the work by Erişir et al. [10]. Same conditions were used for this work but this time the difference of TiAlN and AlCrN were compared in terms of punch wear characteristics. They stated that AlCrN was more durable than TiAlN coated punches and when the wear started, its increase showed more stable characteristics.

Gaudilliere et al. [11] constructed a high speed blanking machine that used an air gun to propel the punch. The punch speed could be adjusted and was between 6 m/s and 18.5 m/s. They used the machine to calculate the cutting forces when blanking micro-alloy steel S600 at punch speed of 7.8 m/s. The clearance was 10%. In their another study [12], they used the same machine to blank C40 steel with 3 mm thickness and under 2% clearance at punch speed of 13.9 m/s. They calculated the cutting loads and tried to observe the adiabatic shear band created at the shear zone due to the high strain rates.

Grünbaum et al. [13] experimentally investigated the effect of high speed and clearance on the cutting edge quality of the blanks. They utilized an electro activated die set as the press with 10 Tons capacity and had the approximate punch speed of 3.65 m/s. They used different materials like low carbon steel, high strength steel, aluminum and copper which have different thicknesses as the workpieces (stocks). The main purpose of the study was to observe the effect of concentrated heat created during high speed blanking and also the effect of different clearance values. The results showed that the heat dissipation is much more rapid in aluminum and copper due to their higher heat conduction coefficients than the steels. Therefore, they suggested that the punch-die clearance has the major influence on the formation of the part edge, regardless which material was blanked or which punch speed was used.

Kanca et al. [14] performed blanking process under low (0,2 m/s) and high speed (10 m/s) to observe the corrosion properties St 37 steel plate. They used 4.5% and 6% clearance values in their work and found out that the surface roughness (R_a) was 25% smoother in high speed blanking. Also in high speed blanked parts, the corrosion resistance showed improvements. Kanca et al. [15] also used AISI 304 stainless steel sheets to blank under two punch speeds which were 0.5 m/s and 12 m/s. They employed a 300 kN hydraulic press for low speeds and a HERF (High Energy Rate Forming) hammer for high speeds and also used laser cutting to observe the effects of different speeds and cutting methods on the surface quality of blanks. It had been observed that the surface roughness is improved by 50% compared to other methods and at the same time the corrosion resistance is improved.

Subramonian et al. [16] used experimental and FEM analysis to observe punch-workpiece and punch-stripper plate interaction during high speed blanking. They conducted blanking experiments with punch velocities ranging from 20 mm/sec to 1600 mm/sec to study the dynamic loading on the punch. They used a press with 250 kN loading capability. The clearance was 6.5% of the workpiece thickness. The thickness of the workpiece was 0.2 mm and the material was C51100 steel. After the completion of experiments they performed FEM analysis by using Deform 2D program. They also tried to put forward an algorithm to obtain the flow stress of the workpiece under high strain rates. They stated that the cutting load increased to a point due to the work hardening of the workpiece. But when the punch speed reached to 1.6 m/s, the temperature rise at the cutting zone overcame the strain hardening and had an influence on the cutting load. As a result the cutting load decreased. They also mentioned that the vibrations of the stripper plate during unpinning applied lateral force on the punch, which could influence the strength and life of slender punches.

Song and Choi [17] tried to observe the effect of punch speed on the heat generation and on the cutting load of mild steel by using FEM methods. For this research, blanking simulations were carried out with punch speeds ranging from 30 mm/s to 60 mm/s with a blank thickness of 4 mm, punch radius of 15.75 mm, tool edge radius between 0.3 mm and 0.9 mm, and clearance between 0.2 and 0.5 mm. they used the

ABAQUS / explicit program to execute the runs. From the results they noted that the cutting load increased to a point due to the strain hardening than began to decrease due to the heat increase caused by the rise in strain rate. Also they stated that the increase in clearance decreases cutting load and also the temperature. Tool radius affected the results by increasing the cutting load due to the blunt edges and also caused a decrease in temperature.

Husson et al [18] studied on the optimization and comparison of the FEM and experimental results in high speed blanking. They used ABAQUS/ explicit program to analyze the results by introducing a nonlinear isotropic model valid for a wide range of strain rates and low homologous temperature. The material was thin copper sheets (approximate to 1. mm thickness). For experimental study, they used a square punch of 3.51 mm×3.51 mm with 50µm tool radius (the radius was also valid for the die). They employed a high speed blanking press with 25 Tons capacity. The clearance was 8% thickness of the workpiece. The predicted cut edge of the blanked part and the punch-force displacement curves were discussed as function of the process parameters such as the punch-die clearance, the wear of the punch and the die. The predicted cut edge of the blanked part and the punch-force displacement curves were discussed. They presented the evolution of the shape errors (roll-over depth, fracture depth, shearing depth, and burr formation) as a function of process parameters.

Murakoshi et al. [19] used an electromagnetically actuated press that can work in the range of 0.06 m/s to 15 m/s. They used an amorphous foil as the workpiece. They investigated the effects of blanking speed and clearance on the blanked surface. Furthermore, they examined the crystallization of the blanked surface with the use of the electron beam diffraction method. Crystallization had been found to take place mainly at the burnished area, very little being found at the fractured area.

Faura et al. [20] proposed a new methodology including the crack initiation and propagation angles to obtain optimum punch-die clearance value in blanking for a given sheet material and thickness by using finite element method. He used ANSYS program to model the blanking process and written an algorithm to calculate the angles created on the surface of the blanks. He used five different clearance values (5%, 8%, 11%, 14% and 17%) to blank AISI 304 stainless steel sheets with 1 mm thickness. He stated that the ideal clearance range in terms of angle created on the surface of the blank was approximately 11% and 12% for AISI 304. He also added that increase in the clearance caused the stroke depth of the punch to increase, lowered the cutting load.

Goijaerts et al. [21] developed a FEM model to simulate the blanking of X30Cr13 stainless steel with 1 mm thickness under two clearance values (2% and 10% of the workpiece thickness). They also validated the FEM results with experimental work. They used a universal testing machine to work as a blanking press that can exert 5 Mpa load on to the specimens. They calculated cutting load and punch displacement. They also used digital image correlation to observe the strain fields and their distribution. They showed that the proposed numerical model and experimental results fit well.

Goijaerts et al. [22] in another study, proposed a two way model to evaluate the ductile fracture mechanism of five different sheet metals. First way was the determination of the punch displacement at ductile fracture initiation, experimentally. Then by using FEM, modelling of the same blanking conditions were executed and went forward until the same punch displacement had been reached. The critical value C which is referred as the characterization of local ductile fracture criteria was calculated at this displacement value and accepted valid for the whole model. The second approach was the calculation of minimum thickness of the neck after fracture by performing a tensile test. They stated that the minimum thickness of the neck determined the ductile fracture initiation moment. Then came the modelling of the tensile test in FEM environment and when the experimentally determined minimum thickness of the neck was reached in the simulation, C was calculated and accepted as the ductile fracture initiation criterion was characterized. They used five different materials (X30Cr13 stainless steel, 316Ti austenitic stainless, Ms64 brass, DC04 high quality and Al51ST steel) and five different clearances (1, 3, 6, 10 and 15% of the sheet thickness of 1 mm) for both modelling and experimental study. They investigated the cutting load and punch displacement in the light of the predictions they proposed and stated that the first method gave best results in terms of accuracy.

Hambli and Potiron [23], used ABAQUS program and its user routine (UMAT) to develop a finite element model (FEM) to observe the shearing mechanism in blanking. They also executed the blanking process experimentally to compare the results. They used AISI 1060 with 3 mm thickness as the stock material and blanking process was executed at 10% clearance by a hydraulic press with 4000 kN capacity. They investigated the geometry of the sheared edges and force-punch displacement through the calculation algorithm and took damage and crack propagation into the account. Also for different radiuses of punch and die, they stated that the tool maximum load did not change but the punch penetration changes which also showed the effect of tool wear. As a result they put forward that the algorithm they created and the experimental results had a good correlation between them.

Hambli and Reszka [24], in another study used an inverse computation methodology technique for their FEM model to predict critical values of fracture criteria of the given material which is in conjunction with experimental studies. By their study, they tried to balance the results (force-penetration curves) of simulations and experimental results in terms of crack initiation and propagation on the sheared edges of the material which is again AISI 1060 but with 3.5 mm thickness. They used the same hydraulic press with 4000 kN capacity. They compared the numerical results obtained by the simulation with the experimental ones to verify the validity of the proposed technique for fracture criteria identification. They stated that their methodology of FEM and experimental results matched and values were very close.

Hambli [25] used artificial neural networks (ANN) to predict the burr height on the surface of AISI 1060 steel. In order to model the relationship between blanking parameters and burr formation, a three-layered feed-forward neural network with two neurons in the input layer, 17 in the hidden layer and one in the output layer was used. They trained the network with the results gathered from blanking simulations and experimental studies. The workpiece material was blanked using a 40 mm diameter die and a range of punch-die clearances from 5% to 20%. The press used was a hydraulic press with 4000 kN capacity. Punches and dies had the edge radii in the range of 0.01–0.2 mm. The training got stabilized after 2000 cycles and the error ratio decreased to less than 0.1% for any point. They presented that the usage of ANN is a reliable method to predict the burr height evolution vs the clearance.

A dedicated program only to compute blanking parameters which was named BLANKSOFT was also developed by Hambli [26]. The program could compute output parameters like blanking force, strain, optimal clearance, fracture angle, wearing of the tools and etc. in the light of the geometrical and material input data's. He also conducted experiments to verify the correctness of the results gathered from the program. He mentioned that a good agreement was observed between the results obtained by BLANKSOFT program and the experimental ones.

Hu et al [27] investigated the developed heat distribution in the blanking region by modelling the process using Deform 2-d. They proposed a methodology using a thermo-mechanical finite element method to predict the temperature values and distribution while blanking 0.12 mm thick phosphorous bronze sheet. They also observed the softening effect of temperature rise and the probable surface improvement on the blank's surface. They conducted experiments to validate the results like the distribution of sheared area and cutting load which were gathered from the models. They reported that they couldn't find any improvement on the surface quality of the blanks due to the thermal effects but the high productivity rate can be attained while maintaining good quality of the finished products using high speed blanking.

Hatanaka et al [28, 29] performed blanking simulations and experiments to observe the distribution of the zones on the sheared surface of the workpiece made of mild steel sheet with 3 mm thickness. They used an algorithm with their own design and node separation method to simulate the process. They employed Jeong fracture criterion which is a modified version of standard Cockroft and Latham fracture criterion in both of the studies. Blanking experiments were carried out to validate the results taken from the simulations. They used a universal testing machine and a special die set with rectangular punch and die (30x30mm) under a punch speed of 1 mm/min. The clearance between the punch and the die was changed from 2% and 20%. The blank holding force hold was changed from 0 to 12 kN. The punch and die had an edge radius of 0.064 mm. It was also assumed that the blanking would be done under no- lubrication condition so the frictional coefficient was taken 0.2. They reported that the clearance has a major effect on the surface distribution. Rollover and the depth of crack initiation increased at high clearances. Shear zone increased at small clearances and the crack propagations were eager to follow a direct path. In the case of high clearances, the propagations started only from the punch corner and propagate drastically causing low surface quality.

Maiti et al. [30] used FEM method to analyze the influence of clearance, sheet thickness, friction, punch/die size and blanking layout on the sheet deformation of mild steel within the range of 0.1-1 mm thickness. They used ANSYS and a package FEPEP which was written by the authors to execute the FEM analysis. They considered the blank diameters in the range 1-4 mm. The clearance values were changed in the range of 0-20%. They also simulated single (conventional) blanking and double blanking on a single sheet workpiece. Furthermore they investigated the size effect that includes the ratio between thickness and blank diameter. Results showed that the decrease in clearance increased the cutting load. Cutting load also increased with the increase in friction. They mentioned that the findings are also similar between two blanking methods. But they mentioned that the interblanking site distance more than twice the sheet thickness is good for reducing the thinning of sheet in the region between the two sites. In case of thickness and diameter ratio, the only finding they reported was the cutting load that decreased with the increase of diameter for the same workpiece thickness.

Marouani et al. [31], performed experimental and numerical analysis on the high speed blanking of FeSi steel sheet with 0.65 mm thickness. They used ABAQUS/Explicit program to execute the numerical analysis. First they carried out material testing of the material by incorporating tensile tests and also video tensile tests to validate the material properties. Then the identified model was used to perform blanking simulations on the software. The clearance was taken in the range of 3.8% to 23% and the speeds of the punches were changed between 23 mm/s and 123 mm/s. For experimental studies, they employed a mechanical press with a capacity of 200 tons and 80 SPM. They reported that the increase in the punch velocity caused strain hardening to a level where maximum cutting load became constant but the stroke depth of the punch increased. They assumed that this result was achieved due to the heat generation in the material that caused softening at the shear zone so the material can be subjected to more plastic deformation.

Vaz and Bressan [32], summarized the general aspects of the blanking process and its related parameters. They also discussed the issues during the modelling of the blanking process due to the many aspects occur at the shear zone like plastic deformations, material failure and heat transfer occurrences. They performed blanking operations to blank a 60 mm diameter with 0.5 mm thickness. E230T/2 electric steel was used in the simulations under no clearance and 8% clearance condition. They shared the cutting loads in terms of radial, axial and shear loads. They stated that those values were directly in conjunction with the friction coefficient between the tool materials. They considered the process as a cold process between the punch speeds in the range of 0.75 m/s or 300 strokes/min due to the limited temperature rising at the shear zone to a value of 92 °C.

High speed blanking offers some specific effects during the deformation of the material at high strain rates. One of the most important of this effect is the occurrence of adiabatic shear bands at the cutting zone. The formations of bands are not restricted to only blanking and can be formed under high speed deformation, compression and penetration situations. The occurrences and mechanisms of the bands on a given material are universal and results are also applicable for blanking process. Probable generation of adiabatic shear bands and their specifications can change according to the material type and the heat treatment of the materials used. Some studies focused on the investigation of these bands. Odeshi et al [33] investigated the effect of ballistic impacts on the plastic deformation behavior of tempered AISI 4340 alloy steel. Samples were first austenitized at 843 ^{o}C for 30 minutes then oil-quenched. The specimens then tempered at various temperatures in the range of 300 and 600 ^{o}C for 1 hour then air cooled. Different strain rates were established using a Split Hopkinson Pressure Bar (SHPB). Strain rates were in the range of 998 s^{-1} and 1420 s^{-1}. Fracture of the workpiece due to the cracks was observed to follow along the shear bands. They stated that the occurrence of cracks followed the path started by the nucleation of voids inside the cutting region, and then this progress leads to the coalescence of voids, grow and resulted with the formation of cracks. They observed that lower the tempered temperature, whiter the shear band. Specimens tempered at 300 and 400 ^{o}C had the whitest shear band but with no microstructural detail specific to tempered martensites. Higher tempered specimens at temperatures 500- 600 ^{o}C had grey and darker shear band colors and indicated extensive formation of shear strain in that zone. Also cracking probability was higher in specimens tempered at lower temperatures and the hardness due to high strain rates were increased 7% more than specimens tempered at high temperatures.

Chou et al. [34] investigated the formation of shear bands through controlled penetration tests by using an air-propelled gun. The air gun was used to fire an indenter to penetrate a test specimen made of AISI 4140 alloy steel. Penetration of the indenter produced the adiabatic shear bands on the specimen and they stated that the lengths of the bands were related with the flow stress of the material and the penetration depth.

Wei et al. [35] performed investigations on tungsten heavy alloy (93W) to observe the deformation and failure behavior and the adiabatic shear localization under different stress conditions. They used split Hopkinson pressure bar to execute the experiments. The specimens were in the shape of cylindrical, step-cylindrical and truncated-conic. The purposes of those particular shapes were to compare the influence of stress conditions. The experiments were performed at strain rates about $10^3 s^{-1}$. They observed that symmetric cylindrical specimens showed no formation of adiabatic shear bands. But step-cylindrical specimens, although under low strain rates, showed strong tendency to form adiabatic shear bands. Within the adiabatic band formation, tungsten grains were heavily deformed and were pulled into stringers along the shear direction. They assumed that the effect of sudden heat creation made the tungsten grains softer and developed large plastic deformation. Truncated-conic specimens also showed adiabatic shear band formations along the impact area. A severe localized deformation band was observed by using an optical microscope. Within the shear band no micro cracking was observed in the tungsten grains. They stated that except for cylindrical specimens, the adiabatic shear band had general trends to initiate and propagate along the direction of maximum shear stress. They also conducted numerical studies to observe the effect of different specimen geometries on the stress condition. They employed Johnson-Cook model to simulate the thermo-viscoplastic behavior of the material. Experimental and modelling studies validated each other.

Roessig and Mason conducted experimental [36] and numerical [37] research separately on the adiabatic shear localization of 1018 steel, 6061-T6 aluminum, and titanium 6%Al±4%V alloy in a dynamic punch test. For experimental work, they employed a servo-hydraulic press, a mechanical press, and a split-Hopkinson bar apparatus. The experiments were performed under the strain rates between 10^{-3} s^{-1} and 10^{4} s^{-1}. They used the same specimens for all strain rates. The specimens were square plates with 3 mm thicknesses. Punch used for the experiments had 30 mm diameter with 0,25 mm corner radius. The clearance between punch and die is 1,6 mm. Tensile tests were performed to obtain the results of yield strengths and strain hardening exponents to create a base for numerical work. Numerical analyses were executed by using finite element package ABAQUS/Standard. They employed Johnson&Cook constitutive law for the crack condition. Both experimental and numerical investigations showed that adiabatic shear bands were formed in the titanium when punched by mechanical press and Hopkinson bar. None of the experiments gave adiabatic shear band formation for 6061-T6 aluminum. The 1018 steel showed some transitional behavior toward shear localization in the Hopkinson bar experiments. They stated that materials with high strength and low strain hardening show more tendencies to adiabatic shear localization in punching process.

Giovanola [38] observed the adiabatic shear band occurrence in VAR (Vacuum Arc Remelted) 4340 steel (HRC 40) which was subjected to pure shearing. The shear stress- strain curves were obtained by using a split Hopkinson bar in the strain rate range of 1000 $s^{-1}$and 8000 s^{-1}. He employed a calculation method consist of etched grid lines on the specimens and high speed photography of the deformed grids which provided a time sequence of the deformation on specimen width. Then he digitized and differentiated the images to estimate the strain rates within the band. Stresses were calculated by means of a strain gage on the output of the Hopkinson bar apparatus. The shear band temperature was recorded by using thermocouples. He stated that strain of 17 and strain rates close to 1,4 10^6 s^{-1} were measured in the adiabatic shear zone. The temperature was reached approximately to 1000 ^oC and a significant strength reduction was observed due to the temperature rise in the zone.

Xue and Gray [39] examined the development of shear bands in annealed 316L stainless steel. To gather the mechanical response of the material, they performed experiments under quasi-static and dynamic compression conditions. They used cylindrical specimens with 5x5 mm dimensions. The quasi-static compression was conducted on a tensile machine at a strain rate of 10^{-6} s^{-1} whereas dynamic compression test were executed by using a split Hopkinson pressure bar at a strain rate of 25 10^3 s^{-1}. For shear localization experiments, they also used split Hopkinson bar and hat shaped specimens. Six different strikers with lengths 61.8, 76.4, 89.1, 101.6, 127.3, and 152.5 mm, were used to shear identical hat shaped specimens. Results showed that the mechanical behavior of annealed 316L stainless steel showed strong strain hardening to deformation to a point where the development of shear localization results in a substantial but not drastic stress drop. But they mentioned that during the micro observations, temperature did not rise significantly which showed that strain localization might be occurred from geometrical perturbations instead of thermal ones.

Meyers et al. [40] studied the effect of high strain rates on the shear localization occurrence taken place. Two methods were used to form the shear bands. One method was the usage of hat-shaped specimens under compressive loading of split Hopkinson bar. The other method was the collapse of a thick-walled cylinder. They used electron backscattered diffraction (EBSD) and Transmission electron microscopy (TEM) to observe the localization on a microscale level. They propounded that two regions were presented in the band. First one was a region consisting of grains having sizes of 0.1- 0.2 μm with low dislocations and grain boundaries with good definitions. The second region showed the properties of a glassy structure which validated that amorphization was valid in the shear band. Outside the band, the deformation took place due to twinning, stacking errors and martensitic deformations. The presence of martensite laths were observed at twinband intersections within individual grains. The martensite laths were generated by a strain induced phase transformation caused by intense plastic deformation. They stated that the evolution of plastic deformation that correlates with temperature rise occurred due to dislocated/twinned/transformed structure that brook up into small regions separated by geometrically-necessary boundaries.

Dixon and Parry [41] studied on the compressive mechanical behavior and thermal softening effect of type-224 carbon steel under different temperatures and strain rates. Temperature range was -110°C to +300°C and strain-rate range was between 10^{-4} s^{-1} and 5000 s^{-1}. The specimens were solid cylinders with two dimensions. First length by diameter was 5.0 mm x 10.0 mm and the second one type was 4.0 mm x 8.0 mm. The specimens were normalized at 880 °C and tests were conducted by using screw driven test machine, a hydraulic press and a split Hopkinson pressure bar. They reported that for strain rate less than 10^{-2} s^{-1} the compression test for 224 carbon steel had been shown to be adiabatic. But for dynamic testing of the material when the strain rate exceeds 4 s^{-1}, the test had shown to be adiabatic. Environmental temperature range played an important role and it was understood that the strain hardening effect of the material overpowered the temperature rise and the softening of the material. The strain hardening of the material due to increased strain rates was more dominant under low temperatures. At elevated environmental temperatures, the differences of stresses between adiabatic and isothermal conditions were explicitly small.

Clous et al. [42] used a split-Hopkinson compression bar and a prismatic specimen to calculate the temperature at the adiabatic zone. The prismatic shape allows the adiabatic zone to be measured. A fast infrared detector array was used to measure the maximum temperature within the band and found out that the temperature value reached to 850 ^{o}C in the shear band.

As it is evident from the literature review, the approaches and investigations covers a wide range of parameters and different conditions. As mentioned before, the main issue in blanking is the amount of parameters and the intricate effects of these parameters with each other. FEM approaches offer more flexible execution and investigation of the process because there is no cost, no labor, no material expense and the variations are virtually limitless. FEM also gives step by step observation of the process that identifies many features during the execution which is difficult to be investigated in experimental studies. But main problems are setting up the numerical model and validation of the results if they are correct or not. Experimental studies give exact results but to investigate different variations cost a big price in many aspects. Also detailed observations of the process are restricted to gaining only direct results. A step by step observation is literally a very difficult task.

Another issue is that the given studies investigated different approaches and parameters but many of them focused on specific parameters and tried to optimize the process by neglecting the other ones which also have effects on the actual targeted parameter. In a blanking process a small change in one parameter can alter the outcomes. This result triggers the alteration of other parameters and desired outcomes may also change. The optimization of blanking is a difficult task to accomplish due to this linked effects and a proper optimization can only be done by the collective understanding of the parameters and their linked effects.

This thesis focused on to clarify the general approach of single parameter oriented complexity and tried to embrace many aspects and effects of the related parameters. However, before proceeding to conclusions, the blanking process and governing parameters mentioned in the literature review should be explained.

CHAPTER 3

THE BLANKING PROCESS

3.1. Fundamentals of The Blanking Process

The blanking process which is also referred as shearing and generally confused with punching (piercing) is the cutting of the sheet workpiece into desired shapes which is pressed on to a die by a blank holder then perforated by the downward movement of the punch. An illustration of an ordinary blanking set up can be seen in Figure 3.1. The setup consists of 3 main parts except the workpiece: The punch which shears the workpiece into the desired shapes; the blank holder which applies pressure on to the workpiece to block the unwanted upper movement due to the bending moments created when the punch pushes the workpiece into the die cavity; and the die which has the same shape but dimensionally a little larger than the punch. This gap between the punch and die which is called "the clearance" lets the punch to dive into the die and make the shearing possible.

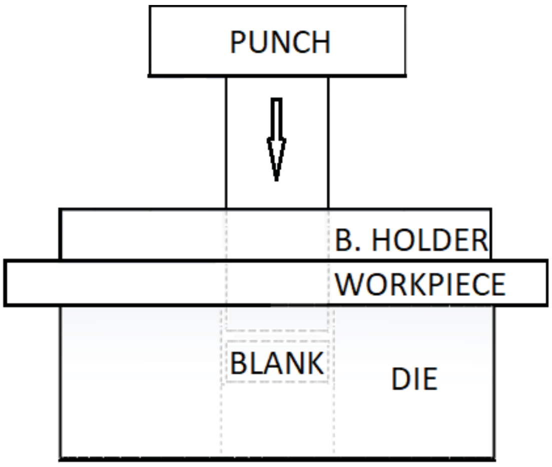

Figure 3.1. An ordinary blanking setup

The concept and working principle of blanking and punching are literally same in every aspect. The only difference and the main reason for their different names is the acceptance of the scrap and the workpiece [43]. In blanking, the sheet metal is th scrap part and the sheared part (blank) is the main workpiece. In punching, the blank is the discarded part or scrap and the perforated sheet metal is the main workpiece which was given in Figure 3.2.

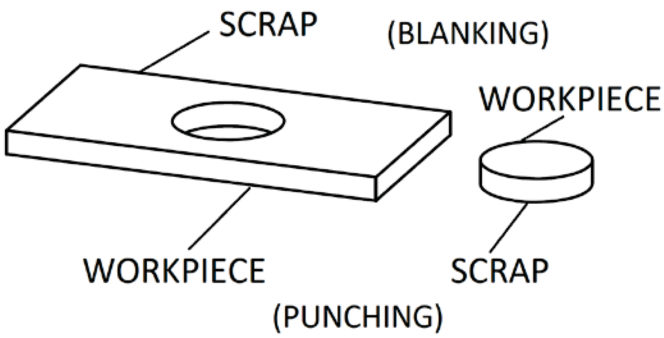

Figure 3.2. The different conceding of blanking and punching

Blanking process can be considered as a series of different phases which the sheet metal first undergoes elastic, plastic deformation then crack formation at the edges that leads to total rupture and at the last phase the sheared part gets separated from the main stock. During the transition of some of these phases, some distinct characteristics pertain to blanking process are formed on the surface. These areas with different characteristics are called zones. The phases can be grouped into 5. At the 2^{th} and 3^{rd} transition of the phases, formations of the zones happen. The explanation of phases and surface zones were given below. The related illustrations were given in Figure 3.3. Because of the axisymmetric structure of tooling, only half of the setup was illustrated.

Step 1. Contact of the punch

The execution of blanking starts with the downward movement of the punch. When the punch surface touches the workpiece and starts to press the material into the die cavity, stresses rapidly built on the workpiece. Compression stresses are created at the upper portion of the workpiece where the punch contacts. Tensile stresses are created at the bottom of the workpiece. Because of the mechanism of shearing, bending moments are also introduced at the direction of punch movement.

Step 2. Elastic / plastic deformation (Rollover and Shear zone)

The punch penetrates into the sheet. Because of the clearance between the punch and die, sheet metal is forced to stuck and pushed into the die cavity which gradually increases the mentioned stresses and starts to cause deformations. Deformations due to the increased stresses begin at the narrow zone which is located between the edges of punch and die. Material first undergoes elastic deformations and extruded depth of the sheet increases. Then plastic deformation starts and this is the point where rollover occurs due to the tensile and bending moments at the bottom of the workpiece. This bending stage called “rollover zone” is small and took 5-10% of the sheet thickness. Also when rollover has happening, the continuous movement of the punch pulls the material into the die cavity. This situation gets the material stuck between the flanks of the punch and die. The surface of the workpiece (the stuck portion) becomes burnished and has lower surface roughness than the other portions. This zone is called “shear zone”. Generally rollover and shear zone merges with each other.

Step 3. Crack formation

Punch penetration and shear zone formation continues up to a point where the load and stresses ultimately surpasses the strength of the material resulting ductile material failure. The crack starts behind the cutting edge on the surface area of the die and spreads out to the surface area of the punch.

Step 4. Breakthrough (Crack zone and Burr formation)

When the cracks at top and bottom meet and coincide, the sheet gets fractured and the surface of that portion is rougher than the sheared edge. This portioned area is called “crack zone”. On the other hand the propagation of cracks can follow a path directly to each other or can follow different paths. The crack propagation path is a crucial parameter and due to its course inside the material the burr or protruding ragged edge formation may be observed. After the occurrence of full fracture, the blank was completely separated from the sheet.

Step 5. Stripping

This is the last phase where the punch penetration reaches to the bottom dead center and ejects the part. Then direction of the punch motion is reversed and starts to move up to the upper dead center to reset the process.

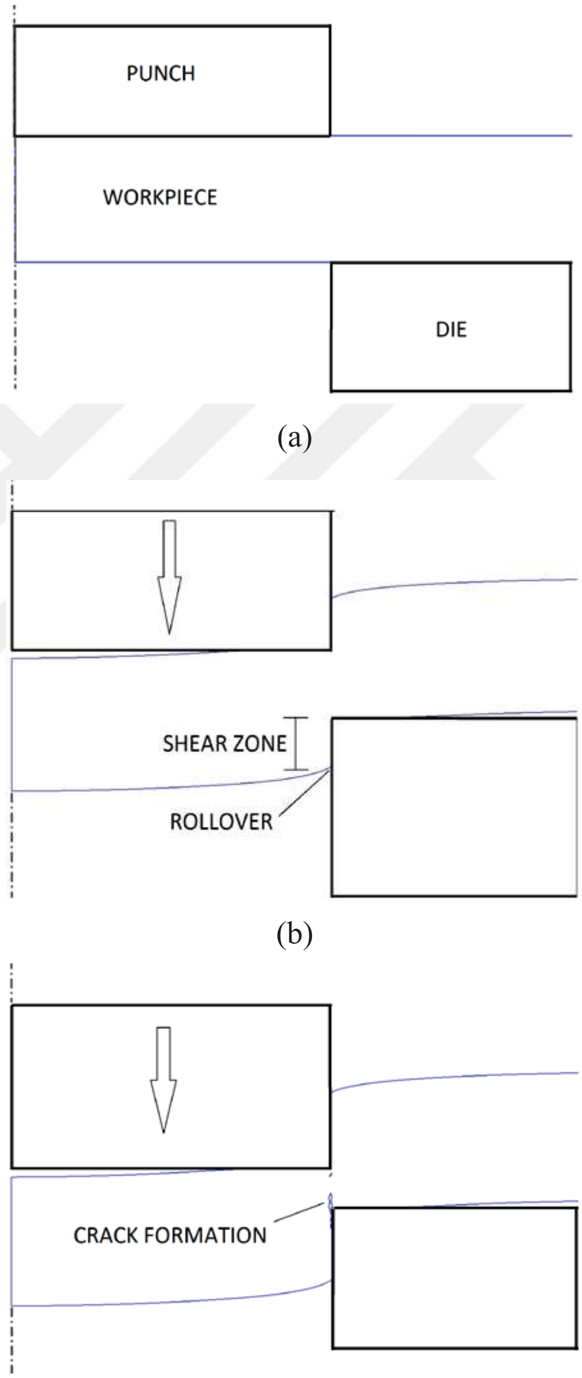

(a)

(b)

(c)

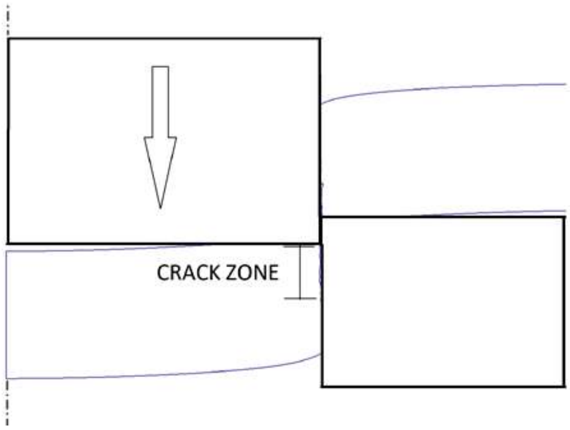

(d)

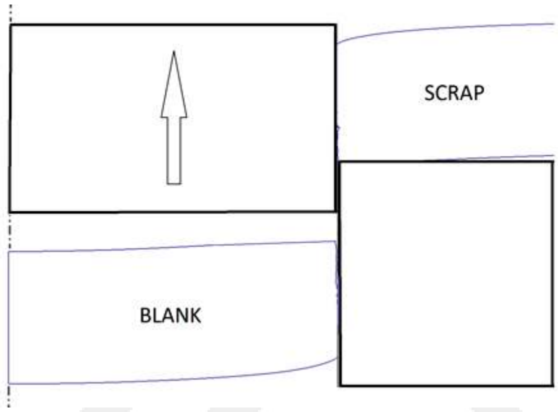

(e)

Figure 3.3. The phase steps that the sheet metal undergoes; (a) contact of the punch, (b) elastic / plastic deformation, (c) crack formation, (d) breakthrough, (e) stripping

3.1.1. Force Components

When the material is subjected to shearing between a punch and die, various forces occur at the cutting sides of the punch and die. A simple distribution of the forces was illustrated in Figure 3.4 where F_V and $F_V^{'}$ stands for the compressive stresses acting non-uniformly on a certain length around the cutting edges. l is the length between the acting forces results in the creation of moment and causes tilt or bending on the workpiece. This moment also creates counter bending moment as a result of bending and normal stresses acting horizontally on both the workpiece and tools. The horizontal forces were represented as F_H and $F_H^{'}$.

Also additional forces may become present if the workpiece does not rest horizontally on the lower die or the application edges of the punch and die do not have 90^{o} perpendicularity. During the studies done in this thesis, these two conditions are applied precisely with the purpose of eliminating additional forces.

On the other hand, the forces created due to the friction forces have to be mentioned. During the furtherance path of the punch, the friction forces act between the punch, die and the workpiece as a result of the forces F_V and $F_V^{'}$. These friction forces can be presented as μF_V and $\mu F_V^{'}$. Additional friction forces are created by the horizontal forces F_H and $F_H^{'}$. The forces can be given as μF_H and $\mu F_H^{'}$ which act through the side surfaces of the tooling [1].

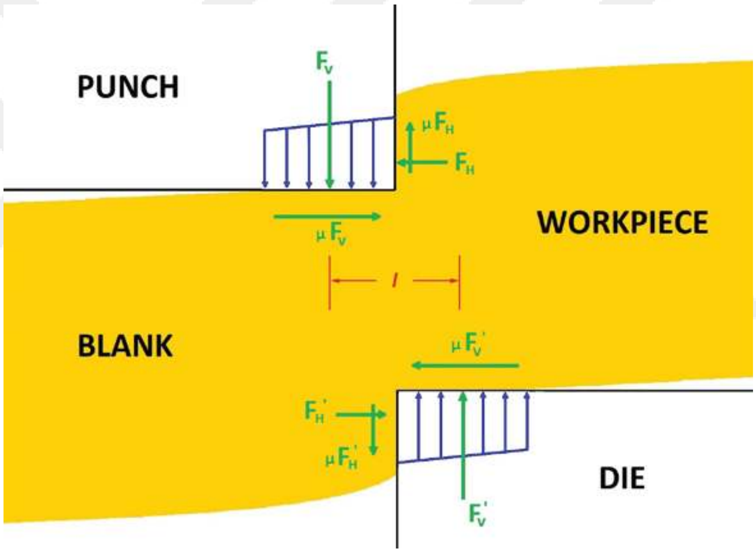

Figure 3.4. Illustration of the force components during the blanking of the workpiece

During the course of blanking, yielding of the material comes to a point where it can no longer deform and fails. When the ultimate strength of the material is surpassed, the initiation of crack happens and follows a path starting at the cutting side of the die and propagates. During the crack formation, the stress condition on the workpiece is considered as triaxial. A simple illustration of the stress generation during the crack formation and the representation of these stresses on a mohr circle based on the tresca yielding criterion were given in Figure 3.5. The principle tensile stress is represented as σ_1 whereas σ_2 is the tangential tensile stress and σ_3 is the principle compressive stress. Principle stress circle is named as “a”.

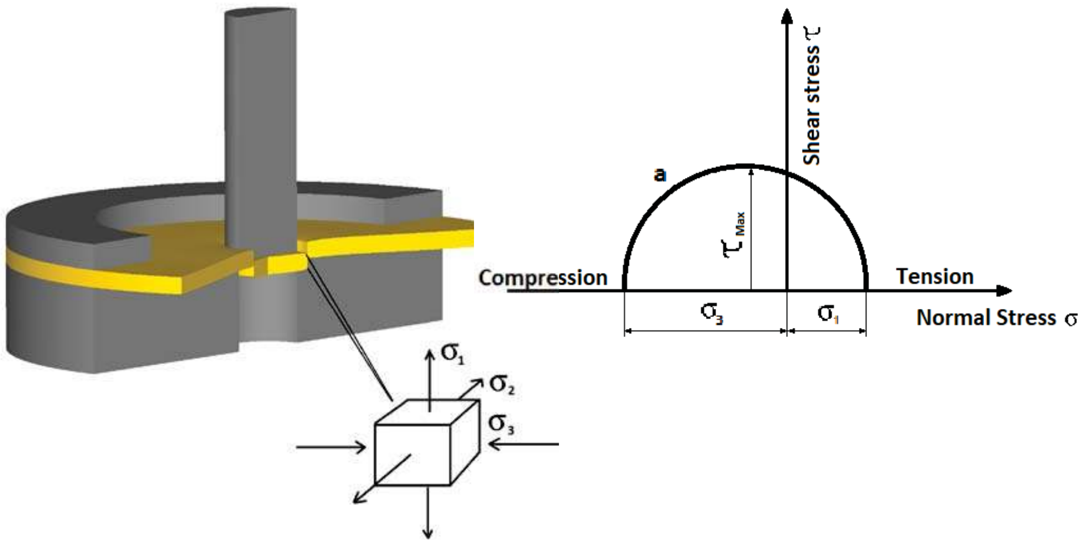

Figure 3.5. Illustration of stress conditions during the shearing

3.2. Blanking Parameters

In blanking, the parameters governing the process can be grouped into two; input parameters and output parameters. Input parameters have effective influences on the output parameters and the effects are valid single or combined. Input parameters generally define the state of the tooling and mechanical aspects whereas output parameters define surface quality, load and related energy consumption. In this context, parameters from both sides that have the most influences were explained. First, output parameters were given carrying a purpose of explaining what they are and the importance they carry. Then input parameters and their effects were explained with respect to the output parameters.

3.2.1. Output parameters

3.2.1.1. Surface Quality

Surface characteristics of the blanks have a big importance in blanking process. The distribution of zones is the direct indication of the surface quality and better quality results in lower correction operations. The main objective is to have the smoothest surface quality so; the shear zone becomes the most desired zone to dominate the surface. Rollover, crack zone and especially the burr formation are the unwanted zones and should be kept small as possible. Burrs are the main reasons for extra cleaning operations and can form in different heights and shapes which should be controlled carefully. In fact, it is difficult to eliminate burr formation completely but it can be minimized with selection of proper clearances and with the maintenance of the cutting tools. Burr formations have the potential to be hazardous during the production or can cause difficulties during forming like early wear of tools and may cause probable workpiece breakage. Also the sights of them give the impression of poor manufacturing quality. The simplest ways to clean the burrs are using hand scrappers but usages of them are limited for soft materials. General removal approach is to grind the surface, also chemical and electrolyte deburring, polishing and ultrasonic methods are available [44]. As a result, spending of labor, time and money can be lowered if a good surface quality without burrs or minimal burrs can be achieved. Figure 3.6 shows the blanking operation and the FEM image of the zone distributions on a blank. (+) sign indicates that the zone is desired and the (-) sign indicates that the zone is wanted to be small as possible.

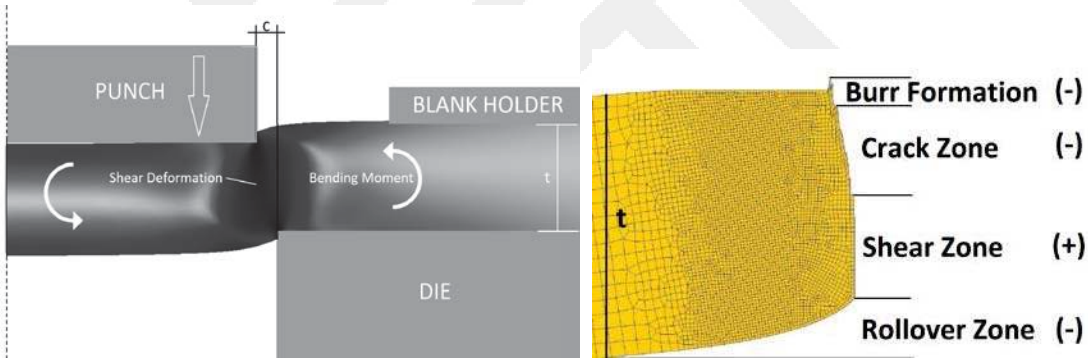

Figure 3.6. Blanking process (left) and a typical sheared-edge profile (right)

Zone distributions of blanks can variate under slight changes. The length of zones can differentiate and dominate each other due to the differences in blanking parameters. Although surface quality is an important parameter, whole system cannot be simplified only to achieve this goal. The process has to be in balance with its parameters meaning that a smooth sheared blank should be manufactured by spending minimal energy.

3.2.1.2. Cutting Load (Punch Force)

The cutting force required to cut the piece is called the cutting load or punch force. In other words cutting load can be identified as the necessary shear force to separate the part from the sheet material. To be able to choose the effective press and tooling for the blanking of a given sheet material, it is necessary to calculate the cutting load. Of course it has to be mentioned that when the cutting load calculation is made, the state of the tooling (sharp die and punch) and the knowledge of correct shear of the material strength should be consider. When die and punches are flat to each other and perpendicular to the motion of the punch, the cutting force can be calculated by multiplying the shear strength of the material by the cut section area of the blank expressed in Equation 3.1 as;

$$F = S_s * t * l \;=\; S_s * t \;* \pi * d \qquad (3.1)$$

where F is the required load of the press (N) (cutting force), S_s is the shear strength of the material (MPa), t is the sheet metal thickness (mm), and l is the cut length or perimeter of the blank (mm). The right side of Equation 1 is valid for round punches.

The cutting load (punch force) changes from the beginning of loading up to the separation of the blank and related events/outer forces at every phase was given in Figure 3.7. Shear strengths of some materials were given in Table 3.1.

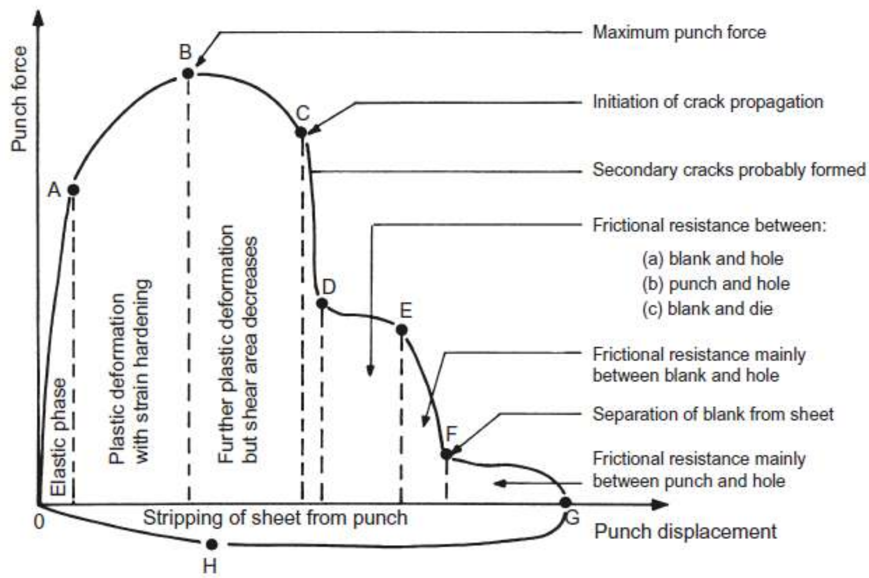

Figure 3.7. Cutting load (punch force)-punch displacement (stroke depth) and related phases [45]

Table 3.1. Shear strengths of various metals at room temperature [45]

Carbon steels	S_s (MPa)	Nonferrous metals	S_s (MPa)
0.10% C	241-296	Aluminum alloys	48-317
0.20% C	303-379	Copper and bronze	152-483
0.30% C	358-462	Lead alloys	13-40
High-strength low-alloy steels	310-439	Nickel alloys	242-800
Silicon steels	414-483	Tin alloys	20-77
Stainless steels	393-827	Titanium alloys	414-483

3.2.1.3. Cutting Energy (Work in Blanking)

Work done aka the cutting energy in a blanking process can be calculated by multiplying the cutting load and stroke depth of the punch expressed in Equation 3.2 as;

$$W = F * s \tag{3.2}$$

where W is the cutting energy (work done) (Nmm), F is the cutting load (N), and s is the stroke depth which is the penetration of punch inside the sheet material before fracture (mm) [45].

Cutting energy can be calculated alternatively from the cutting load- stroke depth graph. The area below the curve gives the cutting energy values. To calculate the area, Equation 3.3 can be interpreted as;

$$W = \int_0^s F(s)ds \tag{3.3}$$

The cutting load-stroke depth and related cutting energy graph were given as an example in Figure 3.8.

The importance of cutting energy lies in the ratio between cutting load and stroke depth. Many studies concerning the effects of parameters on the cutting load only take load parameter as the sole energy saving parameter. If one input parameter can justify lowest cutting load then it can be acceptable. But this kind of an approach can be misguiding. Cutting load and stroke depth can be manipulated by the change in input parameters. There are various versions where cutting load is low but other parameters are worse than expected. So, it becomes much more logical and appropriate to include the cutting energy while investigating the results and then try to optimize the process.

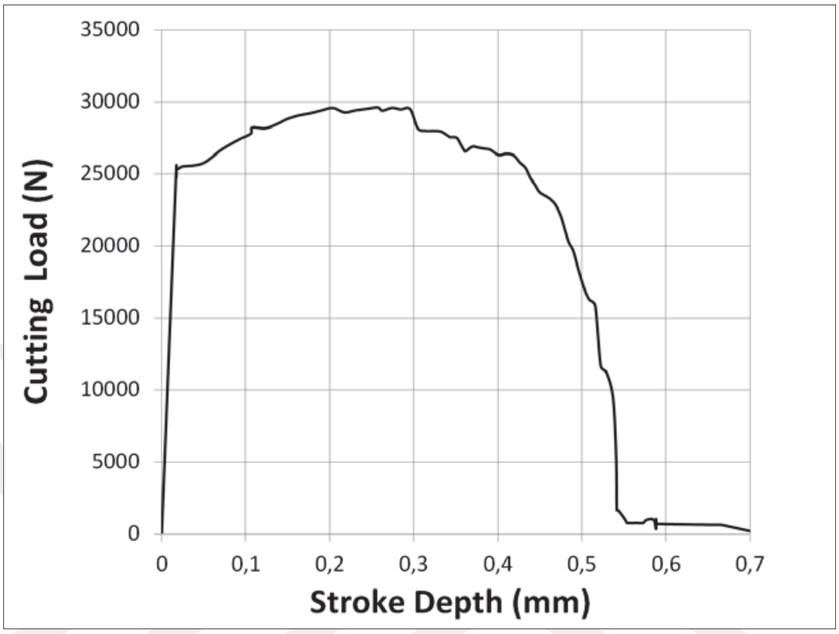

(a)

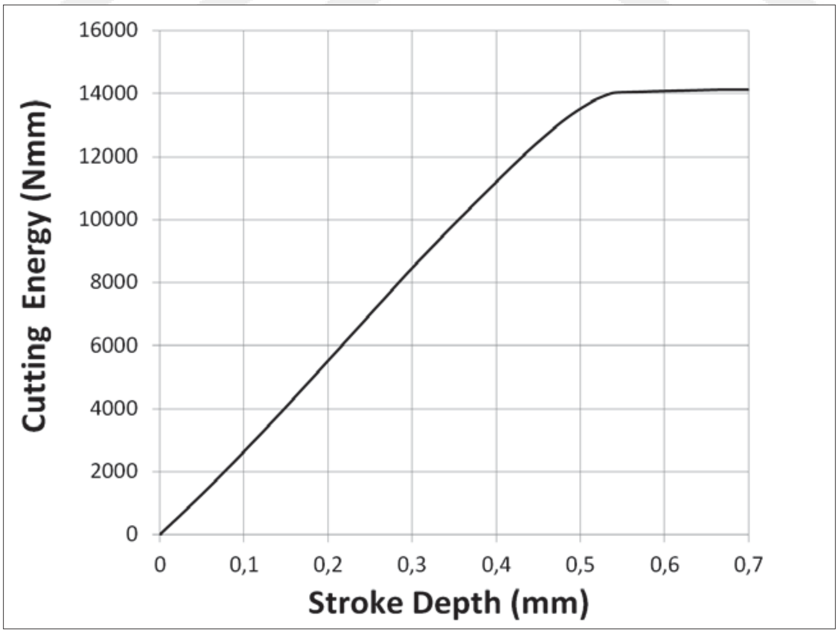

(b)

Figure 3.8. Cutting load and cutting energy graph gathered from a FEM simulation

3.2.2. Input Parameters

3.2.2.1. Clearance

Blanking is a delicate process which the governing parameters have strong influences on the outcomes. Studies deal with the process of blanking showed that clearance has the most influential effects. The differentiation in clearance can alter many parameters from surface zone distributions to load and energy values.

Clearance is simply the relative space between the punch and die. This space makes it possible for punch to enter the die opening and let the shearing possible. The clearance between punch and die was given in Figure 3.9.

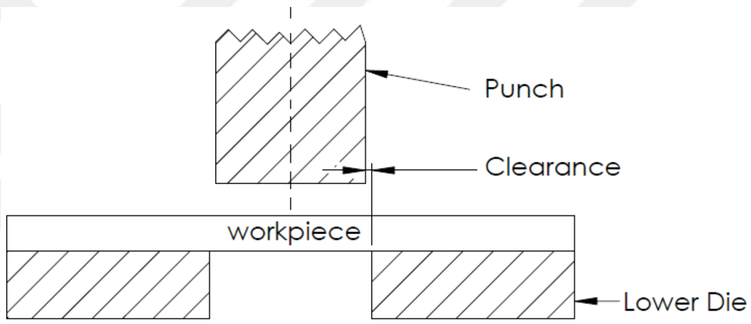

Figure 3.9. Illustration of the clearance on a blanking setup

In a blanking process, clearance is calculated as a percentage of the workpiece thickness expressed in Equation 3.4 as;

$$C = 100 \frac{D_m - D_p}{2t} (\%) \tag{3.4}$$

where D_m is the lower die diameter, D_p is the punch diameter and t is the workpiece thickness.

The effect of clearance can be considered to cause chained events in a blanking process. According to the condition of clearance, tight or loose, the profile on the surface can either be dominated by crack zone or sheared zone and cutting load/energy values also change. There is an interconnected relation between quality and energy and should be considered carefully to balance all aspects.

If tight clearances are chosen for the process, the surface of the blank yields a profile that is mostly covered by shear zone. Amount of materials pulled down and locked inside the die cavity is small but due to the narrow gap and increased friction forces, the pulled down material is grinded between punch and die. This situation causes material to be burnished and the area of this shear (burnished) zones exceeds the area of crack zone. This situation can be interpreted that usage of small clearances are beneficial from the point of surface quality but on the other hand tight clearances and increased friction forces increase the cutting load that results consumption of more energy, moreover the tool life will extremely be shortened due to the excessive contact between the tools and the blank.

Flank wear and galling are the most common types of wear in blanking processes performed under too tight clearances. Also the crack propagation follows a path between the edges of punch and die, but too tight clearance can cause a warp on the course of the cracks resulting secondary cracks which also distorts the surface quality.

Conversely, if the process is considered to be executed under loose clearances, this time the surface quality drastically falls. Excessive material will be pulled into the die cavity because of the large gap between the tools causing larger rollover and a crack zone dominated surface distribution containing a sharp edge with a large burr. However, cutting load reduces due to lower friction and lower contact of blank and tools. Tool life also improves.

Apart from this general knowledge, there is a third approach concerning to gain a blank surface without secondary cracks and minimal burr. This approach is called "the optimum clearance" which is based on the observation of crack initiation and propagation angles at the shear deformation zone.

3.2.2.1.1. Optimum Clearance

Optimum clearance theory investigates the crack formations/propagation directions in the shear deformation zone and tries to deduce an ideal clearance value. When the load and strain exceeds the materials strength and deformation capability, crack formation starts at the edge of the die and quickly propagates to the edge of the punch. Optimum clearance theory mentions that the ideal crack propagation should follow a direct line between the two cutting edges of punch and die or the crack propagation should be close to this line to achieve a high grade surface quality.

Optimum clearance is achieved when the angle of real crack propagation direction β which is the direction of the crack propagation during the blanking coincides with the angle of ideal crack propagation direction θ which is the line (desired path) between the cutting edges of punch and die. This condition can be simplified that closer β to θ, smoother the blank surfaces which was expressed in Equation 3.5 as [46]:

$$\Phi=\beta-\theta\cong 0 \qquad (3.5)$$

The ideal crack propagation angle can be expressed in Equation 3.6 as:

$$\theta = Arc\tan\left(\frac{c}{t-u_p}\right) \qquad (3.6)$$

where c is the clearance; t is the sheet metal (workpiece) thickness and u_p is the punch penetration corresponding to the first crack initiation within the sheet.

The FEM image of crack propagation angles and secondary cracks on a blanked surface was given in Figure 3.10.

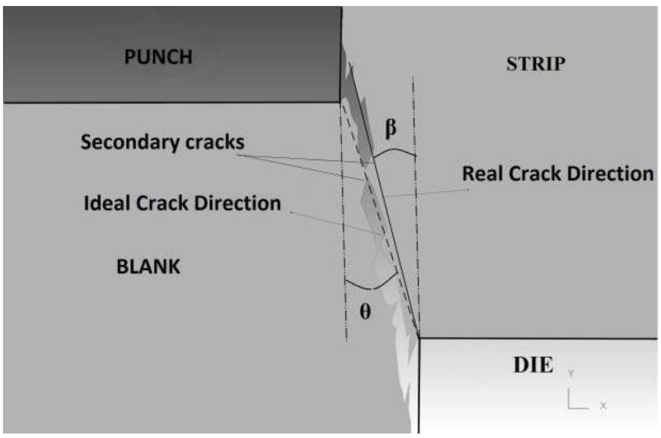

Figure 3.10. Illustration of angle β, angle θ, and secondary cracks

As it is evident from the Figure 3.10 that secondary cracks and a rugged surface is created because β doesn't coincide with θ.

The general concepts and approaches offer some solution in the selection of the clearance. Like optimum clearance method, many put surface quality as the main achievement whereas some investigate the overall energy consumption of the process and place it as the first priority. In theoretical understanding, the selection of clearance is based on logical rules but when the situation comes to the selection of "best clearance" experimentally, there arise a big uncertainty. Generally in practice and many research studies, the user has to be obliged to choose a side. It can be either good surface quality or energy saving. The clearance value is forced to be adjusted to fulfill the purpose of which aspect is much more important to the user. But these forced solutions lead to more problematic results. During literature survey and live observations, it was understood that clearance values advised to be used in a blanking process have an enormous range. Values of the clearance simply range from 1% to 20% of the workpiece thickness according to the sum of the studies. Although the general behavior and effects of different clearance values are known, this range doesn't address or confirm which values should be chosen. "Which value is best for surface quality or cutting load for a given condition? Is there any clearance value that embraces both of these aspects?" are the main questions. On the other hand, in a process where the tooling has to be precise, tolerance limits center around ±0.01 mm and only a minor flaw or change in the value of one parameter can alter many outcomes, this enormous gap of clearance selection values are highly irrational. As mentioned before, blanking outcomes are the combined results of input parameters and the selection of clearance can't be done by neglecting the other parameters. Punch speed which was given in the next chapter, is one of the most important parameter in a blanking process and has a big effect on the overall process.

3.2.2.2. Punch Speed

Clearance may be the most influential parameter in a blanking process but it can clearly be stated that punch speed definitely has an equal importance. Its effects can rival the clearance in terms of surface quality and energy saving. In fact, clearance value should be chosen considering the speed of punch to balance the effects possessed on the blank.

Blanking process can be done at different speeds depending on the press type, but basically divided into two categories as "low speed blanking" and "high speed blanking". The process is regarded as a high-speed blanking process when the punch speed can exceed 5m/s [47]. The effect of punch speed on blanking process can simply be divided into two. First effect is the strain hardening in the vicinity of shear deformation zone due to high strain rates exerted on the blank. When the material is deformed under a high strain rate, material hardens to a point where it can no longer harden and fails by shear localization. If material's formability under high strain rates is low, the hardening mechanism before full rupture causes a big amount of rise in the cutting load.

Second effect and an important advantage of high speed blanking is that the generation of adiabatic shear bands in the shear deformation zone. Adiabatic shear bands are formed under high speed loadings of material. When the material is subjected to high punch speeds, a sudden heat emanation occurs in the shear deformation zone due to the high strain rates. This happens because 90% of the plastic work is converted to heat [48]. This localized heating causes localized plastic flow which can be catastrophic leading to fracture by localized shearing. The heat emanation causes temperature rise in the zone and cannot find time to dissolve in the material and forms a shear zone with high temperature which can be described as adiabatic. With the increase of temperature, workpiece is subjected to thermal softening. By thermal softening, internal stresses are reduced and material can withstand more deformation that causes more smooth surface distribution on the blank [49].

The effect of speed can vary between these two conditions and the eventual shearing happens due to which condition is preponderant. Variations of these effects are directly related with workpiece material's flow stress, strain, strain rate, workpiece material's heat transfer coefficient and temperature rise in the shear zone [50]. As can be understood, mechanical properties of the workpiece material play an important role in a blanking process and should be explained.

3.2.2.3. Properties of Workpiece Material

The main goal of blanking process is to achieve best surface quality by spending minimal energy. All actions are done to accomplish this purpose. However, it is appropriate to mention that the adjustments are forced to be made specifically. Workpiece material is a key point in blanking and its properties can change every outcome in the process. So, selections of the values of parameters should be made specifically for the material planned to be blanked. In this context, some important properties of workpiece materials related to blanking were given in the following sections.

3.2.2.3.1. Stress and Strain

The deformation of a material is only possible with the application of an outer force/load. Stress can be defined as the load per unit area exerted on the material. In blanking and sheet metal forming applications the stress component and the materials behavior against this load plays an important role.

When the material is subjected to stress, deformation starts up and continues to a point (elastic limit) where permanent (plastic) deformation takes place. Strain is the relative change in size (length) due to this external stress (in case of tension) and can be defined as the division of the difference in the initial and last length to the initial length of the material which was given in Equation 3.7 as;

$$e = \frac{\ell - \ell_0}{\ell_0} \tag{3.7}$$

Strain is proportional to the applied stress in elastic region [51] and follows a direct line. But through the course of deformation and after the transition to plastic region, strain and the deformation ratio changes and does not increase linearly. Total strain can be taken as the sum of strains at elastic and plastic region. Therefore it can be written in Equation 3.8 as;

$$e = e_{el} + e_{pl} \tag{3.8}$$

In sheet metal blanking and forming operations, the elastic strain e_{el} is smaller than plastic strain e_{pl}. Elastic strains are in order of 10^{-4} whereas plastic strains are in order of 10^{-1} or 10^{0} [52]. Because of this big difference, general approach about the elastic strain is to neglect it. So, after the removal of the stress, for the final length (ℓ_1), Equation 3.9 can be interpreted as;

$$e_{pl} = \frac{\ell_1 - \ell_0}{\ell_0} \tag{3.9}$$

But this form of the equation which is also called "engineering strain" at the plastic region can't appropriately describe the deformations under the extension or the compression of the workpiece for high strains. To correct this situation "true engineering strain" should be introduced.

Engineering strain can be rearranged in terms of the differential difference of the length $d\ell$ in Equation 3.10 as;

$$de = \frac{d\ell}{\ell_0} \tag{3.10}$$

Integration through whole stretching period leads to;

$$e = \int_0^e de = \int_{\ell_0}^{\ell_1} \frac{d\ell}{\ell_0} = \frac{\ell_1 - \ell_0}{\ell_0} \tag{3.11}$$

In engineering strain, the length is accepted as the specimens starting length. If this length is written as the current length of the material;

$$d\varepsilon = \frac{d\ell}{\ell} \tag{3.12}$$

Integration again through the whole period;

$$\varepsilon = \int_0^e d\varepsilon = \int_{\ell_0}^{\ell_1} \frac{d\ell}{\ell} = \ln\left(\frac{\ell_1}{\ell_0}\right) \tag{3.13}$$

By this approach, the symbol ε is called the true strain of the material and also signifies the plastic true strain. The relation of engineering and true strain can be seen in Equation 3.14;

$$\varepsilon = \ln\left(\frac{\ell_1}{\ell_0}\right) = \ln\left(\frac{\ell_0 + \Delta\ell}{\ell_0}\right) = \ln\left(1 + \frac{\Delta\ell}{\ell_0}\right) = \ln(1+e) \quad (3.14)$$

The correlation of stress and strain is the most important relation for a material going under deformation. True strain usage in blanking is crucial so the stress component should also justify the proper values. As in engineering strain, engineering stress is also based on the initial, original cross sectional area of the workpiece. But true stress uses the instantaneous cross sectional area that was given in Equation 3.15 as;

$$\sigma = \frac{F}{A} \quad (3.15)$$

Where σ is the true stress, F is the load and A is the instantaneous cross sectional area of the workpiece. Under large deformations usage of true stress gives more accurate measures than engineering stress and their relations can be expressed as;

$$\sigma = \frac{F}{A} = \frac{F}{A_0}\frac{A_0}{A} = \sigma_e \frac{A_0}{A} = \sigma_e \frac{\ell}{\ell_0} = \sigma_e(1+e) \quad (3.16)$$

σ_e is the engineering stress of the material, A_0 and ℓ_0 is the starting cross sectional area and length of the material, e is the engineering strain of the material. The difference of true and engineering stress-strain curves were given in Figure 3.11.

In sheet metal forming applications, the elastic deformation of the material is no concern because the main purpose is to obtain the deformation of the sheet material. So, usage of elastic region can be neglected. As mentioned before under the influence of stress, material elastically deforms to a point where it starts to deform plastically. This yielding point's corresponding stress value is called the "flow stress".

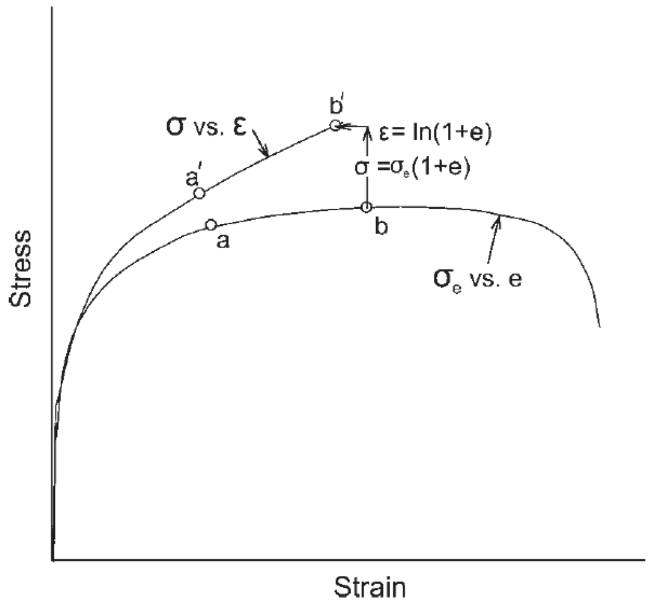

Figure 3.11. Differences between true and engineering stress-strain curves [52].

Flow stress is the required stress to keep the material "flowing". In other words, it is the force that continued the plastic deformation of the material under uniaxial state of the stress. Flow stress of the workpiece material is a considerable specification in a blanking process. Because most metals when deformed at room temperature have a tendency to increase their flow stress. This behavior is called strain or work hardening. Strain hardening is the result of interaction of inclusions or dislocations in the crystalline structure of the metal [52].

Estimation of flow stress is extremely important to measure the required forces and the mechanical behavior of the material. Various approximations are possible that the material work hardens according to the strain. An ideal condition and the simplest model is the non-existence of any hardening which can be expressed in Equation 3.17 as;

$$\sigma = Y \tag{3.17}$$

Where σ the flow stress which is independent of strain and Y is the yield strength of the material. In the situation of linear work-hardening the equation can be written as;

$$\sigma = Y + A\varepsilon \tag{3.18}$$

For many materials the work hardening follows a linear path that increases with increasing strain. But the hardening rate decreases with increasing strain.

For annealed materials experiencing plastic deformation at room temperature, the power law (also known as Hollomon's law) is a good approximation of the flow stress;

$$\sigma = K\varepsilon^n \tag{3.19}$$

where K is the strength coefficient (MPa); and n is the strain hardening exponent. For prestrained materials the power law can be shifted proposed by Swift [53] given in Equation 3.20 as;

$$\sigma = K(\varepsilon_0 + \varepsilon)^n \tag{3.20}$$

where ε_0 represents prestrain of the material and Swift’s equation is useful when the material has undergone a prestrain. Still there proposed a saturation model which predicts the flow stress approaches as an asymptote, σ_0, at high strains suggested by Voce [54];

$$\sigma = \sigma_0\left[1 - \exp(-A\varepsilon)\right] \tag{3.21}$$

Equation 19 generally finds a usage for a number of alloys. The mathematical approximations of suggested stresses and their related true stress–strain curve illustrations were given in Figure 3.12.

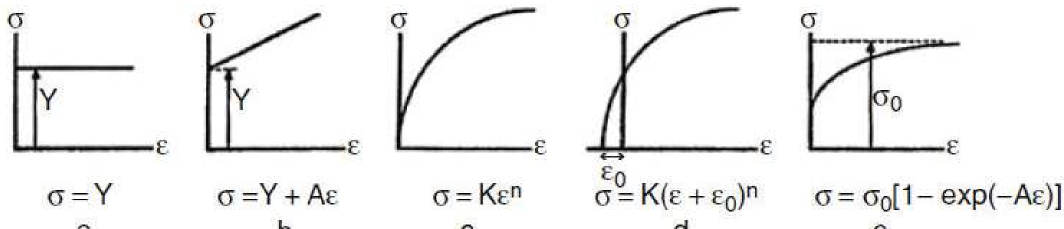

Figure 3.12. Mathematical approximations of the true stress–strain curves [54]

The values of the strain hardening material coefficient, *K* (MPa) and the exponent, *n* for different materials at room temperature were listed in Table 3.2.

Table 3.2. Strain-hardening coefficient, K (MPa) and exponent, n [54, 55, 56]

Material	Strength Coefficient, *K* (Mpa)	Strain Hardening Exponent, *n*
Low-carbon steels	525-575	0.20-023
HSLA steels	650-900	0.15-0.18
Austenitic stainless	400-500	0.40-0.55
Copper	420-480	0.35-0.50
Aluminum alloys	400-550	0.20-0.30
70/30 brass	525-750	0.45-0.60

3.2.2.3.2. Stress and Strain rate

Strain rate is another important factor and the materials strength variation according to the strain rate is known as strain-rate sensitivity. Strain rate in forming is directly related with deformation speed which was given in Equation 3.22 as;

$$\dot{\varepsilon} = \frac{v}{h} \tag{3.22}$$

where, v is velocity of the deformation, h is the instantaneous height of the workpiece being deformed and $\dot{\varepsilon}$ is the true strain rate.

The relation of stress and strain rate can be expressed as;

$$\sigma = C\dot{\varepsilon}^m \tag{3.23}$$

where *C* is the strength constant of the material. The strength constant is similar to *K* in the flow curve equation but not equal. When the strain rate is constant at a speed of 1 s^{-1}, flow stress is defined as strength constant and strength constant is symbolized as *C* [54]. The exponent *m* is called the strain- rate sensitivity exponent. The strain-rate sensitivity of the material can be gathered from the slope of the flow stress and strain rate. The effect of strain rate on flow stress at an elevated work temperature plotted on a log-log coordinates was given in Figure 3.13. Strain rate sensitivities of some materials were given in Table 3.3.

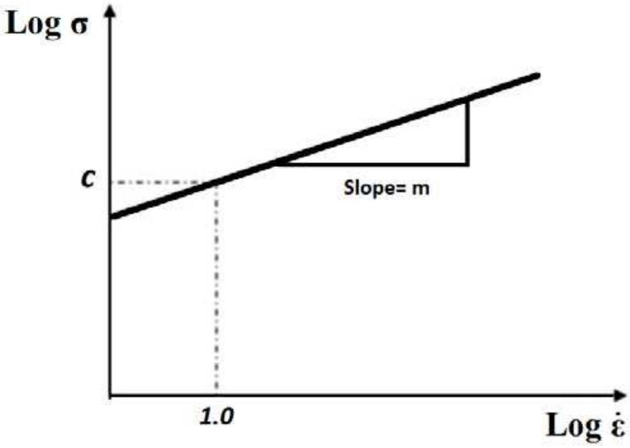

Figure 3.13. Flow-stress and strain rate relation at an elevated working temperature plotted on a log-log coordinates [56]

Table 3.3. Strain rate sensitivities of some materials at room temperature [56]

Material	***m***
Low-carbon steels	0.010 - 0.015
HSLA steels	0.005 - 0.010
Austenitic stainless	(−0.005) - (+0.005)
Ferritic stainless steels	0.005 - 0.010
Copper	0.005
Aluminum alloys	(−0.005) - (+0.005)
70/30 brass	(−0.005) - (0)
α-titanium alloys	0.01 - 0.02
Zinc alloys	0.05 - 0.08

3.2.2.3.3. Stress and Temperature

Temperature of the working condition is an important asset in sheet metal forming because the material's hardening behavior is related to it. For any metal K decrease at elevated temperatures. Both strength and strength hardening reduce at higher temperatures which mean that the plastic deformation operation can be done by using lower forces. The decrease in strain hardening also indicates that the strain hardening exponent (n) decreases with increasing temperature. Also it has to be mentioned that the ductility is higher at elevated temperatures. Figure 3.14 shows the decrease in strength of copper and aluminum and decrease in strain hardening exponent due to increasing temperature.

From the point of strain rate and its relation with temperature, the decrease in C at elevated temperatures is same as K. But this is restricted to higher temperatures because at lower temperatures, the increase in flow stress due to high strain rates is insufficient (approximately 1%- 2% increase). So, for lower temperatures the hardening effect of the strain rate can be neglected. But when the working temperature exceeds the recrystallization temperature of the material which is generally more than the half of melting temperature of the material, there occurs a drastic increase in the material's resistance to deformation with the increasing strain rate. The strain rate sensitivity exponent, m is also temperature dependent and increases with elevating temperature. The flow stress and strain rate change under the influence of different temperatures was given Figure 3.15. The slope of the curves gives m and can be seen that increases with increasing temperature. The variations of m for various metals under homologous temperature $\frac{T}{T_m}$, where T is the initial temperature and T_m is the melting temperature of the material were given in Figure 3.16 (a). The change of m for 2024 and pure aluminum under different temperatures were given Figure 3.17 (b).

A combined approach including strain and strain rate and their effect on the flow stress can be expressed as;

$$\sigma = K\varepsilon^n + m\ln\dot{\varepsilon} \tag{3.24}$$

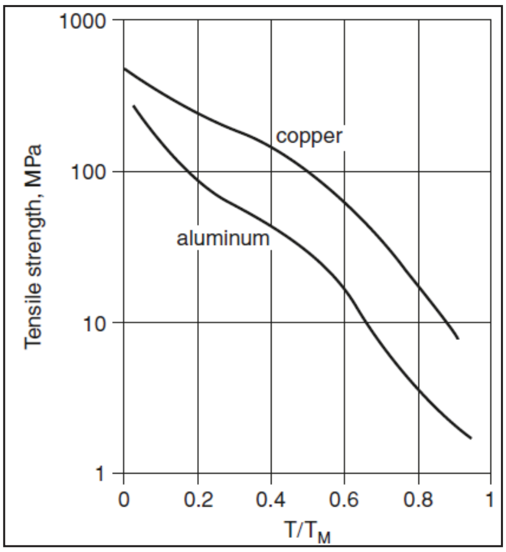

(a)

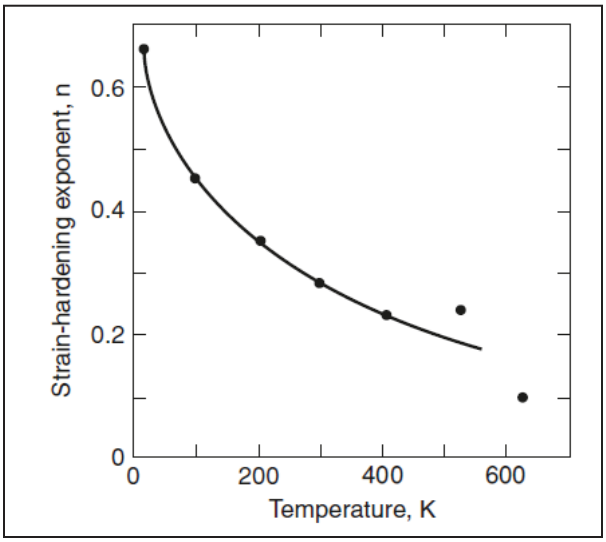

(b)

Figure 3.14. (a) Decrease in tensile strength of aluminum and copper due to increasing temperature (b) Decrease of strain- hardening exponent, *n* of aluminum with increasing temperature [55]

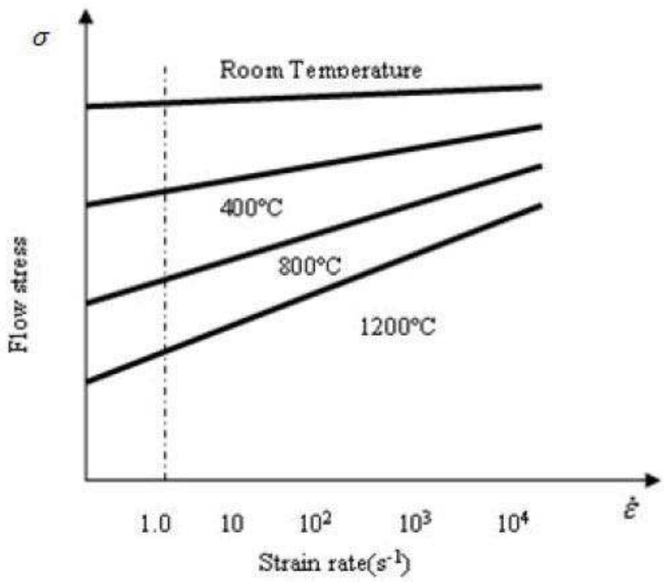

Figure 3.15. Effect of temperature on the flow stress for typical metal [54]

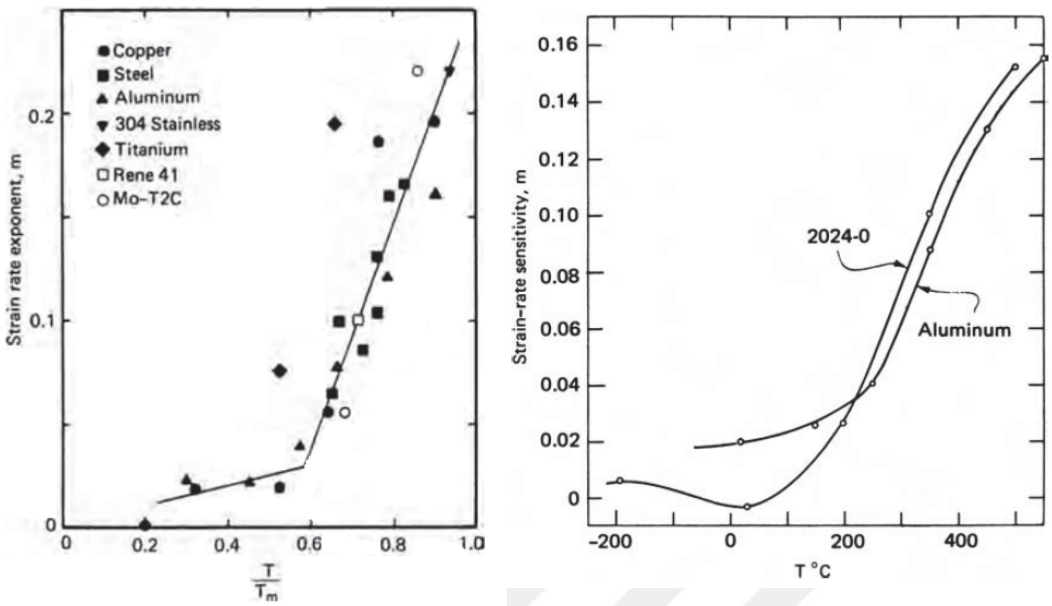

(a) (b)

Figure 3.16. (a) Variation of the strain-rate sensitivity of different materials with homologous temperature, $\frac{T}{T_m}$; (b) Temperature dependence of the strain-rate sensitivities of 2024 and pure aluminum [55].

3.2.2.3.4. Thickness of The Workpiece and Thickness to Die Diameter Ratio

In sheet metal forming industry, blanking of different sized workpieces are common manufacturing events hence the thicknesses and sizes of AISI 304 stainless steel vary greatly. The material finds itself possible usage places like in the manufacturing of very thin and small electric/electronic components to automotive and heavy industrial applications where the material thickness exceeds 6 mm and be considered as bulk forming.

The thickness of the workpiece is an important parameter in blanking process. The clearance, cutting load and cutting energy ought to change according to the thicknesses and should be taken into consideration. For example; clearance values cannot be fixed if the thickness of the workpiece changes. From Equation 3.4, it can clearly be seen that thickness directly influences the value of the clearance. Also, it is not logical to use the same clearance for all thicknesses because the optimal clearance where the surface quality is good or the lowest energy consumption is reached has a probability to change according to the thickness values.

On the other hand, the size of the part to be blanked has to be taken into consideration due to the amplification it adds to the cutting load and cutting energy. The baseline of load calculation that was given in Equation 3.1 includes the change in thickness and also includes the change in diameter. According to Equation 3.1 for a round part ($F = S_s * t * \pi * d$), the required cutting load can be found by multiplying the shear strength, thickness and the diameter of the lower die (the desired diameter of the blank).

However, the equation contains a big gap and it is the absence of the effect of clearance. The equation gives the peak value of the load like there is no clearance between the punch and lower die. A biased interpretation of this situation can lead to a simple explanation that if peak load is known and used, the punch penetrates the sheet for any value of clearance. This may be true if only goal is to pierce the sheet metal no matter the cost or spent energy. But in reality, energy conservation is a crucial part of the manufacturing systems and must be taken care of.

So, the absence of the effect of clearance became the main reason to the investigation of the effect of thickness and thickness to die diameter ratios. The general treatment for larger parts is to find the clearance value as a function of thickness and apply it for all diameters. Also there have been no studies regarding to thickness to die diameter ratios and any suggestions for energy conservation. Thickness and especially the size of the workpiece and their combined effects create a big gap in the literature and should be investigated.

CHAPTER 4

THE EXPERIMENTAL STUDY

Blanking process consists of some key mechanical components to operate fully and produce blanks. These components can be simplified mainly into three main parts which are the press to exert the load, the die setup to execute the shearing and the workpiece material desired to be blanked. In this chapter, the detailed explanation of these three parts used for the experiments will be given in the scope of the work done.

4.1. Presses

In a blanking process, the type of the press holds a vital importance because the required force should be exerted on the workpiece at the required speed. Without the capacity to create the force or the speed needed, the blanking process cannot operate efficiently. The production capability in a blanking process is mainly dependent on the specifications of the press employed.

The main center of this study relied on to obtain the load and speed needed to properly execute the process of blanking. Three different punch speeds were necessary to observe the effect of speed on the properties of blanks. So, to achieve the desired punch speeds, different type of presses were used.

4.1.1. Hydraulic Press

The hydraulic press which was used in the experiments is actually a tension-compression test machine and has an interchangeable capacity between 12, 30 and 60 tons. All experiments were executed under 30 tons and by using the compression side of the machine. The upper ram of the hydraulic press is stationary. However, the lower ram and the die seat, move in upward and downward directions. The velocity of die seat is controlled by means of the velocity control handle. As the seat of the press goes upwards or downwards, the drum rotates by means of the pulleys. Rising and lowering the press bed is carried out by the loading and unloading arm. The press is located in Materials Laboratory of Mechanical Engineering at University of Gaziantep which was given in Figure 4.1. The press is mainly used for the blanking experiments executed under the press speed of 0.1 m/s.

Figure 4.1. The hydraulic press used for experiments

4.1.2. Eccentric Press

For blanking with moderate speeds (1 m/s), a H type high speed eccentric press was used which was located in a private metal forming factory located in Gaziantep organized industrial zone. The press had a capacity of 100 tons. The stroke length of the press could be adjusted between 20- 150 mm and had the adjustable stroke limit of 60-120 strokes per minute. The press used in the experiments was given in Figure 4.2.

Figure 4.2. The eccentric press used for experiments

4.1.3. Powder Actuated Nail Gun

With conventional machines and press types, reaching high punch speeds is a difficult goal. Full embracement of the high speed forming requires a serious investment of machinery, tools and equipment to support the production line and continue the process. Hence this study was a at a research level and did not need to create a production cycle or mass production; an alternative and simpler tool was used to reach high punch speeds which is based on the usage of a powder actuated nail gun and a special die set.

A powder actuated nail gun has the form close to a gun that consists of an outer case (1) ; a trigger mechanism (2) ; a magazine slide inside the handling (3) ; a barrel assembly (4) that houses a piston; a barrel extension (5) at the front which has to be pressed inside against the work surface with approximately 90 N (9 kgf) to squeeze the safety pin at the back of the gun and tension the spring of the firing pin which is actuated by the explosion of the powder; a cocking lever (6) and mechanism to shift the piston (7) to its initial position and also advance the magazine (8) upwards to make the gun ready for firing.

The gun has a max power output value of 400 J. The power output can also be adjusted by a screw mechanism at the side of the gun that regulates the pressure inside the barrel. The gun and the illustration of its inner parts were given in Figure 4.3.

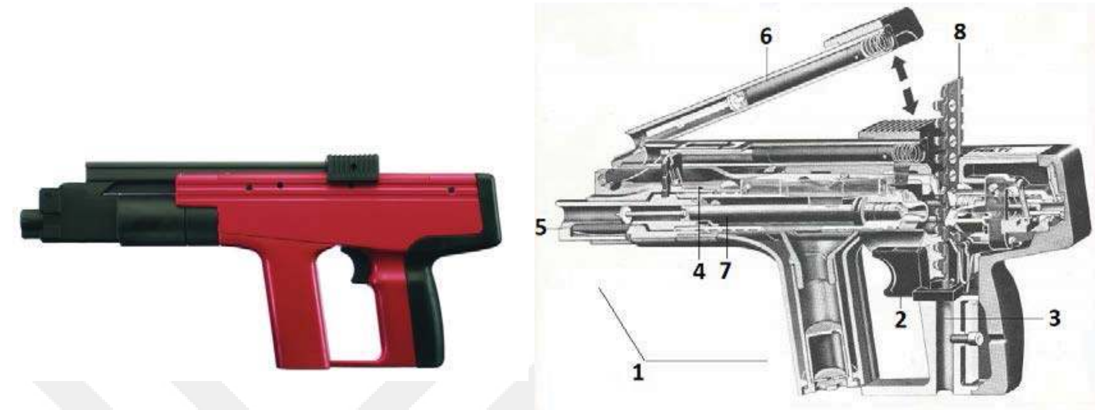

Figure 4.3. The powder actuated nail gun and illustration of its inner parts [57].

4.2. Dies

The process of blanking requires a set up consists of punch and die assemblies. Two different die setups were used to execute the experiments. For blanking at low and moderate speeds a dies set up consists of 6 parts were used. The exploded view of the designed die and its components were given in Figure 4.4. The die consists of six components; upper die block, punch holder, punch, fixed stripper, lower die and lower die block. The upper die block, punch holder, fixed stripper and lower die block was made of St 37 steel whereas the guide rods on the upper die block, punch and lower die was made of heat treated AISI 4140 for long durability.

The second die set was specially designed for blanking at high punch speeds. The die also houses a holder for the gun and designed with the purpose of being much mobile as possible. This die consists of 10 components, mount piece for the nail gun, upper block that can move vertically, 4 shafts to enable the moving of blocks, a punch case to prevent the mechanical damage to the punch that is caused by the explosion force of the nail gun, 4 plain ball cage bushes to conduct the movement of middle block caused by the explosion of the gun with minimum friction, the punch, the middle block that holds the punch and punch case, stripper, the lower die and lower die block . The exploded illustration of the second die set was given in Figure 4.5.

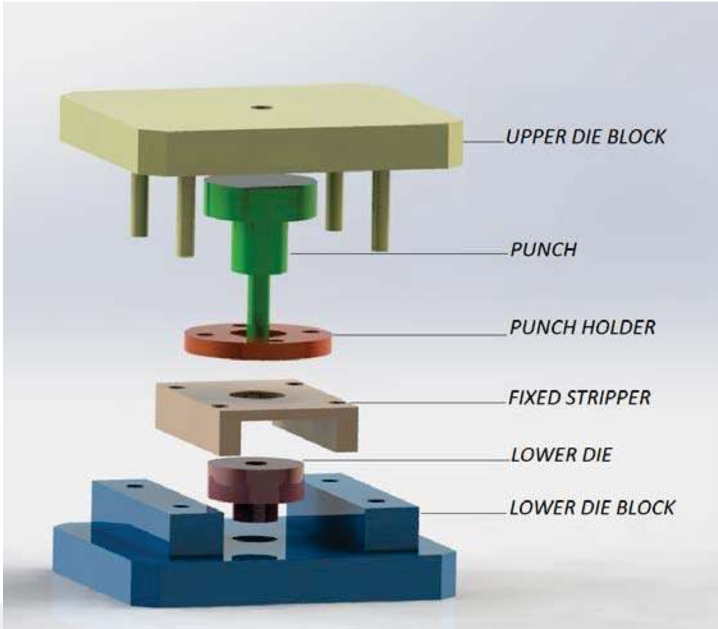

Figure 4.4. The exploded view of the first die used for experiments at low and moderate speeds

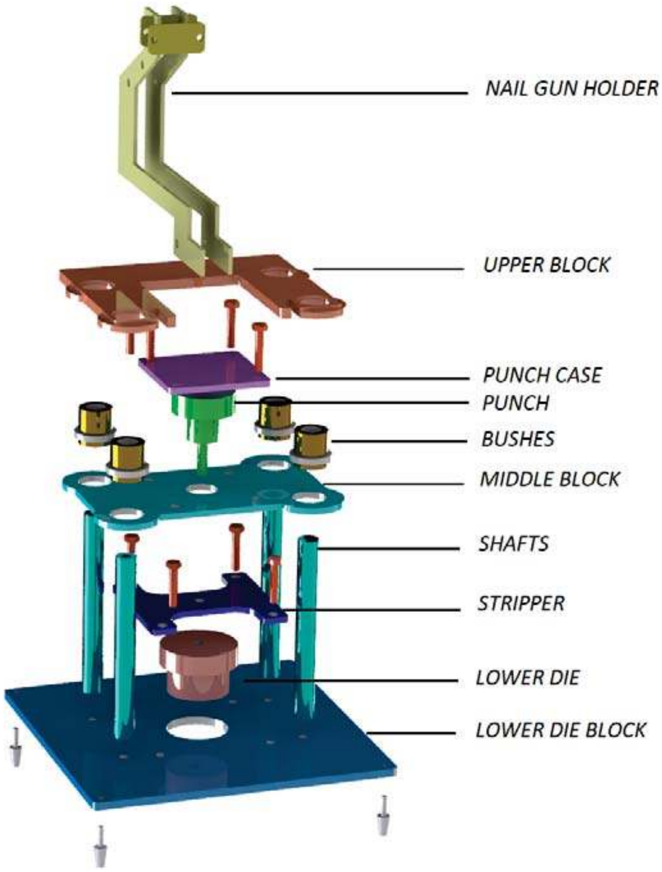

Figure 4.5. The exploded view of the second die used for experiments at high speeds

4.3. Punches

Punches hold a crucial point in the process of blanking. A punch should resist the force exerted on it and should maintain its stability and rigidity. Also the wear resistance should be high due to the friction forces created between the punch, workpiece and lower die. To meet the condition, punches used for the experiments were manufactured from AISI 4140 steel because this type of alloy steel offers a good balance of strength, toughness and wear resistance. Manufactured punches then heat treated with the purpose of retarding the wear and possible crack occurrence at the sides.

The manufacturing of the punches and determination of their dimensions needed to be done according to the predetermined process parameters. Three distinct parameters were mandatory for designating the dimensions; five different clearances (1%, 3%, 5%, 10% and 20%), four different thickness to die diameter ratios (t/D_m=1/5, t/D_m=1/10, t/D_m=1/30, t/D_m=1/50) and three thicknesses (t=2 mm, t=3 mm and t=4 mm).

Due to the variations between these parameters, the necessary number of manufacturing reached to the amount of 70 different punches and 12 different lower dies. Apart from the enormous cost it would bring, if so much production had been done, there would have been no need for simulations. Because of these reasons, certain amounts of sets were manufactured to compare the results of experimental study with the results of simulation study.

After the justification of the parameters and similar results had been achieved between the experimental and simulation results, the remaining experiments were executed under virtual environment and results were taken directly from the simulations accomplished. Two of the manufactured die sets for five different clearances and for t=2 mm; (a) set for ratio t/D_m=1/5; (b) set for ratio t/D_m=1/10 which were used in the experiments were given as an example in Figure 4.6.

(a)

(b)

Figure 4.6. Manufactured die sets for (a) ratio t/D_m=1/5; (b) ratio t/D_m=1/10

4.4. Workpiece Material

AISI 304 stainless steel was used as the workpiece material. AISI 304 is a common type of stainless steel used in several kinds of industrial applications like in the production of equipment for food processing, surgical and operational equipment for health sector, home applications like kitchen sinks and kitchen apparatus, various fasteners, fittings, filters and many equipment working under corrosive and pressurized environment; paper, automotive, marine, oil and nuclear applications [58]. This diverse use makes AISI 304 a material to be further investigated under different production conditions and applications.

The chemical composition of AISI 304 was given in Table 4.1. Mechanical and physical properties were given in Table 4.2 and in Table 4.3.

Table 4.1. Chemical composition of AISI 304 stainless steel

	C	Mn	Si	P	S	Cr	Mo	Ni	N
Minimum	-	-	-	-	-	18.0	-	8.0	-
Maximum	0.08	2.0	0.75	0.045	0.030	20.0	-	10.5	0.10

Table 4.2. Mechanical properties of AISI 304 stainless steel

Min. Tensile Strength (Mpa)	Min. Yield Strength (0.2% Proof) (Mpa)	Min.Elongation (% in 50 mm)	Hardness	
			Rockwell B (HR B)	Brinell (HB)
515	205	40	92	201

Table 4.3. Physical properties of AISI 304 stainless steel

Density (kg/m^3)	Modulus of Elasticity (GPa)	Coefficient of Thermal Expansion ($mm/m/^oC$)			Thermal Expansion (w/m.K)	Specific Heat (J/kg.K)
		0-100 ^oC	0-315 ^oC	0-538 ^oC	100 ^oC-500 ^oC	0-100 ^oC
8000	193	17.2	17.8	18.4	16.2-21.5	500

The sheet materials for all thicknesses were provided in form of 1000x1000 mm sheets and all sheets were cut into smaller strips approximately at the size of 40x200 mm. A prepared sheet strip with 2 mm thicknesses were given in Figure 4.7.

Figure 4.7. AISI 304 sheet metal specimen used for blanking experiments (t= 2 mm)

4.5. Profilometer

Surface roughnesses of the materials were calculated by using a Mitutoyo Surftest SJ-400 model profilometer which is located in Materials Laboratory of Mechanical Engineering at University of Gaziantep.

Arithmetic mean roughness (R_a) was used to determine the surface roughness and was found by taking the average of the values measured from 6 different points of the cut surface of the workpiece including both shear zone and crack zone. The profilometer used for evaluating the surface roughness was given in Figure 4.8.

Figure 4.8. Profilometer used to evaluate surface roughness of the blanks

CHAPTER 5

THE SIMULATION ENVIRONMENT

Investigations of blanking process with experimental approaches require a serious amount of investments, tooling and time. In many industrial applications, the path to achieve the best outcomes for the desired products often rely on time, labor and money consuming trial and error procedures. The failed attempts have little comebacks in terms of material recycling or re-usage.

As an alternative approach, FEM (**F**inite **E**lement **M**ethod) which can simply be identified as the modelling of the experimental setup in a virtual environment offers many advantages over experimental tries. The first and utmost importance of FEM is the investment for the system which can easily be neglected when compared to the investment made on a single experimental setup. The second important advantage is the variations and different aspects of parameters can be examined one by one or all together to observe if the required achievements or adjustments are accomplished. Also detailed investigations of blanking process can be made including the distribution of temperature, effective stress, effective strain rate and etc. in the shear zone which are literally so difficult to be observed at that shearing moment in an experimental environment. The third advantage is the speed and mobility of the FEM simulations. Preparations can be made and results can be gathered in no time compared to the experimental studies that can only be done after a long and precise manufacturing of the sets and other parts, assembling and preparing the system then executing the process and gathering results (if no flaws happen in any of the steps). The only minor disadvantage of a FEM simulation is the justification and the equalization of the results with actual known ones to compare if the virtual environment is compatible with the experimental one.

.

5.1. Software and Model

The program chosen to create the blanking environment and execute the runs was "Deform". The program is a product of **S**cientific **F**orming **T**echnologies **C**orporation (STFC) and mainly used to model forming and forging operations like blanking, close-open die forging, rolling, drawing, compaction and etc. The code that the program uses is based on an implicit Lagrangian routine of computation. The identification of the program is done axisymmetric and whole system is identified on a 2D plane. This means that identification of half of the setup is sufficient to run the simulations [59].

The half of the model can be seen in Figure 5.1. The model consists of four parts; the punch, workpiece, a blank holder and a lower die. The blank diameter of the lower die and punches were modeled separately according to the predetermined dimensional parameters including the clearance (1%, 3%, 5%, 10% and 20%), workpiece thickness (t=2 mm, t=3 mm and t=4 mm) and thickness to die diameter ratios (t/D_m=1/5, t/D_m=1/10, t/D_m=1/30, t/D_m=1/50).

Firstly, to observe the effect of thickness alone under different clearances, no ratios have been taken into consideration. A lower die with 10 mm diameter and matching dies for 5 clearances and 3 thicknesses were modeled and also manufactured separately.

Then, modelling of the sets was continued including thickness to die diameter ratios. The hole dimension of lower die for each parameter were kept constant in itself and mainly punch diameters were changed. The total number of lower dies to be modeled was 12 and the number of punches was 70. Simulations were executed for each condition and also including different punch speeds (0.1m/s, 1m/s, 10m/s). A total of 210 runs were done to cover all the conditions.

The dimensions of the sets according to the thickness to die diameter ratios were given in Table 5.1. The dimensions of the punches and lower die with 10 mm diameter were given in Table 5.2.

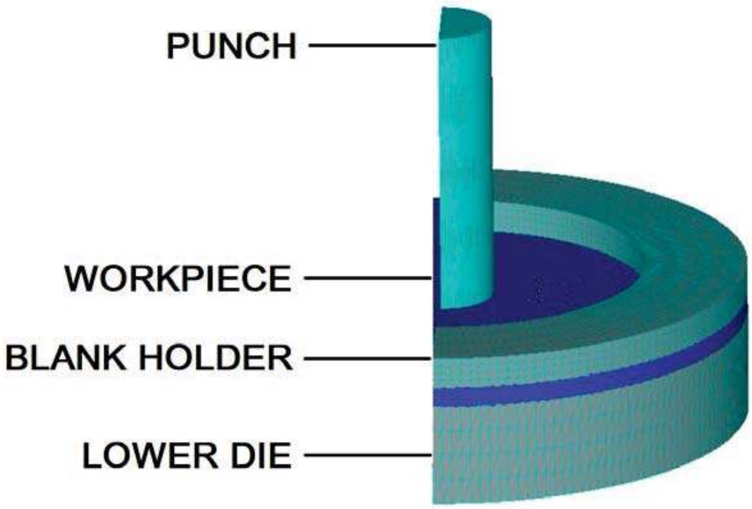

Figure 5.1. The half of the blanking setup identified to the program

Table 5.1. Dimensions of sets including thickness to die diameter ratio

	C	Ratio 1/5 (D_m=10 mm)	Ratio 1/10 (D_m=20 mm)	Ratio 1/30 (D_m=60 mm)	Ratio 1/50 (D_m=100 mm)
t=2mm	1 %	9.96	19.96	59.96	99.96
	3 %	9.88	19.88	59.88	99.88
	5 %	9.80	19.80	59.80	99.80
	10 %	9.60	19.60	59.60	99.60
	20 %	9.20	19.20	59.20	99.20
	C	(D_m=15 mm)	(D_m=30 mm)	(D_m=90 mm)	(D_m=150 mm)
t=3mm	1 %	14.94	29.94	89.94	149.94
	3 %	14.82	29.82	89.82	149.82
	5 %	14.70	29.70	89.70	149.70
	10 %	14.40	29.40	89.40	149.40
	20 %	13.80	28.80	88.80	148.80
	C	(D_m=20 mm)	(D_m=40 mm)	(D_m=120 mm)	(D_m=200 mm)
t=4mm	1 %	19.92	39.92	119.92	199.92
	3 %	19.76	39.76	119.76	199.76
	5 %	19.60	39.60	119.60	199.60
	10 %	19.20	39.20	119.20	199.20
	20 %	18.40	38.40	118.40	198.40

Table 5.2. Dimensions of punches according to thicknesses and fixed die

	C	t= 2 mm	t= 3 mm	t= 4 mm
	1 %	9.96	9.94	9.92
	3 %	9.88	9.82	9.76
D_m=10 mm	5 %	9.80	9.70	9.60
	10 %	9.60	9.40	9.20
	20 %	9.20	8.80	8.40

The workpiece was considered as a plastic object whereas the punch, blank holder and the lower die as non-deformable rigid bodies. 10000 isoparametric quadratic elements which are the maximum definable mesh element number in the program, with 0.03 mm element size were used as the element meshes of the workpiece. Meshes had to be concentrated around the deformation zone for the calculations and visualizations to be precise. The densities of the meshes were concentrated along the area where shear occurs between the cutting corners of the punch and lower die by using equally spaced mesh windows. Mesh windows have the function to hold the mesh density close to a given value which was identified as 1/20 which means that the mesh count was 20 times more in the boundaries of the windows than the other areas on the workpiece. During the course of the punch movement, mesh density windows move within the direction of the punch and discretize the element number of meshes in a specified limit inside the boundaries of the windows. The 2D identification of the blanking setup and its components were given in Figure 5.2.

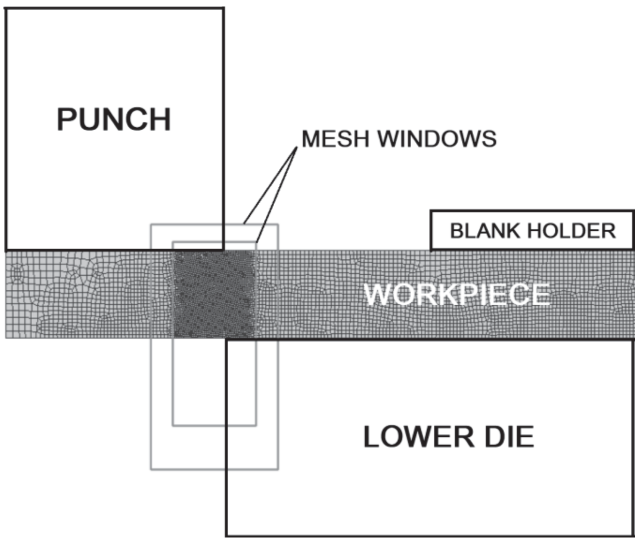

Figure 5.2. The 2D identification of the setup and its components

The presence of constant shear friction was assumed to take place between the workpiece and tools which was expressed in Equation 5.1 as;

$$f_s = mk \quad , \tag{5.1}$$

where f_s is the frictional stress, k is the shear yield stress and m is the friction factor. The formula puts forward that on a deforming body, the occurrence of the friction is directly a function of the yield stress.

Yielding is major event in blanking and yielding happens due to the large plastic strain generated in the narrow shear band. There are many yield criterions to presume the condition. For this study the material was assumed isotropic and Von Mises yield criterion was chosen to calculate the yielding occurrence expressed in Equation 5.2 as;

$$\bar{\sigma} = K\bar{\varepsilon}^n \quad , \tag{5.2}$$

where $\bar{\sigma}$ is the effective stress, $\bar{\varepsilon}$ is the effective strain, K is the material constant, and n is the strain- hardening exponent [60].

The fracture criterion was chosen as Normalized Cockroft and Latham. The criterion is expressed in Equation 5.3 as;

$$\int_0^{\varepsilon^{-f}} \left(\frac{\sigma^*}{\bar{\sigma}} \right) d\bar{\varepsilon} = C \quad , \tag{5.3}$$

where σ^* is the maximum principal tensile stress, ε^{-f} the fracture strain and C is the critical value. $\bar{\sigma}$ indicates the effective stress and $\bar{\varepsilon}$ indicates effective strain. Fracture initiation is determined by the critical value C and is free from the effects of working operation and can be found by performing a tensile test. The critical value for AISI 304 was found before the execution of the simulation and experimental tests. The found and identified value of C into program is 0.534. During the blanking process, it is already mentioned about the narrow shear band generated on the workpiece where the shearing occurs. The deformation gets severely concentrated at the shear band. The ratio between maximum principal stress and effective stress $\left(\frac{\sigma^*}{\bar{\sigma}}\right)$ are assumed to be constant. This assumption leads to the implementation of this constant into the Cockroft and Latham criterion. The approximation becomes $\varepsilon^{-f} = C*$ at the shear band and states that the initiation of the crack happens when the effective strain reaches and becomes equal with the fracture strain of the work material [20].

The progress of the blanking visualization was based on element deletion method which means that when the predetermined critical values are reached in the deformation zone, simulation stops and the program performs element deletion. Program deletes the elements permanently that reach the critical values and this action is governed by two parameters; "fracture steps" and "fracture elements". Fracture steps value determines the step interval where the simulation stops and performs element deletion. This value was chosen as '1'. That means that in every step, program stops and check the elements if they surpass the critical values or not. If so, the element deletion takes place, if not program continues to the next step. Fracture elements are the number of the elements that must be above the critical damage value for the simulation to stop and perform element deletion. This value was chosen as '4'. Too much or too low values cause visualization and also calculation flaws. After many precise comparisons between modelling and experimental work, the best value to match was found 4 and used for all simulation studies.

The calculation of heat occurrence and heat transfer is always a tough achievement in a blanking process where the generation and dissipation happens in milliseconds. The design of an experimental setup for observing this event is seriously a difficult one because of the place that the shearing happens where no probe, socket or any other detection device can be placed. Studies mainly rely on the experimental surface roughness comparisons or uses simulation results to see the effect of heat generation especially if the blanking process is executed under high punch speeds. Deform program has the ability to calculate and visualize the distribution of the temperature among with the other parameters like effective stress, effective strain and effective strain etc. Distributions of temperature during the shearing of a workpiece in bar style (a) and in line style (b) were given in Figure 5.3.

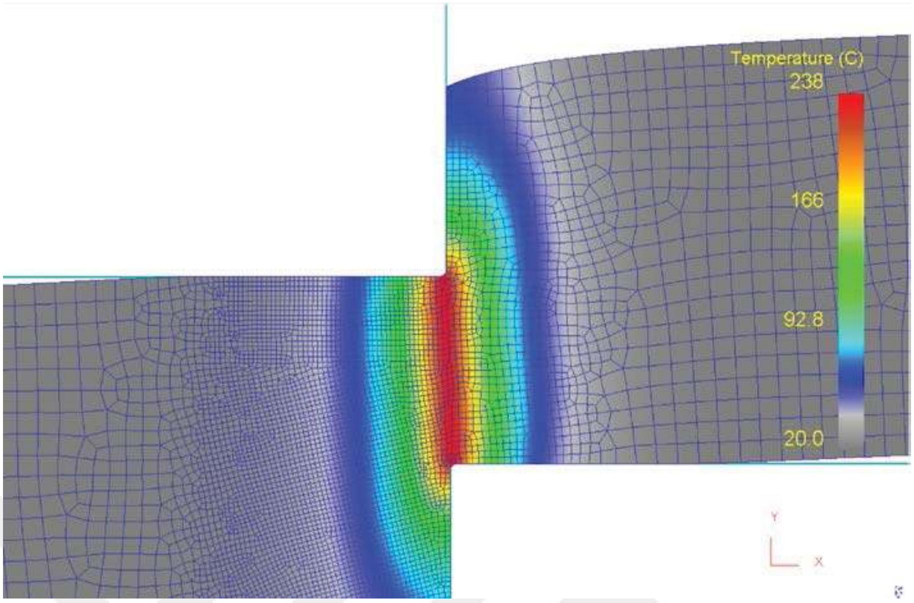

(a)

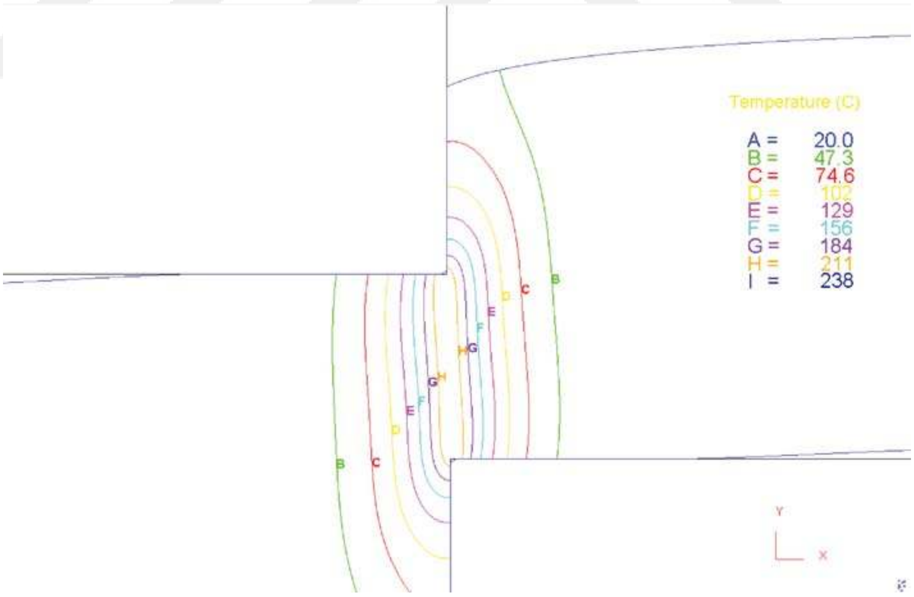

(b)

Figure 5.3. Temperature distribution (a) in bar style and (b) in line style

CHAPTER 6

RESULTS AND DISCUSSION

6.1. Validation of The Results

When performing experimental and FEM studies in synchronization with each other or to use simulation results to observe specific parts of the process with more detail which cannot be done by experimental methods, there rises the problem of "result validation". Validation is the most problematic part when extracting the results from the executed simulations because there occurs a big uncertainty about the values whether they are correct or not, as mentioned in the previous chapter. Reaching to conclusions without strong proof provided from some well-known results or experimental studies have a potential to lead to irremediable faults.

To eliminate the probable instability between experimental and numerical work in this study, the validation of the results was the first action taken before proceeding forward. The first step of validation in blanking is the comparison of cutting load-stroke depth diagrams of experiment and simulation results. To achieve the best results, the deformation information of the material should be defined correctly into the program for modelling work and the exact same material should be chosen for the experimental work. The deformation behavior of the material is represented by the flow stress chart and the charts for AISI 304 under different strain rates (a) and temperatures (b) were given in Figure 6.1.

The validation work was accomplished at room temperature (20 ^{0}C) by using a workpiece with 2 mm thickness and under the punch speed of 0.1 m/s. Five different clearances (1%, 3%, 5%, 10% and 20%), and two thickness to die diameter ratios (t/D_m=1/5, t/D_m=1/10) were used to observe the value differences between experimental and numerical results.

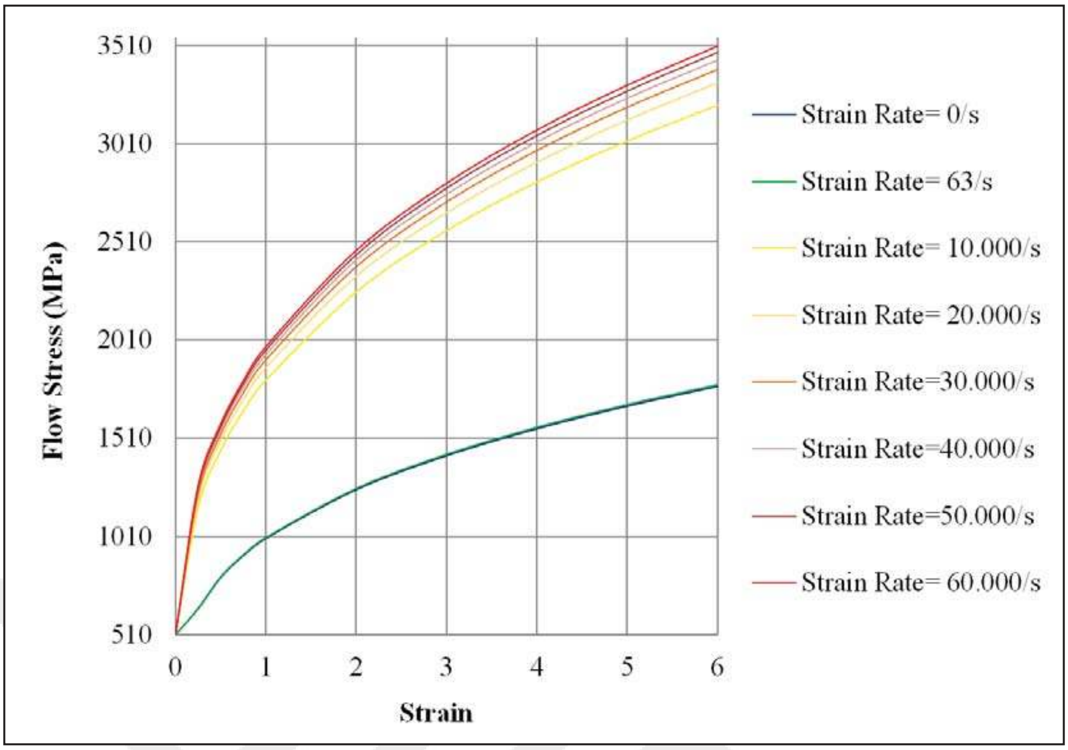

(a)

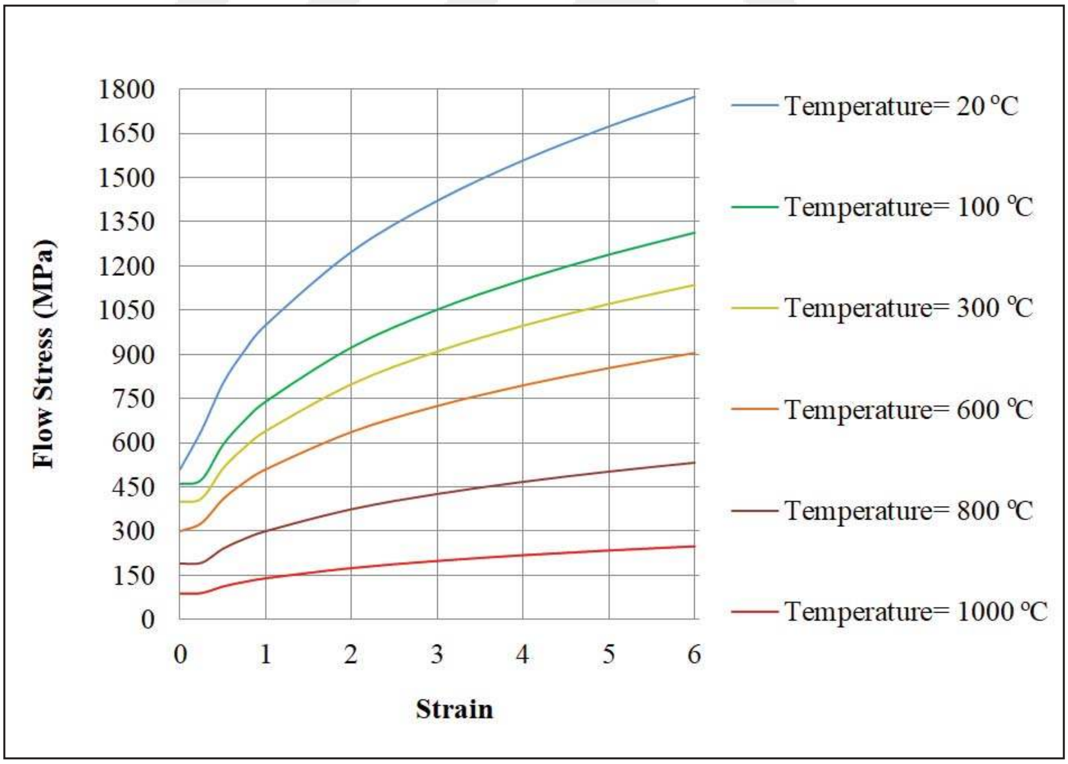

(b)

Figure 6.1. Flow stress change of AISI 304 according to (a) strain rate and (b) temperature [61]

It was observed that cutting load-stroke depth diagrams had very similar results after many tests except the experimental results had slightly higher values than the numerical ones. These slight discrepancies between the values are the result of conditions between real and virtual environment. The environmental effects like vibration, dirt, unforeseen frictions or movements between tools and margin of error of the load cell located in the press change the outcomes slightly during the experimental studies. These external effects are none present in the virtual environment and the modelling was considered to be executed under perfect conditions. The difference between experimental and numerical result was given in Figure 6.2 for 5% clearance and t/D_m=1/5 under the punch speed of 0.1 m/s as an example.

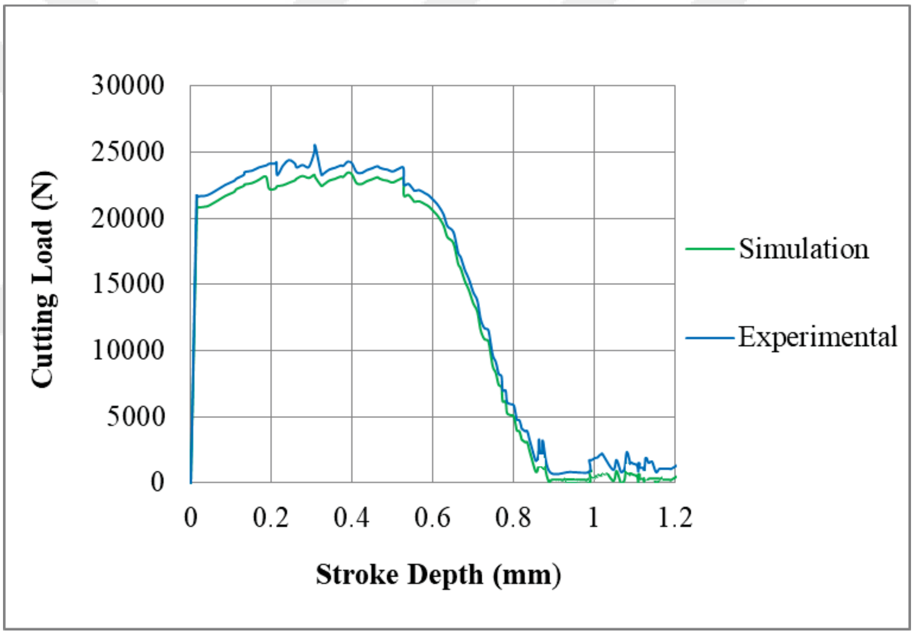

Figure 6.2. Cutting load change between simulation and experimental results

The justification of cutting load-stroke depth diagram similarities stated that the numerical outcomes for different variations could be successfully modelled and the extracted results would be so close to experimental ones. However, this was the first step of the total validation process as fore stated. Numerical data is a crucial part when modelling a blanking process but surface quality of the sheared edge is also so important. The visualization of crack propagation and zone distributions should also be consistent between numerical and experimental studies which constitutes the second part of the validation step.

The second validation step was accomplished by comparing the workpiece's lateral cut edge with the image gathered from the Deform program. From the point of experimental side; the sheared workpiece was cut into two with a thin, precise automated saw. The inner part of the workpieces then polished and examined under a microscope.

On the modelling side, the concentrated meshes by using mesh windows which were mentioned in the previous chapter provided the opportunity to observe the surface with more detail. 10.000 mesh elements were compressed at the shearing zone with a ratio of 1 to 20 (20 times more than the other sections of the workpiece) which resulted in the formation of a very concentrated area with very tiny elements. As a result, the distribution of the zones and the crack directions were observed to be consistent between simulation and experimental results. An example of the comparison of zones for t= 2 mm thickness under 5% clearance and t/D_m=1/10 was given in Figure 6.3.

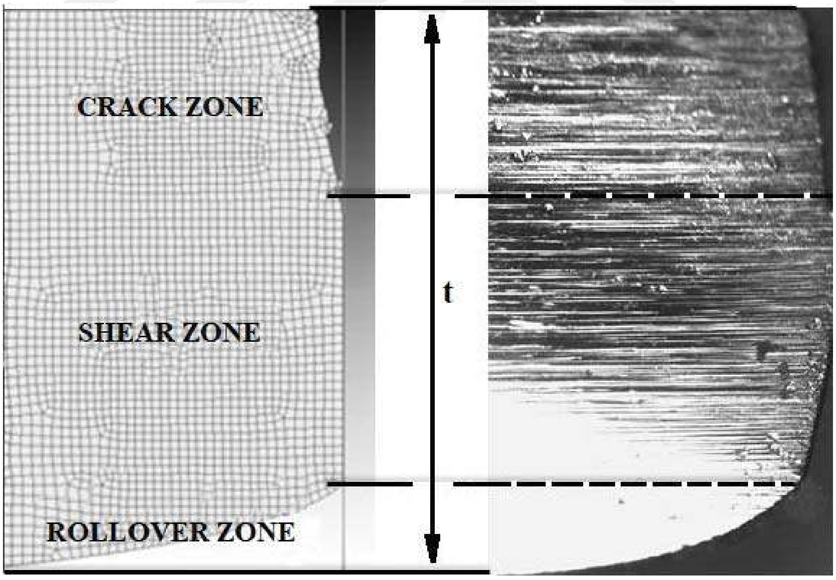

Figure 6.3. Visual consistency between simulation and experimental results

After the completion of result validation, the remaining FEM executions were completed while doing the experimental studies at the same time. The observed outcome results with respect to input parameters were given below.

6.2. Cutting Load and Cutting Energy

Cutting load is the required load to separate the workpiece from the stock and one of the most dominant outcome parameter accepted by the literature. Many studies take the values of cutting load as the sole energy saving parameter or the pure efficiency of the system. However, this kind of an approach can be fallacious because there is the existence of cutting energy parameter which takes both cutting load and the depth of punch penetration (stroke depth) into account at the same time. Also cutting energy doesn’t follow a linear value change pattern as cutting load because of its natural determination order that is the ratio of two parameters. This is the main reason that the cutting energy parameter gives more realistic results if the main concern is energy saving. Therefore, the input parameters and their effects on both cutting load and cutting energy should be investigated.

6.2.1. The Effect of Clearance

Clearance and cutting load are so close to each other in terms of influence. A slight change in clearance can alter the load dramatically. The change in cutting load-stroke depths according to five clearances (1%, 3%, 5%, 10% and 20%) were given in Figure 6.4 (t=4 mm, t/D_m=1/5 and punch speed= 0.1 m/s).

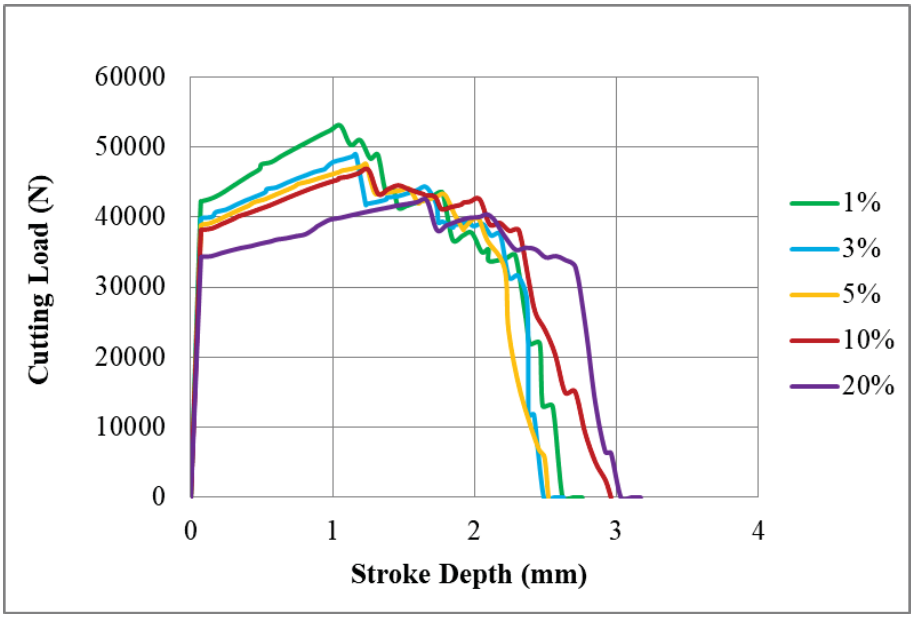

Figure 6.4. Cutting load change according to clearances

As it is evident form Figure 6.4 that clearance has a major effect on the cutting load. The cutting load values where the crack initiations happen decrease with increasing clearances. For instance, there is approximately 20% fall in cutting load between 1% and 20% clearances. The maximum required cutting load for every clearance was depicted in Figure 6.5.

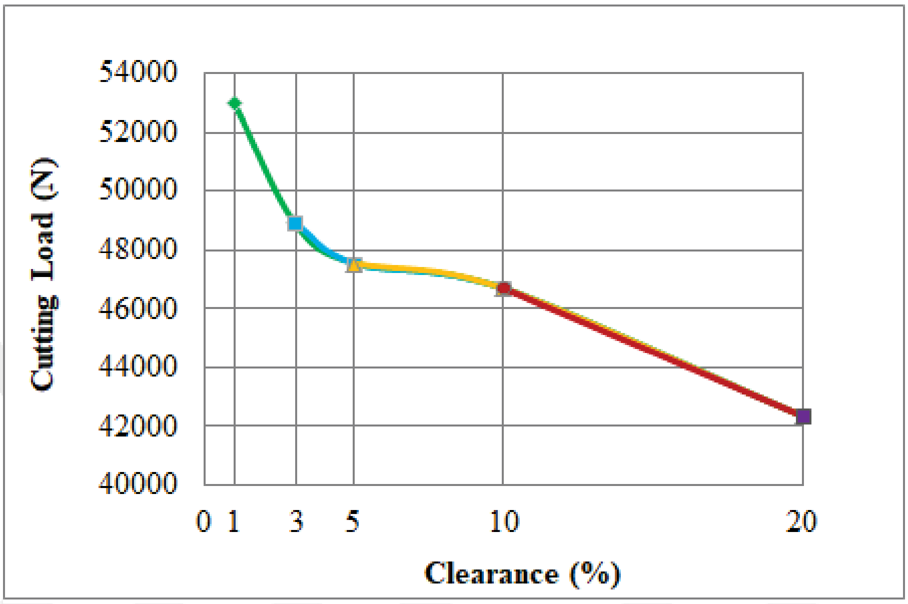

Figure 6.5. Maximum cutting loads and their decreases according to clearances

Decrease in the required cutting load is the result of an increase of the length between the cutting edges of punch and die due to the shrinkage in the diameter of the punch at higher clearances or simply in other words; increase of the gap between two cutting edges due to the clearance. The increase of length allows the punch edge to touch the workpiece from more distance which creates more bending moment and this is the main reason for the reduction in cutting load. However, this reduce in cutting load may be interpreted as usage of higher clearances has more benefits in terms of energy saving but that approach is a deficient one. Tight or loose clearance selections have their own perks but one parameter oriented actions generally result in other outcomes to become much worse. Apart from the cutting load decrease due to the increase in clearance, a closer look to the Figure 6.4 reveals another parameter to be considered and that parameter is the stroke depth.

Stroke depth of the punch is generally a non-visible parameter and doesn't taken into account in many studies of the literature, but has some strong influences on the blanking process especially if energy saving is of concern because of its necessary usage on the designation of cutting energy.

The areas under the cutting load–stroke depth graphs give the values of cutting energies for each clearance. The change in stroke depth can be seen from Figure 6.4. With increasing clearance, penetration depth of the crack initiation shifts to the right slightly. This means that the initiation of the crack formation at high clearances require more punch penetration in contrast to the penetration at lower clearances.

The gap between the cutting edges of punch and die is again the reason of the shift in stroke depth. Due to the increased length, the punch pulls more material into the die cavity and bends the material more before shearing. As a result, the change in the clearance alters the stroke depth; and the change in stroke depth alters the value of the cutting energy.

The benefit of the cutting energy is in the gathering of the values that rely on the ratio between cutting load and stroke depth. The independent changes in these parameters give more realistic insight to the energy consumption of the process. Cutting load may decrease with increasing clearance and follow a linear path but the behavior of the stroke depth doesn't follow a predictable line. So, the cutting energy values can change widely according to the situations of blanking. The changes in maximum cutting energies according to the clearances were given in Figure 6.6 (t=4 mm, t/D_m=1/5 and punch speed= 0.1 m/s).

It can be well observed from Figure 6.5 that the cutting load at 5% clearance is not the lowest. However, cutting load-stroke depth graph given in Figure 6.4 shows that the stroke depth is minimum for 5% clearance. The ratio between two parameters makes 5% clearance the point where lowest energy consumption can be achieved for t= 4 mm and punch speed of 0.1 m/s which was depicted in Figure 6.6.

As a conclusion, it is evident from the found results that clearance has a strong influence on both cutting load and cutting energy. Nevertheless, given results covers only one thickness value which is t= 4 mm. Thickness should also have some influences and was also investigated.

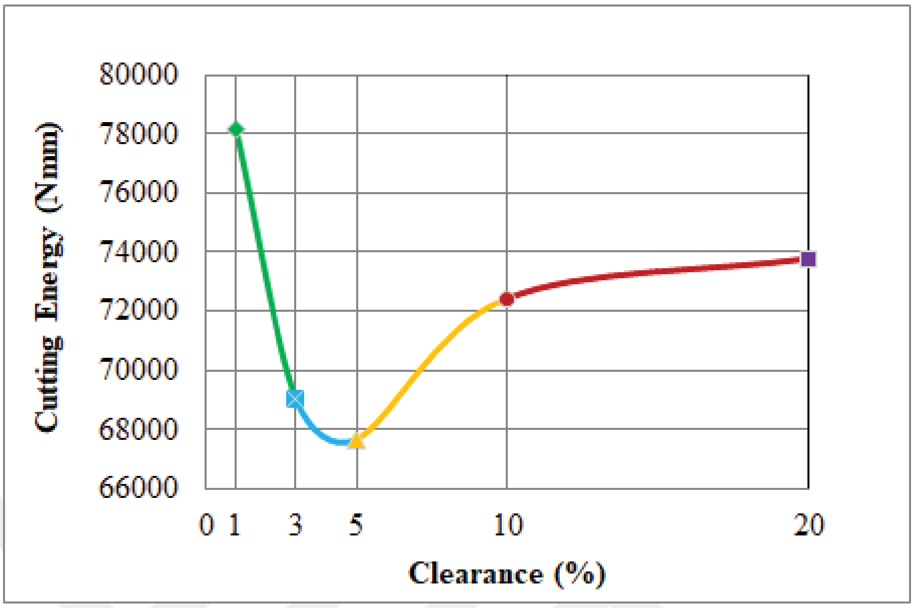

Figure 6.6. Maximum cutting energy changes according to clearances

6.2.2. The Effect of Workpiece Thickness

As mentioned before, three thicknesses were used for blanking AISI 304 workpiece which were t= 2 mm, t= 3 mm and t= 4 mm with the fixed lower die diameter of 10 mm. The punch speed was 0.1 m/s.

Observed changes in cutting loads and cutting energies were given Figure 6.7 and Figure 6.8.

Cutting loads increase with increasing workpiece thicknesses as expected. The behaviors of load changes according to the clearances follow the same path. Cutting loads decrease with increasing clearance but get elevated to higher values due to the effect of thickness.

The change in cutting energy is similar to the results of cutting load. It can be understood that thicker the material gets, higher the cutting load and energy become. The only difference here is the achievement of lowest cutting energy with regard to clearances.

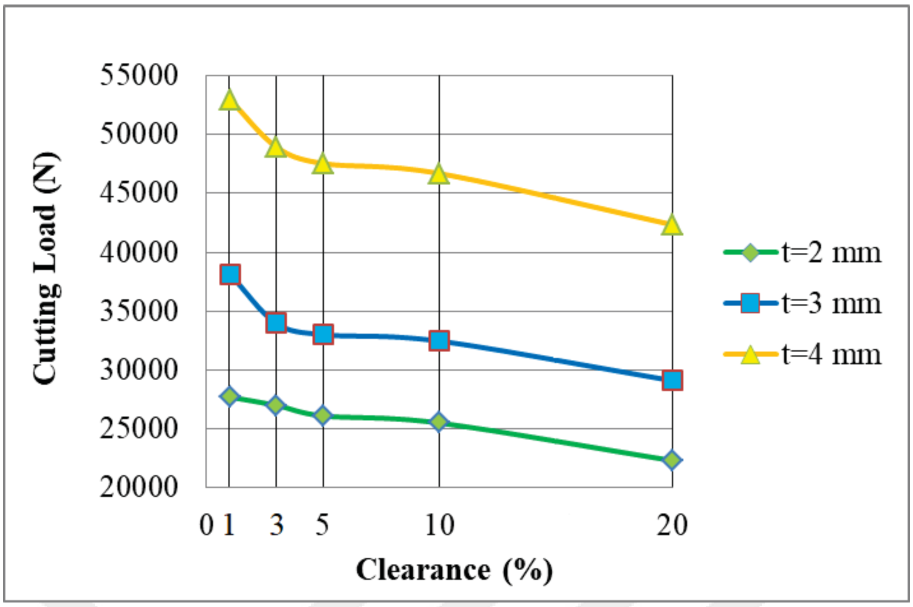

Figure 6.7. Maximum cutting load changes according to thicknesses

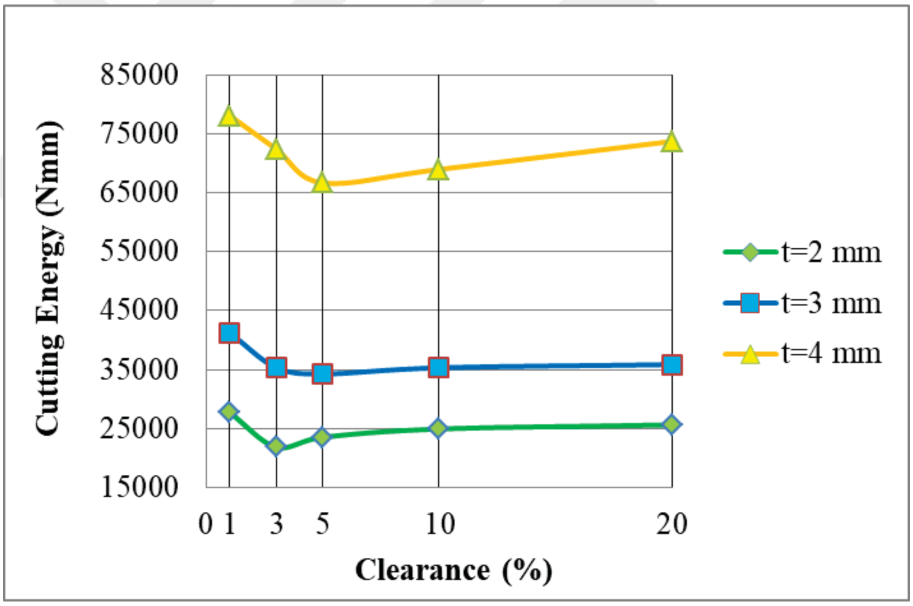

Figure 6.8. Maximum cutting energy changes according to thicknesses

Figure 6.8 shows that thickness has also have influence on the clearance where the lowest energy is achieved. For AISI 304 stainless steel, the ideal clearance to attain the lowest cutting energy is 3% for t= 2 mm and 5% for t= 3 mm and t= 4 mm. The related blanks gathered from experiments were given in Figure 6.9.

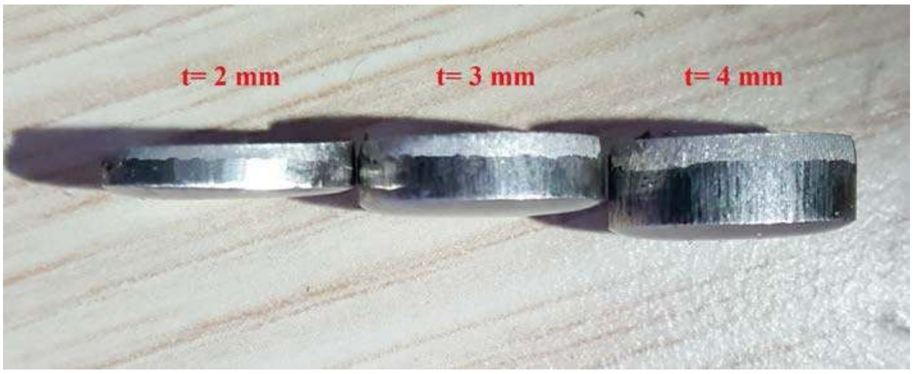

Figure 6.9. Blanked parts from experiments with different thicknesses

6.2.3. The Effect of Thickness to Die Diameter Ratio

Four different thickness to die diameter ratios as; $t/D_m=1/5$, $t/D_m=1/10$, $t/D_m=1/30$ and $t/D_m=1/50$ were studied to observe the effect of thickness to die diameter ratio on cutting load and cutting energy. The thickness was chosen as; t = 2 mm. Punch speed used was 0.1 m/s.

Cutting load-stroke depth differences for a fixed clearance (5%) under different ratios were given in Figure 6.10.

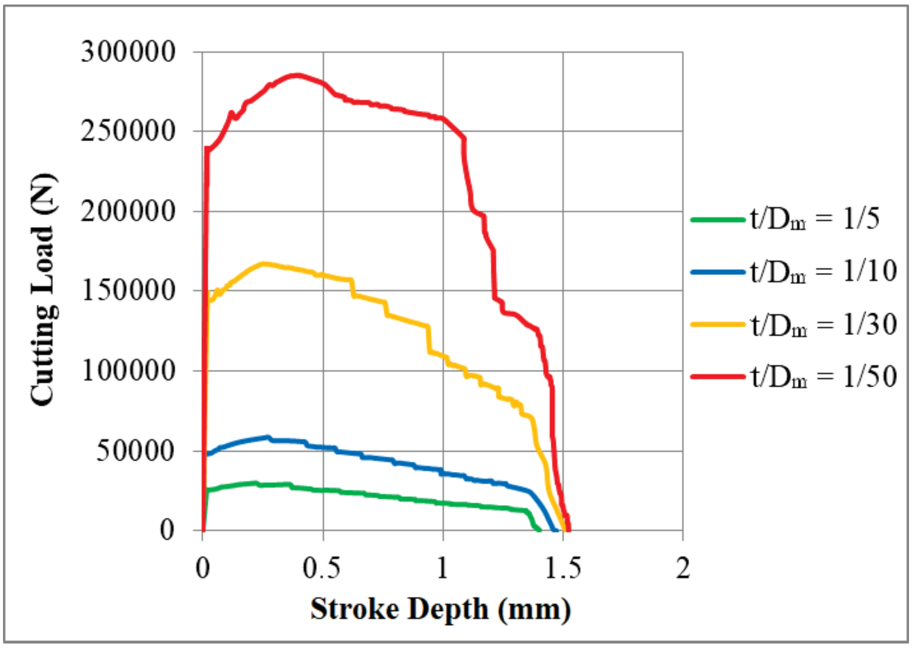

Figure 6.10. Change in cutting load according to t/D_m ratios

The required cutting force to execute the blanking increases with increasing die diameter although the thickness is kept constant. This is an expected result and valid with respect to the Equation 3.1. The related blanks for $t/D_m=1/5$ and $t/D_m=1/10$ gathered from experiments were given in Figure 6.11.

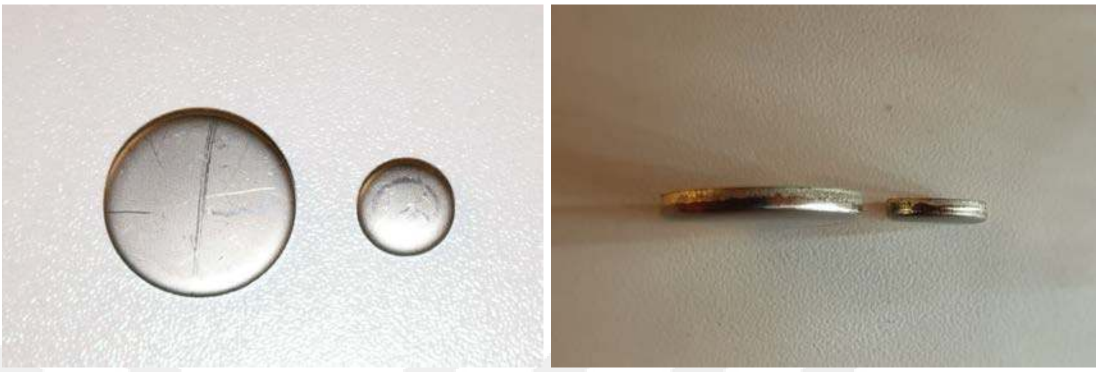

Figure 6.11. Blanked parts with different thickness to die diameter ratios

However, the important part when dealing with thickness to die diameter is the effect of clearance which is absent in the literature and the true deviation of the cutting load.

True deviation of the load emerged from the question that cutting load should increase due to the increase in diameter according to Equation 3.1, but what happens if the cut parameter is neglected? Determination of the effect of thickness to die diameter ratio on the cutting load can be more realistically done if the relative values of cutting load are used. In this context, the values were taken to a base level for comparison by dividing the load values with its specific diameter. The change in cutting load according to clearances and thickness to die diameter ratios were given in Figure 6.12 (a). The relative values of cutting load under same conditions were given in Figure 6.12 (b).

Figure 6.12 (a) and (b) prove that the behavior of the cutting load to increasing clearance shows similarity to the previous results. Cutting load has a tendency to decrease with increasing clearance and this is valid for all ratios and conditions.

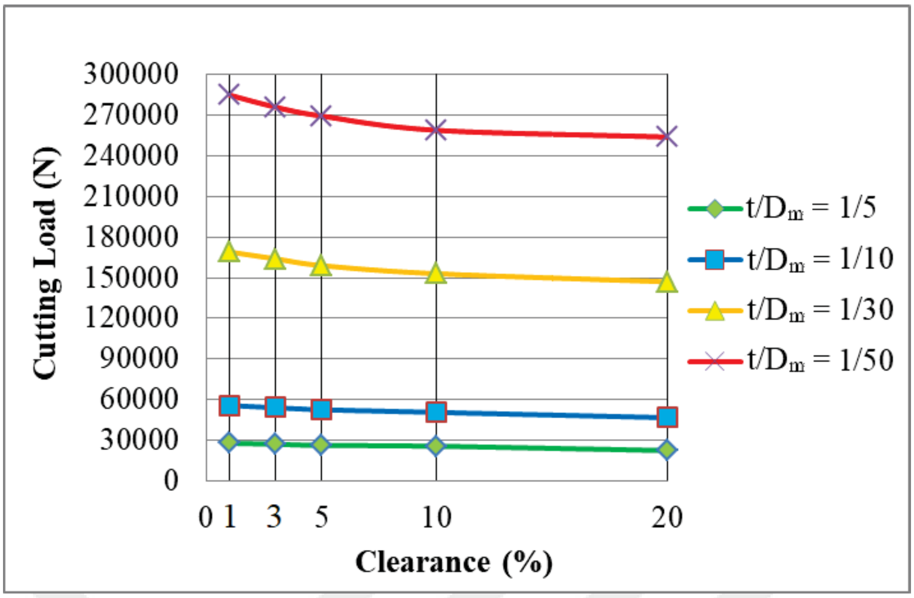

(a)

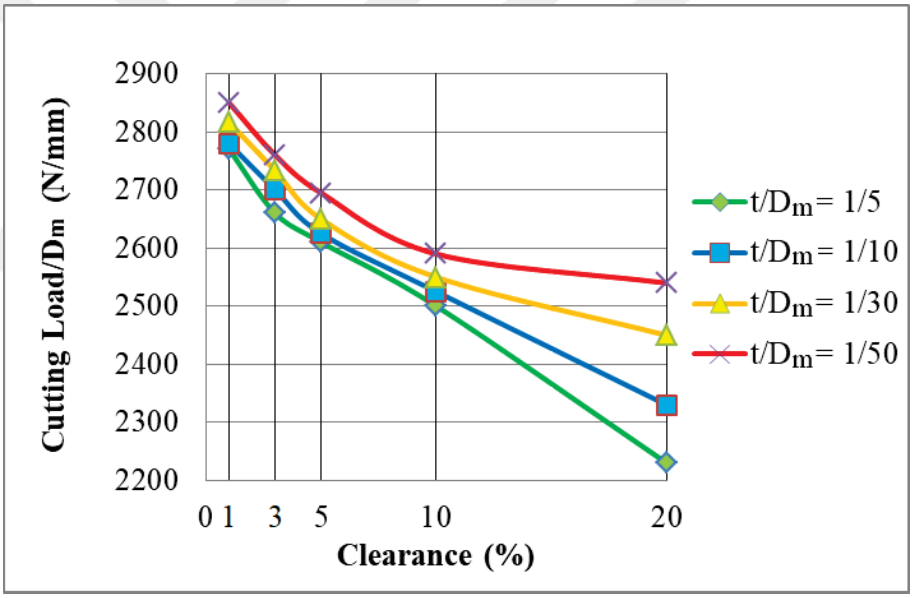

(b)

Figure 6.12. Change in cutting load according to t/D_m ratios; (a) Diameter included, (b) Relative values (Diameter excluded)

According to Equation 3.1, if the diameter is taken away, the determinants become functions of thickness and shear strength of the material. In that case, cutting load value for all t/D_m ratios should be equal. However, Figure 6.12 (b) shows otherwise. The effect of clearance on load is same regardless of diameter absence meaning that increasing clearance causes the cutting load to decrease under every condition. The interesting part is the trend that cutting load followed. The values under different

t/D_m ratios have to be equal but they are not. The values are close to each other but increase with increasing t/D_m ratios and also deviate with increasing clearance. The explanation for this phenomenon lies within the dishing of the material during blanking. Workpiece with a bigger diameter is subjected to more bending than a workpiece with a smaller diameter. This causes the creation of dishing that spreads through the middle section of the workpiece. The separation of the upper section of the workpiece from the punch causes a much narrow contact plane. Lesser contact plane at the edge needs slightly more cutting load to shear the workpiece. This is the physical reason of the rise in cutting load no matter the diameter is included or not, numerically. Illustration of this situation was given for a workpiece with 2 mm thickness in Figure 6.13 (a) for $t/D_m = 1/5$ and in Figure 6.13 (b) $t/D_m = 1/50$.

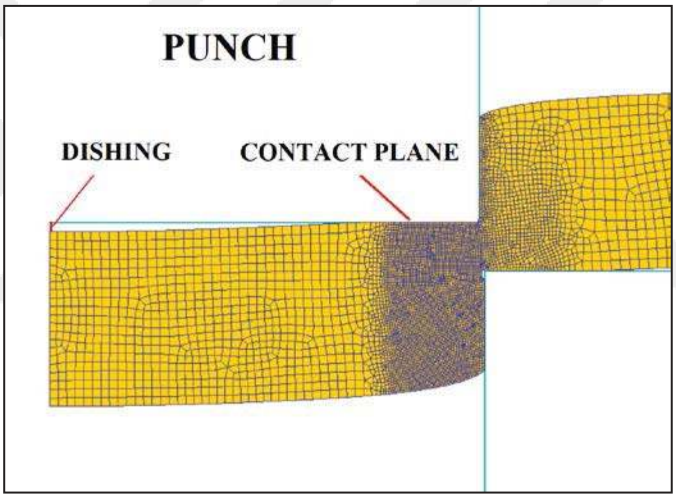

(a)

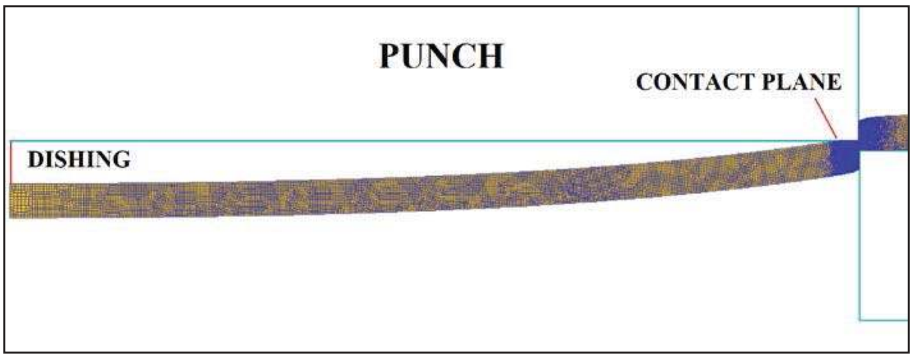

(b)

Figure 6.13. Dishing of the workpiece; (a) $t/D_m = 1/5$, (b) $t/D_m = 1/50$

Again, it should to mentioned that taking cutting load and related clearance value has a high potential to misguide for fully comprehending the situation. So, investigating the cutting energy differences for different ratios becomes essential.

The cutting energy (a) and relative cutting energy (b) change for four different ratios and five different clearances for the blanking of the workpiece with t= 2 mm thickness and under 0.1 m/s were given in Figure 6.14.

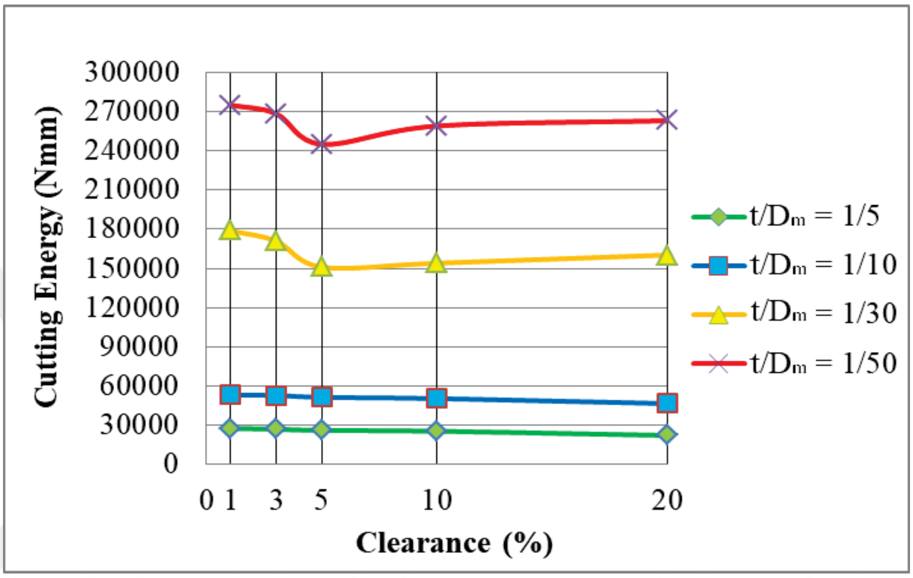

(a)

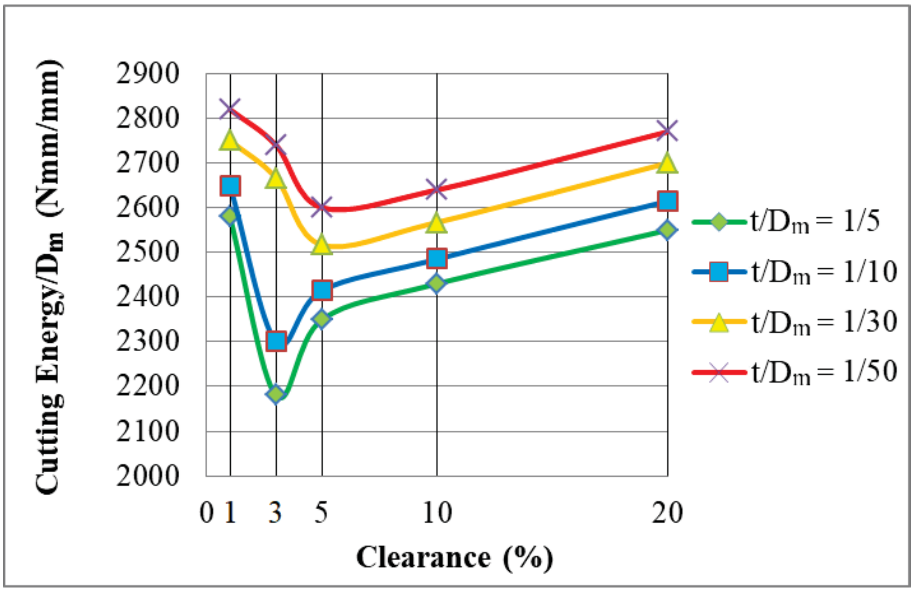

(b)

Figure 6.14. Change in cutting energy according to t/D_m ratios

The increase in thickness to die diameter ratio for the same thickness causes the clearance value to shift with respect to the cutting energies. The lowest cutting energies were achieved at 3% clearance for t/D_m=1/5, and t/D_m=1/10 whereas 5% clearance for t/D_m=1/30 and t/D_m=1/50 ratios. The results are similar for normal and relative conditions because the cutting energy is the ratio of cutting load and stroke depth. The relative values are again different in itself due to the change in cutting load as a result of contact plane difference. On the other hand, the probable reason for the shift of the clearance is related with the crack propagation directions and will be explained in the forthcoming sections.

6.2.4. The Effect of Punch Speed

Punch speed refers to the velocity of punch hence the velocity of cutting. The velocity change alters the strain rate of the workpiece at the shear zone which means that the deformation at the shear zone changes, accordingly. The mechanical behavior of the workpiece to the increased deformation holds a vital point when dealing with high speeds. The effectiveness of the punch speed lies in the balance of strain hardening (work hardening) or the occurrence of adiabatic formation at the shear zone due to the generated heat under high punch speeds which the details were given in previous chapters.

First the cutting load change should be given to fully comprehend the situation and the effect of heat generation. The cutting load-stroke diagrams gathered from simulation results for t= 2 mm workpiece thickness under 10 m/s punch speed by including/excluding the heat generation at the shear zone were given in Figure 6.15.

The strain hardening behavior of the material can easily be seen from Figure 6.15. If no heat generation occurs and no stress relief happens in the shear zone, strain hardening dominates the situation and required stress to initiate the fracture shows an important increase. Also stroke depth of crack initiation and overall cutting energy increases due to the increased area below the curve.

On the other hand if the effect of temperature on the shear zone due to the generation of heat is included, cutting load and the point of crack initiation falls to a lower point, also the cutting energy decreases correspondingly.

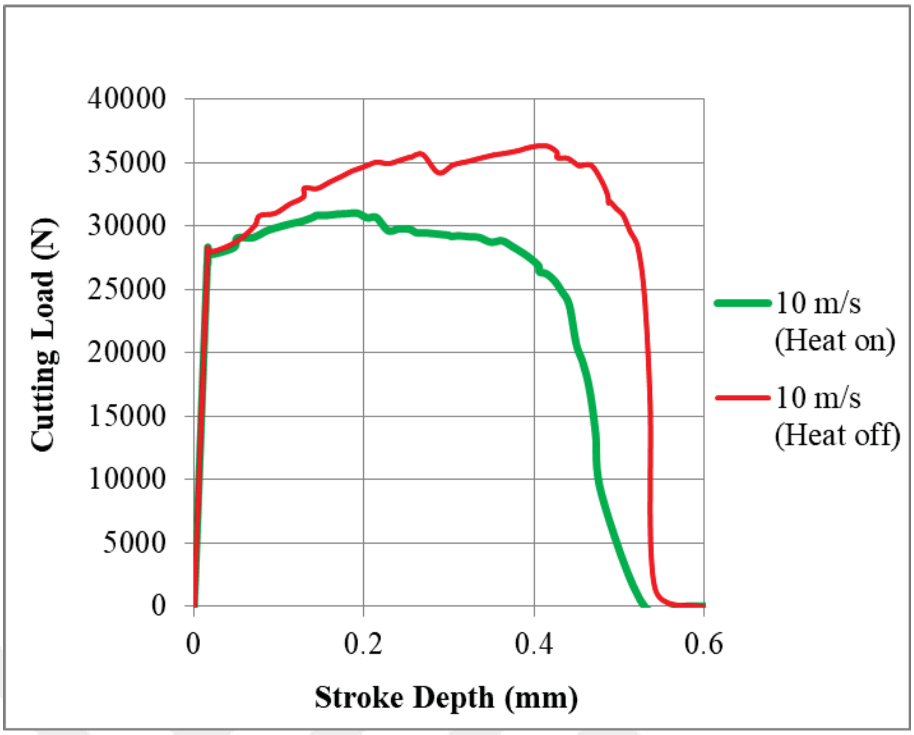

Figure 6.15. Difference between results by including/excluding the heat generation

This means that thermal effects pull the strength (flow stress) of the material to a lower level and the stroke depth of crack initiation happens much quickly.

Whole executions were made by including the thermal effects at the shear zone. The localized temperature escalation at the shear zone is the key point. Workpiece thickness were chosen as t= 2 mm. Three speed values; 0.1 m/s, 1 m/s and 10 m/s were used as the punch speed to execute the processes. The clearance value which was found 3% optimal when t= 2 mm was chosen.

Figure 6.16 and Figure 6.17 shows the temperature and the strain rate distribution at the point of fracture initiation.

Figure 6.18 depicts the change in effective stress whereas Figure 6.19 depicts the change in effective strain under the mentioned conditions and at the exact matching steps.

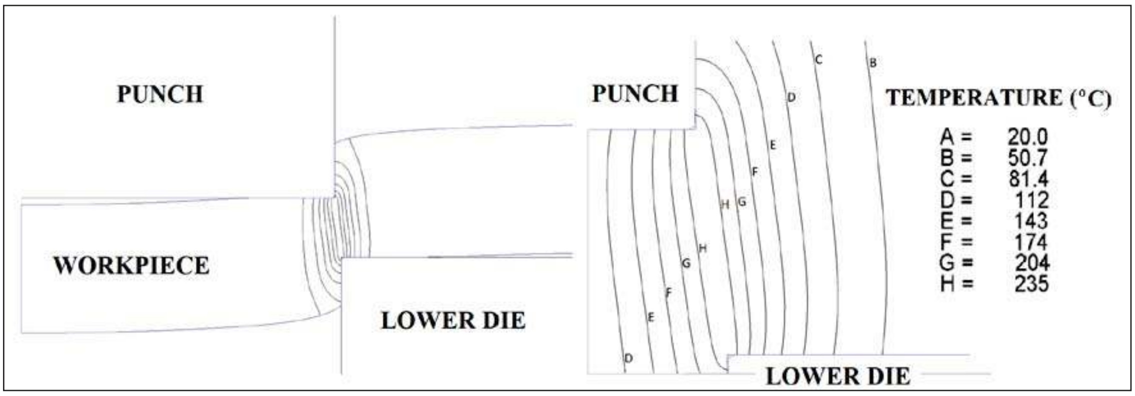

(a)

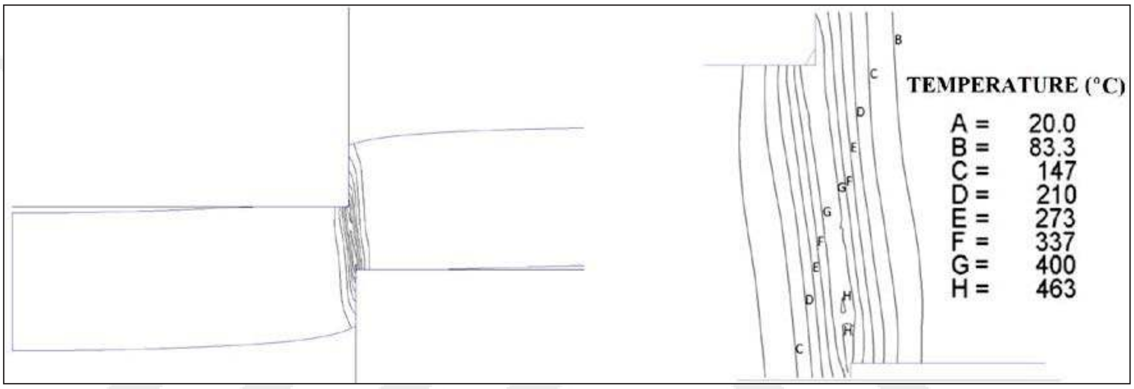

(b)

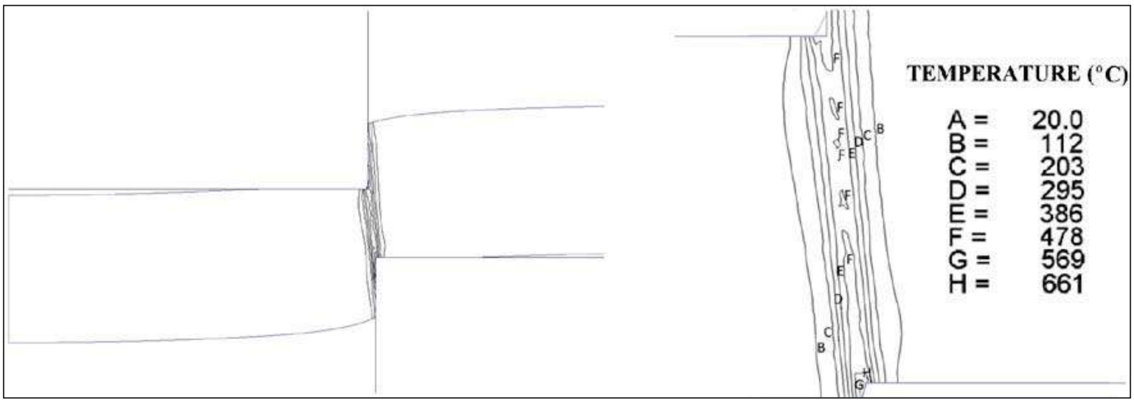

(c)

Figure 6.16. Change in temperature at the shear zone according to different punch speeds; (a) 0.1 m/s, (b) 1 m/s, (c) 10 m/s

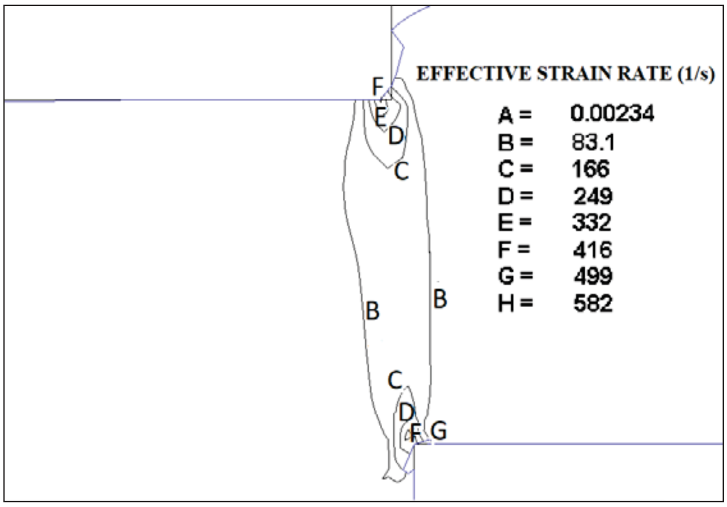

(a)

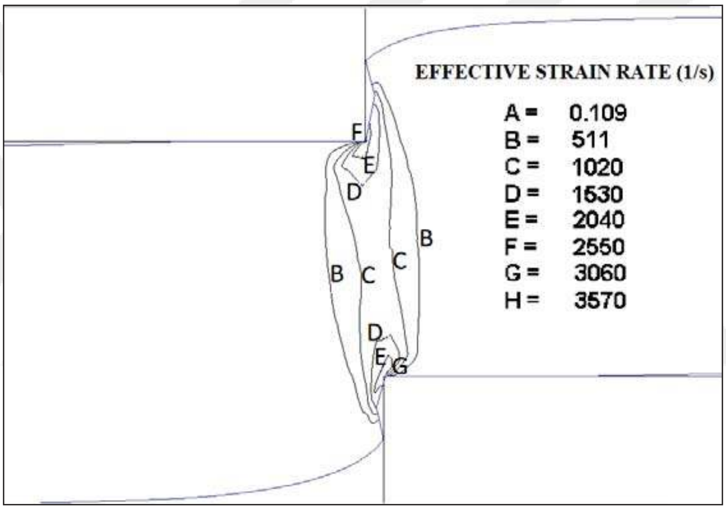

(b)

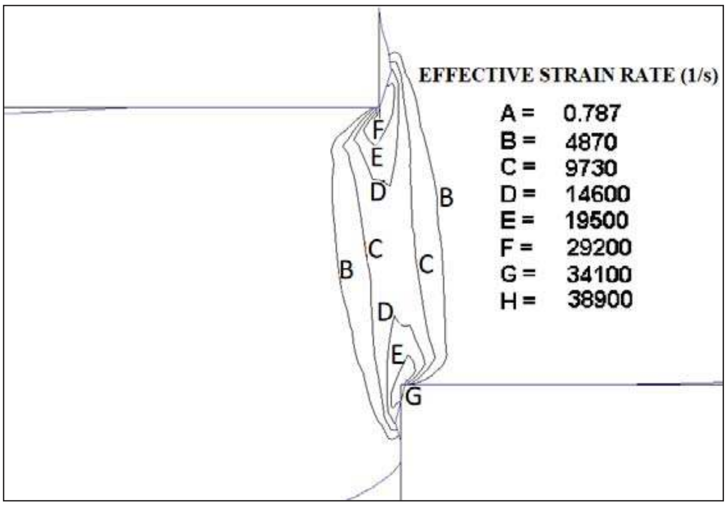

(c)

Figure 6.17. Strain rate change under (a) 0.1 m/s, (b) 1 m/s, (c) 10 m/s punch speed

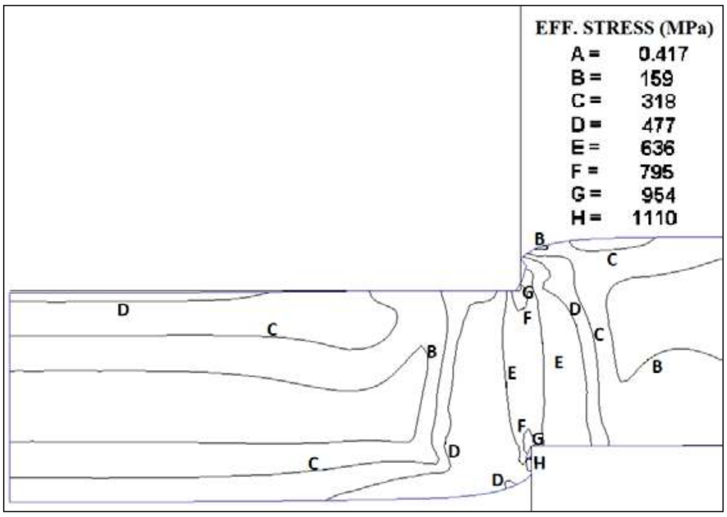

(a)

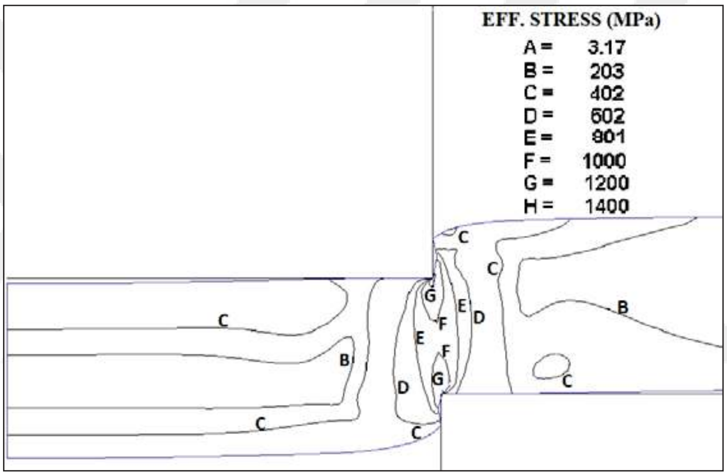

(b)

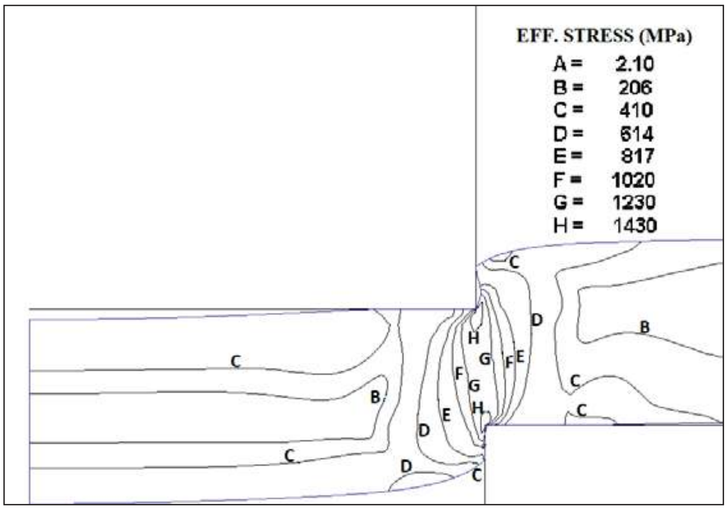

(c)

Figure 6.18. Eff. stress change under (a) 0.1 m/s, (b) 1 m/s, (c) 10 m/s punch speed

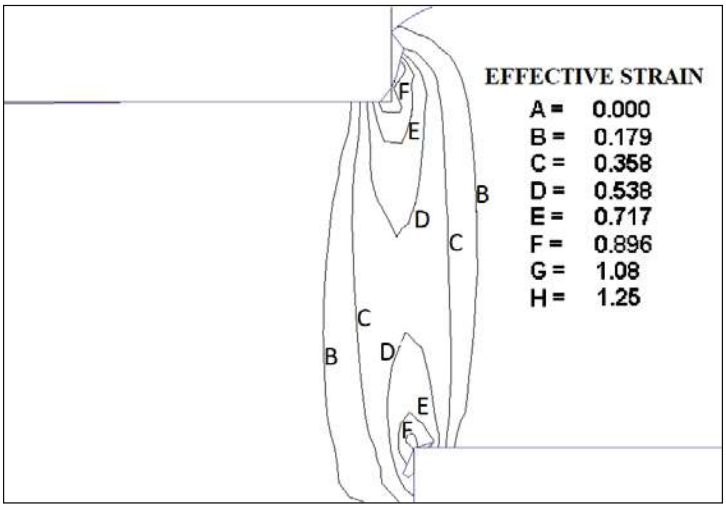

(a)

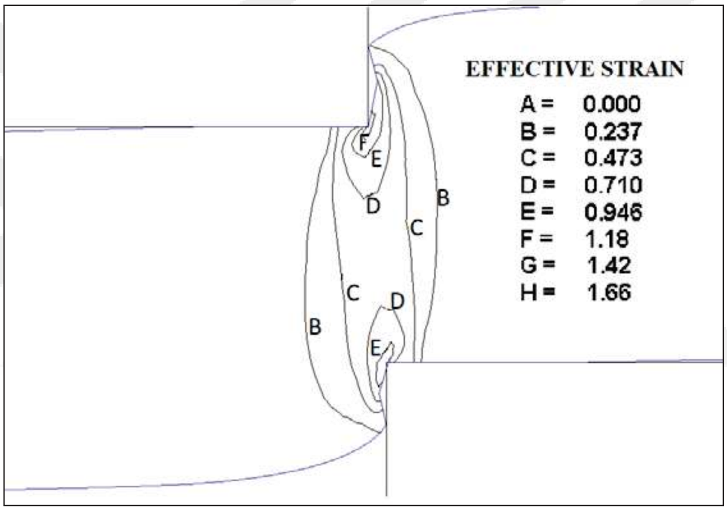

(b)

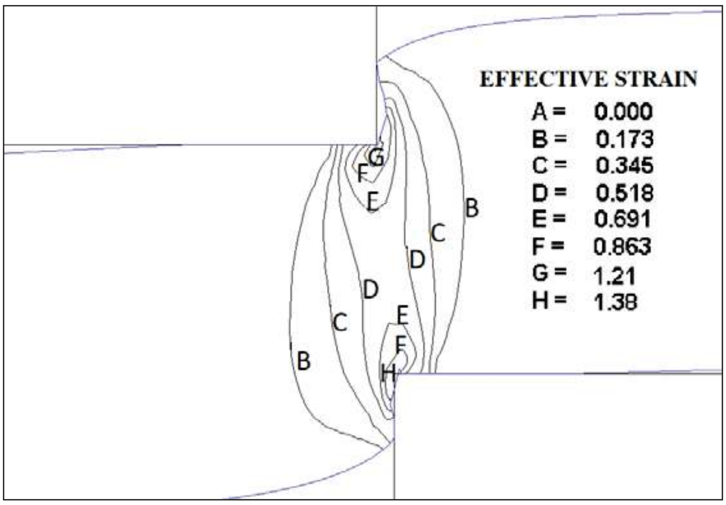

(c)

Figure 6.19. Eff. strain change under (a) 0.1 m/s, (b) 1 m/s, (c) 10 m/s punch speed

It is evident from Figure 6.16 that a difference of about 426 °C is present between 0.1 m/s and 10 m/s, as a result of the increase in punch speed. The generated heat is trapped in an area that gradually narrows directly proportional with increasing speed. Dixon and Parry [41] demonstrated that in compression test using carbon steel, the temperature distribution in the sample can be considered isothermal at a slower deformation rate than 10^{-2} s^{-1}, while at a deformation rate exceeding 4 s^{-1} they claimed that the distribution is definitely adiabatic.

The strain rate of AISI 304 caprioles nearly ten times for every punch speeds. The gradual increase in the punch speed causes the deformation rate to reach 30000 s^{-1} at 10 m/s. According to the literature, the shear zone should definitely have adiabatic properties.

The localization and intensity of local effective stress increases with increasing punch speeds. However, the ratio of increase does not follow a linear path. Especially if the difference between 1 m/s and 10 m/s is examined, it is obvious that the increasing effective stress doesn't elevate as expected for a "high speed" process. This shows the strain hardening holds a dominant position over the softening effect of heat but not entirely. The increase in local effective stress should reach to the values given in Figure 6.1(a) due to the high strain rates but nearly remain same in comparison with the values of 1 m/s punch speed. There are little differentiations between the results of 1 m/s and 10 m/s. Also the final stress values at 10 m/s punch speed are similar to the values found under elevated temperatures which were given in Figure 6.1(b).

Moreover, the values of effective strain increase to a point and intensify as same as the effective stress but decreases to some degree at 10 m/s punch speeds. This behavior may lead to early crack initiation if combined with the decrease in flow stress of the material. Both behaviors of AISI 304 stainless steel hold the sign that thermal effects have some effective influences on the shear zone.

To support the interpretation of this situation, cutting load-stroke depth diagram (a) and related temperature values (b) for each speed should be investigated. The diagram was given in Figure 6.20.

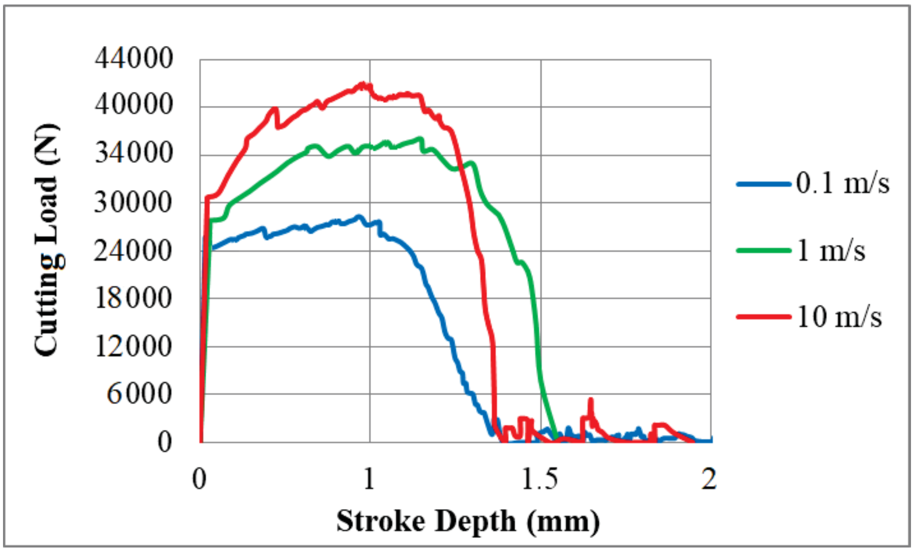

(a)

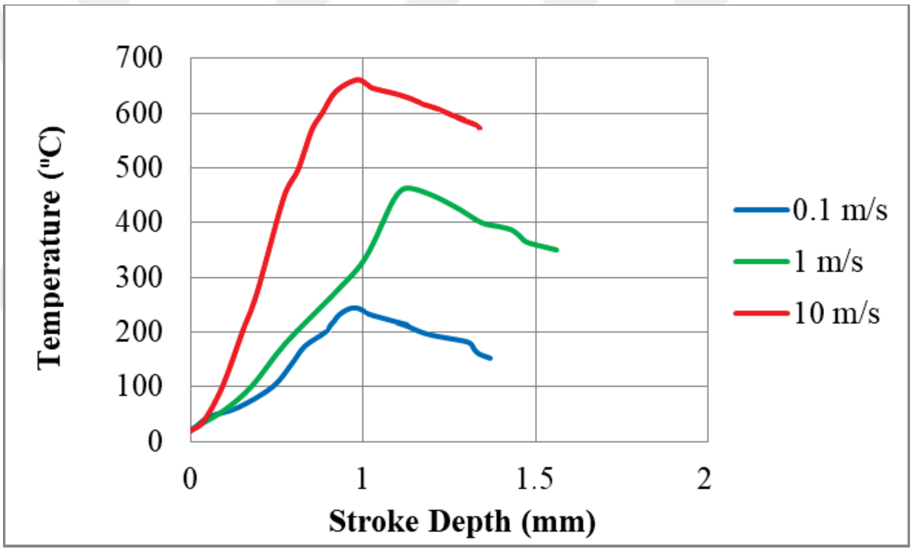

(b)

Figure 6.20. Cutting load-stroke depth change for three different punch speeds

It is determined that the cutting loads are increased with increasing punch speeds. AISI 304 stainless steel's susceptibility to deformation and high tendency to strain harden causes the material to increase its strength with increasing strain rates. However, for a punching speed of 10 m/s, the required cutting load rises to a certain level, but the stroke depth is lowered. This shows that the material breaks more quickly. These data's are accommodative with previous findings from Figure 6.18 and Figure 6.19. The required cutting load rises but not high enough, the localization and decrease in strain around the cutting edges of punch and die causes the material to break at a more shallow depth. In the light of these findings, it can clearly be propounded that the generation of heat and rise in temperature definitely have influences on the shear zone during high speed blanking.

Apart from the results gathered from the condition of one clearance (3%) which was used as an example, the remaining distribution of maximum cutting loads and cutting energies have to be investigated.

The change in maximum cutting load of the blanked AISI 304 workpiece with 2 mm thickness according to five different clearances and under three different punch speeds were given in Figure 6.21.

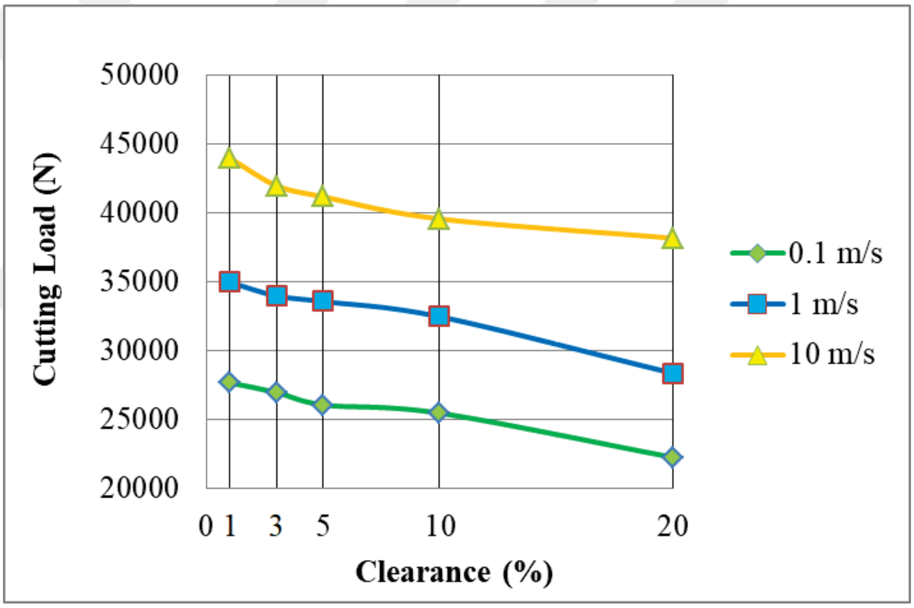

Figure 6.21. Maximum cutting load change for different punch speeds

Figure 6.21 puts forward that the behavior of the cutting load is same to the increasing clearance meaning that increasing clearance causes the cutting load to decrease. The change in punch speed only changes the required cutting load to blank the workpiece. So, a general assumption can be made about the cutting load is that for every condition of the parameters including thickness, thickness to die diameter ratio or punch speed, the cutting load decreases with increasing clearance.

It is observed that the effect of strain hardening is valid for all clearances also with thermal effects. Increase in punch speed elevates the required cutting load but influence of thermal effects precludes the flow stress to reach its top value. Softening of the material lowers the flow stress and this effect can be observed from Figure 6.21. The differences between the increase rates of the cutting loads are not even. The value differences between 1 m/s and 10 m/s punch speeds are closer than the values between 0.1 m/s and 1 m/s, although it should be much higher.

Figure 6.22 shows the change in maximum cutting energy under three different speeds and five clearances.

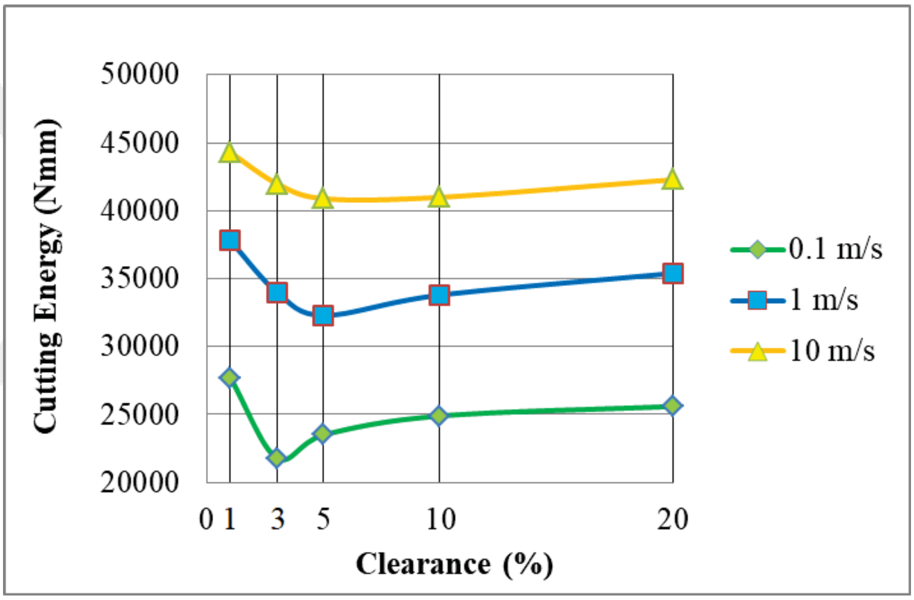

Figure 6.22. Maximum cutting energy change for different punch speeds

Cutting energies also increase depending upon the cutting load that increase with punch speed but there occurs a shift in the clearance where the lowest value is achieved. Cutting energy is lowest when the clearance is 3% for 0.1 m/s punch speed. But when the punch speed reaches to 1 m/s, clearance value shifts to 5%.

The cutting energy difference becomes more interesting when the blanking is executed under the punch speed of 10 m/s. From Figure 6.22, the close difference of the cutting energy between 5% and 10% clearance can easily be observed. There is not a keen cutting energy drop between these two values. The cutting energy becomes lowest at 5% clearance but in comparison with the values under other speeds, there seems like another point may exist between 5% and 10%. This is probably true given the situation of clearance shift due to the increased speed for 1 m/s.

The investigation of this probability could not be completed because of the predetermined values and related manufactured tools. However, in another investigation, the blanking of AISI 304 stainless steel with 2 mm thickness were executed by using a HERF hammer under 12 m/s punch speed and the results showed that lowest cutting energy was achieved at 8.75% clearance [54]. This result confirms the probability to achieve the lowest cutting energy at a clearance which is located between 5% and 10% when blanked under 10 m/s punch speed.

This shift of the clearance to higher values can be explained by the increase in the strength of the material. In literature, from the perspective of material properties, the advice for achieving a good cutting condition is to increase the value of the clearance with the increasing strength of the material [62]. In the case of high speed blanking, increase in punch speed causes high strain rates and high strain rates cause a rise in the flow stress due to strain hardening. So, some shift in the clearance seems to be required to keep the balance between the cutting load and stroke depth to lower the cutting energy.

As a conclusion to this section, it is clear that cutting load and energy holds an important place in blanking process. Clearance, thickness of the workpiece, thickness to die diameter ratio and punch speed are the main determinants on cutting load and energy. Cutting load is very important but only covers a limited area about energy conservation. Instead usage of cutting energy which is the ratio of cutting load and stroke depth offers a more detailed approach to the situation. In a blanking process, the conservation of energy has to be ensured and related parameters should be adjusted.

Apart from the cutting load and cutting energy, surface quality is another important outcome parameter that has to be ensured. A sheared part with a good surface quality has many benefits for the following processes that come after the process of blanking. During the investigations, some relation between the cutting energy, clearance and surface quality in terms of crack propagation angles were observed which will be given in detail in the next section.

6.3. Surface Quality

In a blanking process during the shearing, different zones are transpired on the cut edge surface. These zones are named as; rollover zone, shear zone, crack zone and the formation of burrs. The detailed explanation and distribution of these zones were given in the 3rd chapter. Also there is the concept of optimum clearance which concerns about the optimal value of clearance where energy conservation and surface quality reach their peak point. In this section, the governing parameters/concepts and their effects on the surface quality will be examined.

6.3.1. The Effect of Clearance on Surface Quality

From the perspective of influence level, it can be mentioned that clearance is as effective on the surface quality as on the cutting load and energy. The change in clearance alters the distribution of the zones on the blanked surface. The comparison of the crack propagation direction gathered from experiments by microscope and FEM results were given for the workpiece with t= 2 mm and t/D_m=1/5 at 3% clearance in Figure 6.23.

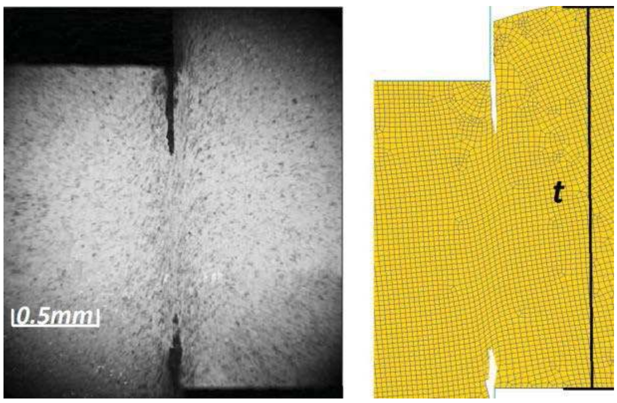

Figure 6.23. Crack propagation comparison of experimental and FEM studies

Figure 6.24 shows the FEM and the experimental results of the surface distribution of the workpiece with 2 mm thickness and t/D_m=1/5 under five different clearances (1%, 3%, 5%, 10%, 20%) and punch speed of 0.1 m/s. The related values of the zone distribution in percentages and values of crack propagation differences were given in Table 6.1.

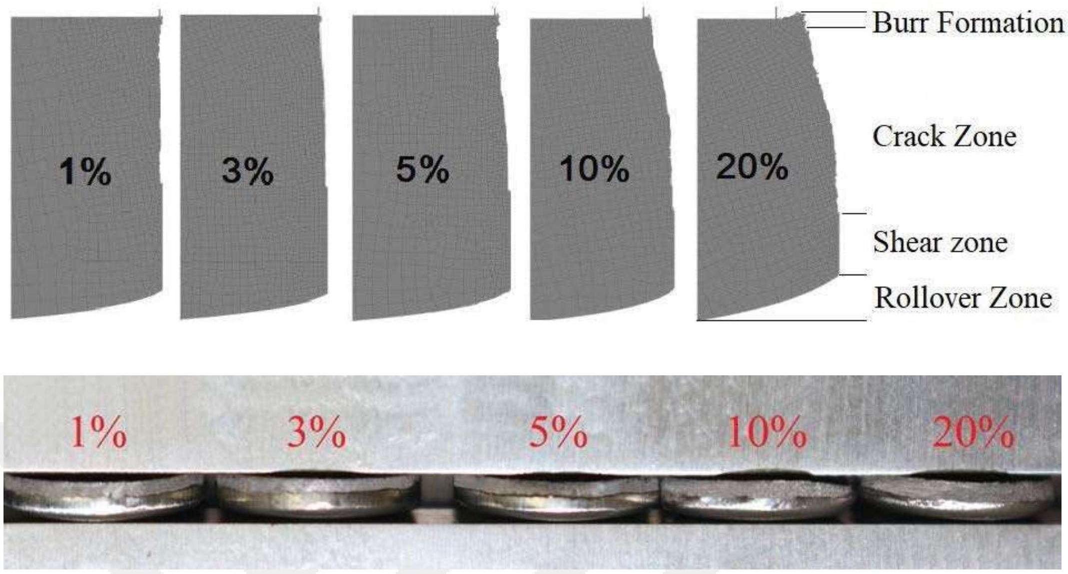

Figure 6.24. Surface distribution comparison of experimental and FEM studies

Table 6.1. Distribution of zones in percentages (%) and difference of angles

Zones	Clearance				
	1%	**3%**	**5%**	**10%**	**20%**
Rollover	8.33%	8.88%	10.76%	12.5%	15.27%
Shear	39.10%	38.80%	35.70%	30.70%	26.30%
Crack	51.19%	51.49%	51.54%	53.70%	54.27%
Burr	1.38%	0.83%	2%	3.10%	4.16%
$\Phi=\beta-\theta$	0.5	0.2	1.6	3.2	7.2

As it is evident from Figure 6.24, increasing gap between the punch and lower die aka the clearance has a big influence on the distribution of the zones transpired on the surface.

The quality of the blanked surface is determined by the surface roughness and surface roughness of the material is lowest on the shear zone (burnished area on the blank). This is the main reason for the demand of shear zone to dominate the surface. Best condition is to have a surface dominated by shear zone with minimal rollover zone, crack zone and no burrs, if possible.

In literature, for AISI 304 with the same thickness and diameter, the ideal clearance was reported approximately 10-11% [20]. However, mentioned research heavily depended on the algorithm written specifically to execute FEM analysis with nearly no experimental evidence.

The deterioration on the surface can easily be seen when the clearance becomes 10% and more which proves both experimentally and virtually that 10-11% clearances are not the optimal values to gain the best surface quality. Both from Figure 6.24 and Table 6.1, it can clearly be seen that the dominant shear zone is present when the clearance is at 3% of the thickness. With increasing clearance, zone distribution shifts towards from shear to crack zone that results more protruded faces and has more burr formation. The amount of shear zone is slightly higher for 1% clearance but secondary crack occurrences are unavoidable for very tight clearances with that amount and the wear of the tools much more rapid. The optimum clearance should be taken into consideration which postulates that surface quality becomes better due to the possible avoidance from secondary cracks when the difference between real crack propagation angle and ideal crack propagation angle is closer to zero. The closest value to zero is achieved when the clearance is 3%. On the other hand, energy consumption has to be included. The cutting energy is lowest at 3% clearance when the thickness is 2 mm and $t/D_m=1/5$.

The shear zone percentage can be slightly higher for 1% but the other determinants points out that 3% clearance is best for all other aspects.

The results prove that clearance alters the surface quality of the blanks in terms of crack propagation angles and change in zone distribution. It is also clear that there is the existence of an optimal clearance value for 2 mm thick AISI 304 stainless steel where the combination of surface quality and energy efficiency can reach a common peak value. The optimal clearance was found to be 3%. But again it has to be mentioned that this value is restricted to this thickness. So the other thicknesses have to be investigated to validate the consistency of the results.

6.3.2. The Effect of Thickness on Surface Quality

Previous results showed that the cutting energy changes according to the thicknesses. The energy values become lowest when the clearance becomes for 3% for t= 2 mm and 5% for t= 3 mm and t= 4 mm. The optimal clearance value for t= 2 mm is verified through experimental results and observation of surface quality. The same procedure was accomplished for the remaining thicknesses.

The surfaces of the blanks (a) t= 3 mm and (b) t= 4 mm gathered from experiments executed under 0.1 m/s punch speed were given in Figure 6.25.

(a)

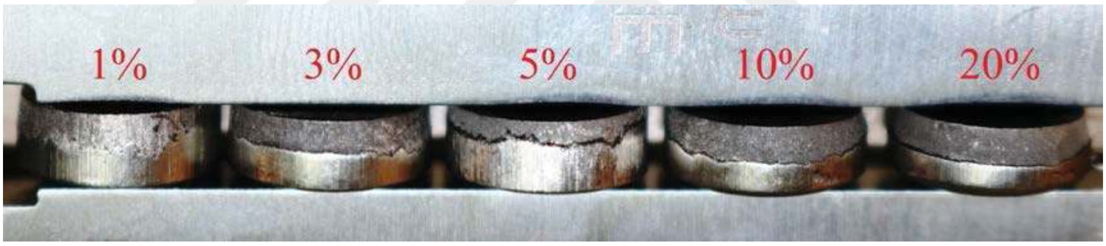

(b)

Figure 6.25. Zone distributions of blanks with (a) t= 3 mm, (b) t= 4 mm thicknesses

The results are coherent with each other. The dominant shear zones for blanks with t= 3 mm and t= 4 mm thicknesses are achieved at 5% clearance. The cutting energies also have the lowest values at the 5% clearance. So, the crack propagation angles should follow the same trend. Crack propagation angle differences for two thicknesses were given in Figure 6.26. The results show that subtraction of angles get close to zero when the clearances become 5% for both thicknesses. It is clear that, 5% is the optimal clearance value for both thicknesses where surface quality and cutting energy becomes lowest when sheared under 0.1 m/s punch speed.

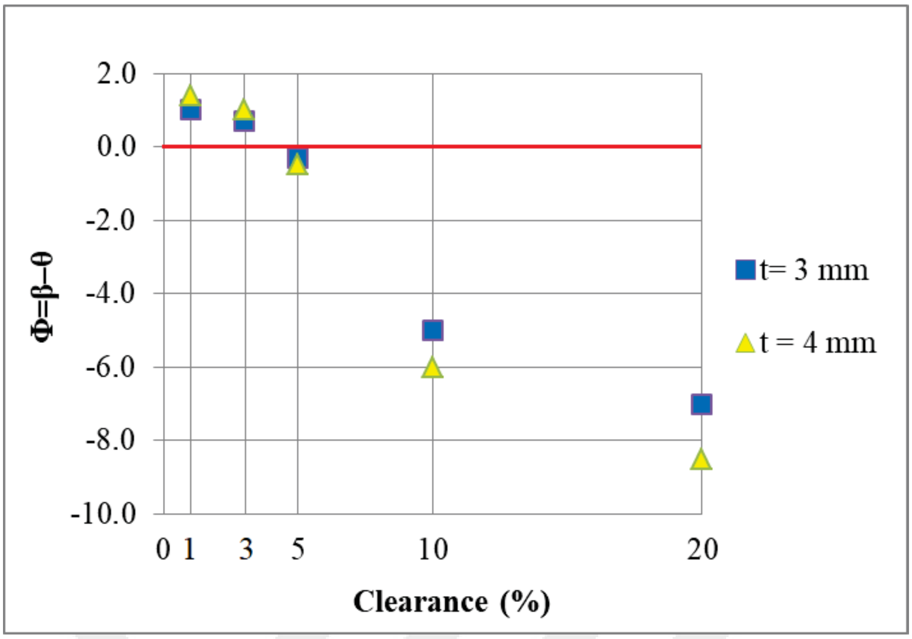

Figure 6.26. The differences in crack propagation angles for t= 3 mm and t= 4 mm

6.3.3. The Effect of Thickness to Die Diameter Ratio on Surface Quality

When blanking workpieces with big sizes, the mechanical results can vary. Although the variables were kept same like clearance, thickness and punch speed; the change in cutting loads due to different diameters were observed and shown in Figure 6.12. Main difference of load was the result of dishing on workpiece and this situation also effects the distribution of zones and surface quality.

Figure 6.27 shows the change in dishing taken from FEM simulations for four different thickness to die diameter ratios (t/D_m= 1/5, t/D_m= 1/10, t/D_m= 1/30 and t/D_m= 1/50) when the thickness is t= 2 mm. The bending of the material is obvious as a result of increasing diameter. This bending reduces the contact plane where the punch touches and slightly increases the cutting load as mentioned before. Also, it can be said that with increasing diameter, the rollover increases due to the creation of dishing that begins from cutting sides and spreads through the middle section of the workpiece. A higher load and higher rollover results with slightly more shear zone at the surfaces. Also the crack propagation angles have small shifts reverse clockwise because of the moments created at that direction.

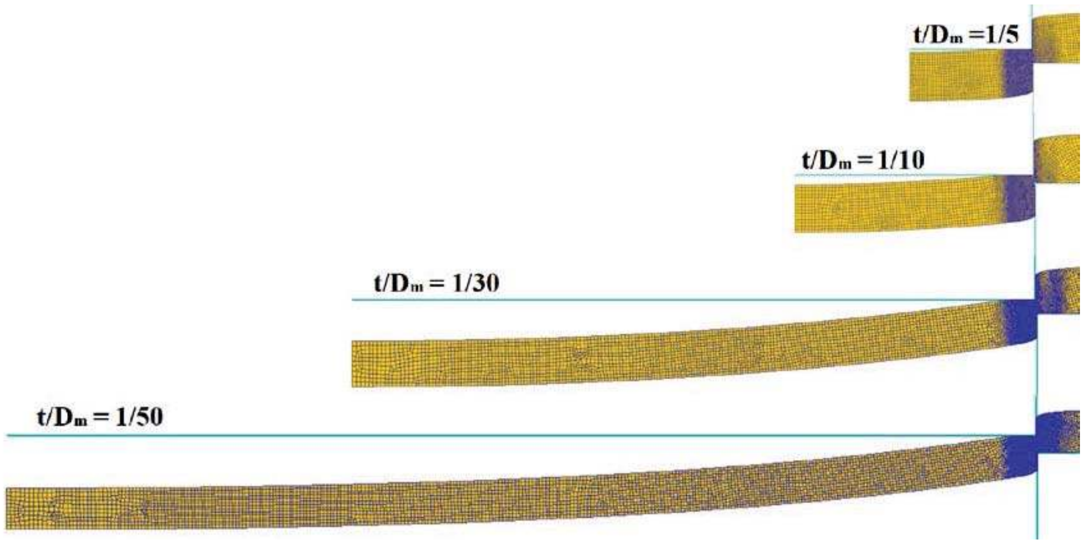

Figure 6.27. Dishing amount for different t/D_m ratios

Figure 6.28 shows the zone distribution for 2 mm thick workpieces under two different thickness to die diameter ratios (a) t/D_m=1/5 and (b) t/D_m=1/10 that were blanked under 0.1 m/s punch speed.

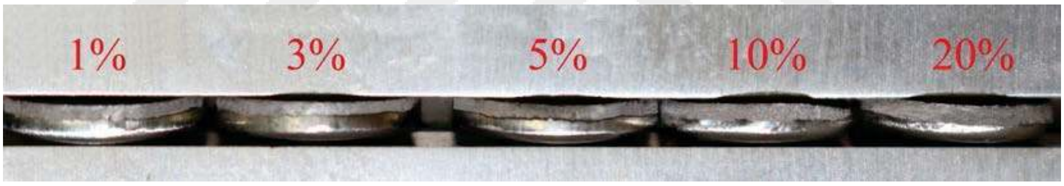

(a)

(b)

Figure 6.28. Zone distributions of blanks for (a) t/D_m=1/5 and (b) t/D_m=1/10

As the main concept is the domination of shear zone on the sheared surface, remaining investigations targeted this aspect of the blanked parts. The shear zones for the remaining t/D_m ratios were given in Figure 6.29 as percentages.

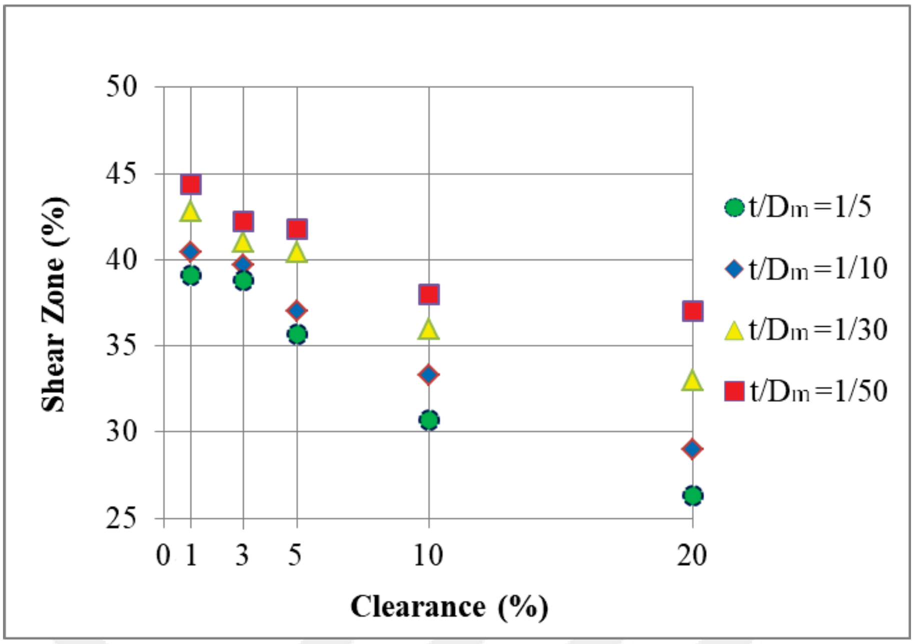

Figure 6. 29. Shear zone change for different thickness to die diameter ratios

Shear zones behavior to clearance for all t/D_m ratios follow the same trend as previous examples. The shear zone length that covers the surface decreases according to increasing clearance. But extra introduced load values and the amount of dishing cause a slight increase in the shear zone for higher t/D_m ratios which can be seen from Figure 6.29.

Shear zone amounts are highest when the clearances are 1% for all t/D_m ratios but determinations of the optimal values have to be in harmony with other aspects. The minimum energy values were achieved at 3% clearance for t/D_m=1/5 and t/D_m=1/10 while 5% clearance for t/D_m=1/30 and t/D_m=1/50.

Besides, differences of the shear zone percentages are close between 1% and 3% for t/D_m=1/5 and t/D_m=1/10, and 3% and 5% for t/D_m=1/30 and t/D_m=1/50. So, it is much more logical to choose the best values which cover all the aspects at the peak points, possible.

Before come to a conclusion, crack propagation angles have to be checked if they conclude the results. Figure 6.30 depicts the differences of crack propagation angles according to the clearances for different t/D_m ratios.

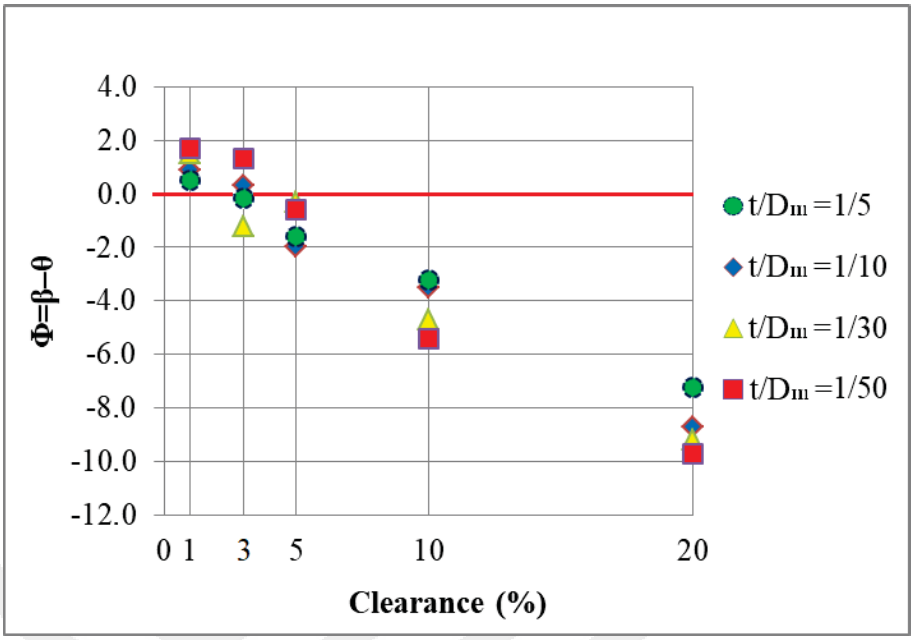

Figure 6.30. Crack propagation angle differences for different t/D_m ratios

Crack propagation differences show that they are closest to zero when the clearance is 3% for t/D_m=1/5 and t/D_m=1/10 and 5% for t/D_m=1/30 and t/D_m=1/50 which are also in conjunction with cutting energy values. As a result, although the shear zone is slightly higher for lower clearances, it is best to choose the clearance that justifies the other outcomes which are 3% for t/D_m=1/5 and t/D_m=1/10 and 5% for t/D_m=1/30 and t/D_m=1/50 under these circumstances.

6.3.4. The Effect of Punch Speed on Surface Quality

In previous sections, influence of punch speed on the shear zone was described. High strain rate in the shear zone results in heat generation that causes softening but AISI 304 stainless steel's sensitivity to deformation causes strain hardening that puts the situation in a struggle between hardening and thermal softening. The localization of heat limits the hardening and stroke depth shows a big drop before full rupture which means that the material rapidly goes to cracking and the shear zone length should be much lower than the shear zone lengths of other punch speeds.

Changes in zone distributions of workpieces for t/D_m=1/5 ratio and t= 2 mm thickness under three different punch speeds (0.1 m/s, 1m/s and 10 m/s) and five different clearances (1%, 3%, 5%, 10% and 20% of thickness) were given in Figure 6.31. The pictures in Figure 6.31 were purposefully given upside down to support better and understandable visualization.

Clearance	Zone Distributions		
	0.1 m/s	**1 m/s**	**10 m/s**
1%			
3%			
5%	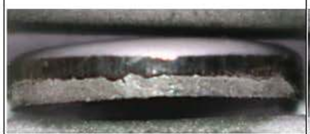		
10%	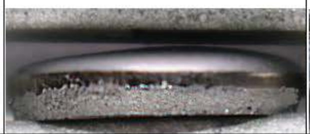		
20%			

Figure 6.31. Zone distributions according to punch speeds

It is evident from Figure 6.31 that increase in the clearance cause the material to bend more and with every increase; shear zone on the surface decreases, rollover and crack zone length increases. The effect of clearance is same for all speed values.

From the perspective of speed; when punch speed reaches to 1 m/s, the rollover starts to cover less area on the surface. This is due to the increasing strength of the material by strain hardening without the obvious softening effects of heat generation. The punch obliged to move much deeper to initiate the crack and this situation slightly increases the depth of the shear zone. So, it can be put forward that general and practical concept of shear zone domination is valid for 0.1 m/s and 1 m/s. Also, results are in harmony with cutting energy values where lowest energies are reached at 3% clearance for 0.1 m/s punch speed and 5% for 1 m/s punch speed that were given in Figure 6.22.

However, when the punch speed reaches 10 m/s, "dominant shear zone" approach starts to lose its importance. The full rupture of the material follows the cutting load-stroke depth diagram depicted in the Figure 6.20 (a). The increased strength of the material due to strain hardening causes the formation of less rollover, but the localization of heat by high deformation rates takes the material to early breakage which means that the length of the shear zone becomes less and crack zone length becomes more.

If the determination of surface quality only follows the concept of shear zone domination, then high punch speeds should never be used because of the excessive length of the crack zone. But, this is untrue. As mentioned in previous sections, the desired situation on the surface is the presence of less rollover, less crack zone and less burr formation while more coverage of the shear zone. This comes from the idea of surface roughness which is lowest on the shear zone. So, surface roughness is the actual key property to be considered when blanking with high punch speeds.

For this reason, it becomes crucial to evaluate the surface roughness of the blanked parts to be able to compare the differences amongst them. The microscopic image of zones and surface roughness values of the workpiece blanked under the punch speed of 10 m/s and 3% clearance was given in Figure 6.32, as an example.

Surface roughness values for three different punch speeds and five different clearances were evaluated by the profilometer and the results were given in Table 6.2.

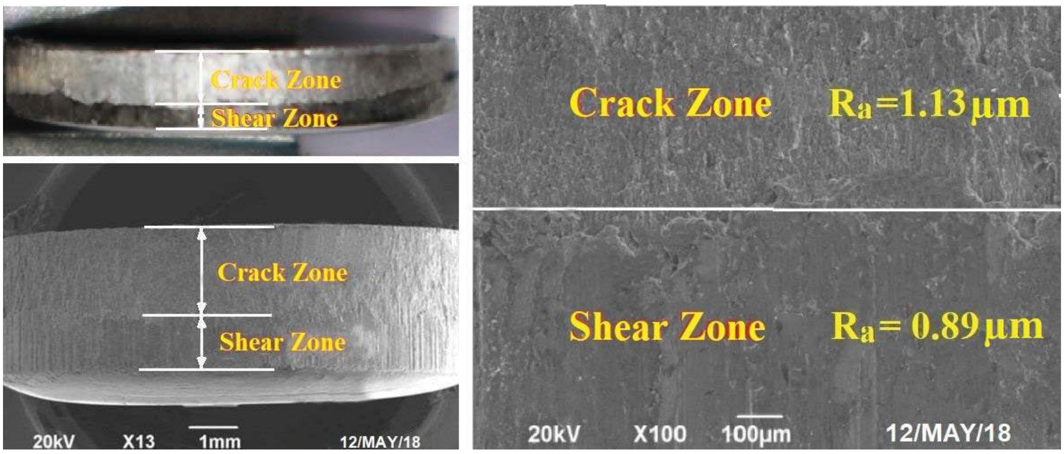

Figure 6.32. Microscopic image of a blank and related surface roughness values

Table 6.2. Surface roughness of blanks under different punch speeds

	Surface Roughness (µm)					
	0.1 m/s		1 m/s		10 m/s	
Clearance	**Shear Zone**	**Crack Zone**	**Shear Zone**	**Crack Zone**	**Shear Zone**	**Crack Zone**
1%	1.23	1.62	1.18	1.51	0.77	0.98
3%	1.28	1.68	1.22	1.56	0.82	1.06
5%	1.30	1.73	1.24	1.58	0.89	1.13
10%	1.41	1.81	1.33	1.67	1.04	1.19
20%	1.59	1.89	1.43	1.73	1.21	1.26

It is observed that blanking under increased speeds lowers the surface roughness for all clearance values. Data's in Table 6.2 confirm that surface qualities of blanks at higher speeds are better. The big drop on surface roughness values for 10 m/s punch speed is much more noticeable.

If blanking is executed at 10 m/s punch speed, surface roughness of the blanks drastically falls and overall surface qualities are improved for all clearances despite the fact that surfaces have the lowest shear zone lengths and mainly dominated by crack zone. Altan and Tekkaya [52], stated that high speed blanking results in the average surface roughness of 0.3-1.2 μm which supports the findings of this study. This situation alters the common knowledge for shear zone domination.

As a result, increasing punch speeds has the influence to lower the surface roughness. If low or moderate punch speeds are planned to be used, then shear zone domination can be a practical helper to determine the surface quality of blanks because the distribution zones on surface are easily noticeable and in harmony with cutting energy values. But it should be noted that it is better to use moderate punch speeds if available because it enhances the length of shear zone, lowers the surface roughness and lowers the rollover.

If high speed blanking is planned to be used, the concept of shear zone is rendered useless. The surfaces have the lowest shear zone lengths and mainly dominated by crack zones. But, overall surface roughness is reduced which means that the blanks executed under high punch speeds have the smoothest surfaces than shear zone dominated blanks which are executed under low and moderate speeds.

CHAPTER 7

CONCLUSIONS AND FUTURE STUDIES

This study focused on the cutting surface quality of the blanks executed by using high speed blanking. But, by only taking quality and speed parameter and neglecting the other governing parameters, a comprehensive understanding could not be achieved. Blanking is a complex process although the working principle seems simple. The governing process parameters are many and their combined effects make the prediction of outcomes quite difficult.

Investigated parameters were divided into two parts as input and output parameters. Input parameters include; clearance, punch speed and thickness of the workpiece. Also the concept of thickness to die diameter ratio was introduced which was never considered in the literature before. The output parameters include the cutting load, cutting energy and surface quality of the blanks.

To designate the boundaries of the study, five different clearances (1%, 3%, 5%, 10% and 20% of thickness) were used to blank 2 mm, 3 mm and 4 mm thick workpieces made of AISI 304 stainless steel under four different ratios (t/D_m=1/5, t/D_m=1/10, t/D_m=1/30, t/D_m=1/50) and under three different punch speeds (0.1 m/s, 1 m/s and 10 m/s) by using FEM and experimental work.

The found results were summarized below;

- The mechanical properties of the material hold the foremost importance. Every outcome has a potential to differentiate if the material changes. So, it has to be mentioned in the first place that every result presented in this study is restricted to AISI 304 stainless steel and its mechanical properties.

- The ultimate goal in blanking is to achieve the best surface quality by spending minimum energy. All efforts in this study and in many other literature studies carry the purpose to find an optimal point that satisfies both aspects.

- The determinants of the energy side are the cutting load and the cutting energy. Cutting load is the required load to shear the workpiece. Cutting energy is the ratio of cutting load and stroke depth. The determinant of surface quality side is the surface roughness on the sheared edge. When a material is blanked, the formation of zones happen on the sheared edge which are rollover zone, shear zone (burnished area), crack zone and burr formation. Surface roughness is lowest on shear zone. A blank's edge dominated by shear zone is most welcome and a practical way to evaluate the surface quality. The remaining zone lengths should be kept as short as possible.

- Another approach follows the crack propagation angles and the difference between them at the sheared surface which is called the optimum clearance theory. The theory claims that if the angle of real crack propagation direction coincides with the angle of ideal crack propagation direction, the sheared edge should have the smoothest surface without secondary cracks. And the clearance value that this condition comes true is the optimum clearance.

- The values of output parameters; cutting load, cutting energy and surface quality can vary according to any change in input parameters.

- The clearance which is the gap between the cutting edges of punch and die is considered to be the most effective input parameter by the literature. The change in clearance directly alters the cutting load, energy and also the surface quality. The increase in clearance lowers the cutting load. The decrease in cutting load is due to the occurrence of more bending moment as a result of the shrinkage in punch diameter and increased gap. This behavior of cutting load to clearance is same regardless of other input parameters and generally considered to be the sole energy saving parameter in many studies. However, this is not all true.

- When the clearance increases, more material is pulled into the die cavity. This situation leads to two results; surface quality degradation and stroke depth increase. Because of the excessive material, the initiation of crack happens at more depth. On the other hand, excessive material and increased moments bend the workpiece more. This result in the drastic decrease of shear zone, increase of rollover, crack zone and possible occurrence of burr formation that remains a rugged surface. Hence, the main goal is to find an optimal point between quality and energy, surface deterioration has to be seriously taken into account.

- Furthermore, the stroke depth change alters the total energy consumption of the process. The cutting load only represents one side of the energy concerns neglecting the status of the stroke depth. So, usage of the cutting energy brings a more thorough approach to the situation. Contrary to popular belief, increase in clearance does not lower the total energy consumption of the process. Consumption changes at every clearance due to the decreasing cutting load and increasing stroke depth. Too tight clearances spend more energy because the load is very high; but on the other hand, too loose clearance's energy consumption can rival with tight clearances because of the increased stroke depth. Thereupon, with the addition of surface degradation, the usage of loose clearances should be considered, carefully.

- If the surface quality is no concern, the only benefit of using too loose clearances is to delay the wearing of the tools because of the decreased cutting load and decreased friction.

- The lowest energy consumption of the process in terms of clearance was found as 3% of the thickness when the thickness is t= 2 mm. Also lowest difference of crack propagation directions and best surface quality was achieved at this clearance.

- Thickness of the material is another important parameter, because the industrial use of AISI 304 stainless steels includes many thicknesses specific to the application. The equation to find the clearance values is also a function of workpiece thickness. The increase in thickness caused the cutting load and energy to increase as expected. The results showed that the clearance where the lowest energy consumption achieved was 5% for t= 3 mm and t= 4 mm. This means that there occured a shift in the clearance with increasing thicknesses. Surface qualities followed the same path and both surface quality values became best at 5% clearance.

- Industrial applications can vary not only in thicknesses but also in different sizes. However, clearance selection only considers the thickness of the workpiece. On the other hand, the equation to find the cutting load for a given diameter doesn't include clearance and only gives the peak load. Furthermore, if the diameter is taken out of the equation, cutting load values should become same and should not be change. However, these were proven wrong. The results showed that with increasing diameter size, the cutting load increased not because of the diameter itself but remaining of less contact plane of the punch due to the occurrence of dishing through the middle of the workpiece that separates the upper portion of the material from the punch. Another finding is about the clearance values where the cutting energy is lowest. The clearance values have a tendency to shift with increasing t/D_m values. Results showed that lowest cutting energies were reached when the clearance is 3% for $t/D_m=1/5$ and $t/D_m=1/10$, whereas 5% clearance for $t/D_m=1/30$ and $t/D_m=1/50$ along with surface qualities. There have been no studies in the literature that focused on the thickness to die diameter ratios and observed the change in cutting energies and surface qualities which these findings may have a contribution to these situations.

- The main topic, punch speed is another parameter that has strong influences on the outcomes. When a material is blanked under high speeds, two effects can be seen in the shearing zone. First effect is the emanation of heat where shearing occurs due to high deformation rates. This generation of heat results in temperature rise and because of high speed, heat cannot find time to dissipate to relative regions. As a result, a narrow zone with concentrated temperature occurs which is called the adiabatic shear zone. Concentrated temperature at the zone causes the material to soften and a drop in the flow stress of the material. This effect has catastrophic results that the initiation of crack happens rapidly and the material has gone under full rupture at shallow stroke depths while causing a decrease in the cutting load. The second effect is the strain hardening of the material. Again due to the deformation rate, material can show a resistance to the exerted deformation that causes an increase in the strength of the material hence the required cutting load. It can be mentioned that there is a constant struggle between these two negative effects and the outcomes can change due to which effect outweighs the other one.

- In the situation of AISI 304, two effects were observed at the same time effecting at different levels. When the punch speed increased from 0.1 m/s to 1 m/s, the cutting load and stroke depth increased. This was the effect of strain hardening fully dominating the zone. However, when the punch speed reached to 10 m/s, heat generation and softening limited the increase in strength to a certain level and material had cracked at a lower stroke depth. However, the cutting energies still increased with increasing punch speeds.

- From the perspective of cutting energy, the lowest values for the materials with same thicknesses were achieved at different clearances. The lowest cutting energy value for 0.1 m/s punch speed was achieved at 3% clearance whereas 5% for the punch speed of 1 m/s. The cutting energy for 10 m/s gave the impression that an intermediate value was present between 5% and 10% clearance where the lowest value could be reached for that specific punch speed.

- The surface qualities in terms of zone distributions gave matching results and verified the findings between 0.1 m/s and 1 m/s punch speeds. But when the punch speed reached to 10 m/s, zones were altered drastically resulting minimum rollover, minimum shear zone and maximum crack zone which were nearly the worst case from the concept of zone distribution. However, the base idea of quality depends on the value of surface roughness. For this reason, surface roughness values for all punch speeds were investigated and found out that surface roughness at high speed blanking (10 m/s) gave the lowest values. These results proved that although the cutting load/energy got higher as a result of material properties, the increased clearance values which could improve tool life and achievement of smoothest surfaces that invalidated the need of shear zone domination brought big advantages over the use of conventional speeds.

7.1. Future Studies

The following areas that required further investigation have become evident during the course of this study;

- The investigation of more clearance values between 5% and 20% to determine the existence of clearance where the lowest cutting energy can be achieved especially for 10 m/s punch speed.
- Investigation of different materials that have different mechanical properties to enrich the range of the study.
- Design of a new high speed blanking setup with higher capacity and suitable for serial production that uses natural gas or Liquid Petrol Gas (LPG) to meet the requirements of the metal-working industry.

REFERENCES

[1] Lange, K. 1994. Handbook of metal forming. 2nd edition. Michigan: Society of Manufacturing Engineers.

[2] Tekiner, Z., Nalbant, M., Gürün, H. (2005). An experimental study for the effect of different clearances on burr, smooth-sheared and blanking force on aluminium sheet metal. *Materials and Design*. **27**, 1134–1138

[3] Greban, F., Monteil, G., Roizard, X. (2007). Influence of the structure of blanked materials upon the blanking quality of copper alloys. *Journal of Materials Processing Technology*. **186**, 27-32.

[4] Breitling, J., Altan, T. (1997). Blanking of non-round parts. *Stamping Journal*. 27-30.

[5] Lubis, Z. D., Mahardika, M. (2016). Influence of clearance and punch velocity on the quality of pure thin copper sheets blanked parts. *IOP Conference Series: Materials Science and Engineering*. **157**, 1-6.

[6] Wu, X., Bahmanpour, H., Schmid, K. (2012). Characterization of mechanically sheared edges of dual phase steels. *Journal of Materials Processing Technology*. **212**, 1209-1224.

[7] Akyürek, F., Yaman, K., Tekiner, Z. (2017). An experimental work on tool wear affected by die clearance and punch hardness. *Arabian Journal for Science and Engineering*. **7**, 1-10.

[8] Mucha, J. (2010). An experimental analysis of effects of various material tool's wear on burr during generator sheets blanking. *The International Journal of Advanced Manufacturing Technology*. **50**, 495-507.

[9] Çöl, M., Kir, D., Erişir, E. (2013). Wear and blanking performance of AlCrN PVD-coated punches. *Materials Science*. **48**, 514-520.

[10] Erişir, E., Çöl, M., Kir, D. (2013). Investigations on wear of PVD coated punches for sheet metal blanking. *3rd International Conference of Engineering Against Failure* (ICEAF III). 428-434.

[11] Gaudillière, C., Ranc, N., Larue, A., Maillard, A., Lorong, P., (2013). High speed blanking: an experimental method to measure induced cutting forces. *Experimental Mechanics*. **53**, 1117-1126.

[12] Gaudilliere, C., Ranc, N., Larue, A., Lorong, P. (2010). Investigations in high speed blanking: cutting forces and microscopic observations. *In EPJ Web of Conferences*. **6**, 19003.

[13] Grünbaum, M., Breitling, J., Altan, T. (1996). Influence of high cutting speeds on the quality of blanked parts. *ERC Report*. **19**, 5-96.

[14] Kanca, E., Eyercioglu, O., Karahan, I. H., Günen, A., Göv, K. (2016). Effects of blanking speed on the shear surface of mild steel (st37). *Acta Physica Polonica A*. **130**, 370-374.

[15] Kanca, E., Eyercioglu, O., Karahan, I. H. (2008). Shear-surface improvement of the austenitic stainless steel AISI 304 using high-speed punching. *Optoelectronics and Advanced Materials-Rapid Communications*. **2**, 822-827.

[16] Subramonian, S., Altan, T., Campbell, C., Ciocirlan, B. (2013). Determination of forces in high speed blanking using fem and experiments. *Journal of Materials Processing Technology*. **213**, 2184– 2190.

[17] Song, S. H., Choi, W. C. (2016). FEM investigation on thermal effects on force in high-speed blanking of mild steel. *International Journal of Precision Engineering and Manufacturing*. **17**, 631-635.

[18] Husson, C., Ahzi, S., Daridon, L. (2006). High-speed blanking of copper alloy sheets: Material modeling and simulation. *Journal De Physique IV*. **134**, 1189-1194.

[19] Murakoshi, Y., Takahashi, M., Terasaki, M., Sano, T., Matsuno, K., Takeishi, H. (1992). High-speed blanking of an amorphous alloy. *Journal of Materials Processing Technology*. **30**, 329-339.

[20] Faura, F., Garcia, A., Estrems, M. (1998). Finite element analysis of optimum clearance in the blanking process. *Journal of Materials Processing Technology*. **80-1**, 121-125.

[21] Goijaerts, A. M., Stegeman, Y. W., Govaert, L. E., Brokken, D., Brekelmans, W. A. M., Baaijens, F. P. T. (2000). Can a new experimental and numerical study improve metal blanking?. *Journal of Materials Processing Technology*. **103**, 44-50.

[22] Goijaerts, A. M., Govaert, L. E., Baaijens, F.P.T. (2001). Evaluation of ductile fracture models for different metals in blanking. *Journal of Materials Processing Technology*. **110**, 312-323.

[23] Hambli, R., Potiron, A. (2000). Finite element modeling of sheet-metal blanking operations with experimental verification. *Journal of Materials Processing Technology*. **102**, 257-265.

[24] Hambli, R., Reszka, M. (2002). Fracture criteria identification using an inverse technique method and blanking experiment. *International Journal of Mechanical Sciences*. **44**, 1349-1361.

[25] Hambli, R. (2002). Prediction of burr height formation in blanking processes using neural network. *International Journal of Mechanical Sciences*. **44**, 2089-2102.

[26] Hambli, R. (2003). BLANKSOFT: a code for sheet metal blanking processes optimization. *Journal of Materials Processing Technology*. **141**, 234-242.

[27] Hu, D. C., Chen, M. H., Ouyang, J. D., Yin, L. M. (2015). Finite element analysis of the thermal effect in high-speed blanking of thick sheet metal. *The International Journal of Advanced Manufacturing Technology*. **80**, 1481-1487.

[28] Hatanaka, N., Yamaguchi, K., Takakura, N. (2003). Finite element simulation of the shearing mechanism in the blanking of sheet metal. *Journal of Materials Processing Technology*. **139**, 64-70.

[29] Hatanaka, N., Yamaguchi, K., Takakura, N., Lizuka, T. (2003). Simulation of sheared edge formation process in blanking of sheet metals. *Journal of Materials Processing Technology*. **140**, 628-634.

[30] Maiti, S. K., Ambekar, A. A., Singh, U. P., Date P. P., Narasimhan, K. (2000). Assessment of influence of some process parameters on sheet metal blanking. *Journal of Materials Processing Technology*. **102**, 249-256.

[31] Marouani, H., Ismail, A. B., Hug, E., Rachik, M. (2009). Numerical investigations on sheet metal blanking with high speed deformation. *Materials & Design*. **30**, 3566-3571.

[32] Vaz, M., Bressan, J. D. (2002). A computational approach to blanking processes. *Journal of Materials Processing Technology*. **125**, 206-212.

[33] Odeshi, A.G., Al-ameeri, S., Mirfakhraei, S., Yazdani, F., Bassim, M. N. (2006). Deformation and failure mechanism in AISI 4340 steel under ballistic impact. *Theoretical and Applied Fracture Mechanics*. **45**, 18-24.

[34] Chou, P. C, Hashemi, J., Chou, A., Rodgers, H. C., (1991). Experimentation and finite element simulation of adiabatic shear bands in controlled penetration impact. *International Journal of Impact Engineering*. **11**, 305-321.

[35] Wei, Z., Yu, J., Li, J., Li, Y., Hu, S. (2001). Influence of stress condition on adiabatic shear localization of tungsten heavy alloys. *International Journal of Impact Engineering*. **26**, 843-852.

[36] Roessig, K. M., Mason, J. J. (1999). Adiabatic shear localization in the dynamic punch test, part I: experimental investigation. *International Journal of Plasticity*. **15**, 241-262.

[37] Roessig, K. M., Mason, J. J. (1999). Adiabatic shear localization in the dynamic punch test, part II: numerical simulations. *International Journal of Plasticity*, **15**, 263-283.

[38] Giovanola, J. H. (1988). Adiabatic shear banding under pure shear loading part I: direct observation of strain localization and energy dissipation measurements. *Mechanics of Materials*, **7**, 59-71.

[39] Xue, Q., Gray, G. T. (2006). Development of adiabatic shear bands in annealed 316L stainless steel: Part I. Correlation between evolving microstructure and mechanical behavior. *Metallurgical and Materials Transactions A*, **37**, 2435-2446.

[40] Meyers, M. A., Xu, Y. B., Xue, Q., Perez-Prado, M. T., McNelley, T. R. (2003). Microstructural evolution in adiabatic shear localization in stainless steel. *Acta Materialia*, **51**, 1307-1325.

[41] Dixon, P. R., Parry, D. J. (1991). Thermal softening effects in type 224 carbon steel. *Journal de Physique IV Colloque*, **1**, 85-92.

[42] Clous, R., Schreppel, U., Veit, P., (2000). Experimental study of shear band formation in various steels, advances in mechanical behavior, *Plasticity and Damage*, 463-468.

[43] Totre, A., Nishad, R., Bodke, S. (2013). An overview of factors affecting in blanking processes. *International Journal of Emerging Technology and Advanced Engineering*. **3**, 390-395.

[44] ASM. 2006. Handbook Volume 14B: Metalworking: Sheet Forming. Ohio: ASM International.

[45] ASM. 1993. Handbook Volume 14: Forming and Forging. 9th Edition. Cleveland: ASM International.

[46] Engin, K. E., Eyercioglu, O. (2017). The Effect of the Thickness-to-Die Diameter Ratio on the Sheet Metal Blanking Process. *Strojniški vestnik-Journal of Mechanical Engineering*, **63**, 501-509.

[47] Marinov, V. 2010. Manufacturing processes for metal products. Bulgaria: Kendall Hunt Publishing Company.

[48] Dodd, B., Bai, Y. 2012. Adiabatic shear localization. 2nd Edition. Massachusetts: Elsevier Insights Publishing.

[49] Lee, W. S., Sue, W. C., Lin, C. F. (2000). The effects of temperature and strain rate on the properties of carbon-fiber-reinforced 7075 aluminum alloy metal-matrix composite. *Composites Science and Technology*. **60**, 1975-1983.

[50] Batra, R. C., Lear, M. H. (2005). Adiabatic shear banding in plane strain tensile deformations of 11 thermoelastoviscoplastic materials with finite thermal wave speed, *International Journal of Plasticity*. **21**, 1521-1545.

[51] Sandor, B. I., Roloft, R., Birn, S.M., Brown, M. L. 1999. Mechanics of solids. Boca Raton: CRC Press LLC.

[52] Altan, T., Tekkaya, A. E. 2012. Sheet metal forming: fundamentals. ASM International.

[53] Gronostajski, Z. (2002). The constitutive equations for fem analysis. *Journal of Materials Processing Technology*. 1, 40-44.

[54] Kanca, E. (2009). Design and construction of a compact high energy rate forming (herf) hammer. Phd thesis. Gaziantep University, Graduate School of Natural & Applied Sciences (Mechanical Engineering).

[55] Hosford, W. F. Caddell, R. M. (1983). Metal forming: mechanics and metallurgy. London: Prentice-Hall Publishing.

[56] Groover, M. P. (1996). Fundamentals of modern manufacturing. London: Prentice-Hall Publishing

[57] HILTI. Dx 450 operating instructions, part 1. 2017. https://ikestrftso.cf/dx-450-hilti-manual. 11.4.2018.

[58] ASM Aerospace Specification Metals Inc. AISI Type 304 Stainless Steel. 2015. http://asm.matweb.com/search/SpecificMaterial.asp?bassnum=MQ304A. 10.02.2018.

[59] Fang, G., Zeng, P., Lou, L.L., (2002). Finite element simulation of the effect of clearance on the forming quality in the blanking process. *Journal of Materials Processing Technology,* **122**, 249-254.

[60] Samuel, M. (1998). FEM simulations and experimental analysis of parameters of influence in the blanking process. *Journal of Materials Processing Technology*, **84**, 97-106.

[61] Boyer, H. E. 1987. Atlas of stress-strain curves. Ohio: ASM International.

[62] Keeler, S., Kimchi, M. 2015. Advanced high-strength steels application guidelines V5. World Auto Steel.

CURRICULUM VITAE

PERSONAL INFORMATION

Name-Surname: Kaan Emre ENGİN

Nationality: Turkish

Birth place and date: İstanbul-1981

Marital status: Married

GSM: +90541 396 80 69

Email: kengin@adiyaman.edu.tr

EDUCATION

	Graduate School	Year of Graduation
Master	Mersin University	2008
Bachelor	Cumhuriyet University	2005
High School	Amasya High School	1999

WORKING EXPERIENCE

	Place	Enrollment
2010-Present	Adıyaman University	Research Assistant
2009-2010	European Tobacco	Production Manager
2009-2009	Metrans Makina	Sales Manager

PUBLICATIONS

1. SCI, SSCI, AHCI Journals:

1.1. Engin, K. E., Eyercioğlu, Ö. (2017). The Effect of the Thickness-to-Die Diameter Ratio on the Sheet Metal Blanking Process. *Strojniški vestnik - Journal of Mechanical Engineering*, **63**(9), 501-509., Doi: 10.5545/sv-jme.2016.4272**.**

2. Other Journals:

2.1. Engin, K. E., Eyercioğlu, Ö. (2017). Purpose Oriented Clearance Selection. *European International Journal of Science and Technolog*y, **6**(7), 66-76.

2.2. Engin, K. E., Eyercioğlu, Ö. (2016). Investigation of the Process Parameters on the Blanking of AISI 304 Stainless Steel by Using Finite ElementMethod. *Journal of Mechanics Engineering and Automation*, **6**(7), 356-363., Doi: 10.17265/2159-5275.

2.3. Soğukpınar, H., Tali B., Alğın, E., Çerçi, S., Sunar, Ç. D., Engin, K. E., Kaya, A. İ. (2016). Prototype Solenoid Electromagnet Design and Production for Turkish Proton Accelerators Mdis Ion Source. *Balkan Physics Letters*, **24**(1), 1-14.

2.4. Soğukpınar, H., Bozkurt, İ., Baran, M. F., Türkmenler, H., Pala, M., Engin, K. E., Kaya, A. İ. (2015). Micro Turbine Design and Production and Testing. *International Journal of Engineerıng Technologies*, **1**(4), 141-145.

2.5. Engin, K. E., Koyuncu T., Lüle F. (2015). Production Of Different Composite Materials And Determination Of Some Technical Properties. *Anadolu Journal of Agricultural Sciences*, **30**(1), 43-50., Doi: 10.7161/anajas.2015.30.1.43-50.

2.6. Koyuncu T., Engin, K. E., Kaya, A. İ., Lüle, F., Baran, M. F., Yükçü, N., Soğukpınar, H. (2015). Krom Bir Güneşli Su Isıtıcısının Tasarımı Yapımı ve Denenmesi. *Tarım Makineleri Bilimi Dergisi*, **11**(1), 61-68.

3. Conferences & Symposiums:

3.1. Engin, K. E., Eyercioğlu, Ö. (2018). The Effect of Thickness to Die Diameter Ratio on the Blanking of Dp600 Steel Sheet. *International Automotive Technologies Congress (OTEKON)*, **9**, 1551-1560.

3.2. Engin, K. E., Eyercioğlu, Ö. (2016). Investigation of the Process Parameters on Sheet Metal Blanking Process by Using Finite Element Method. *International Conference on Advanced Technology&Sciences*, **1**(1), 1141-1145.

3.3. Soğukpınar, H., Bozkurt, İ., Baran, M. F., Türkmenler, H., Pala, M., Engin, K. E., Kaya, A. İ. (2015). Wind Blade Design and Production by Using Aluminum. *International Congress on Natural and Engineering Science*s, **1**(1), 19.

3.4. Koyuncu, T., Engin, K. E., Lüle, F. (2014). Design Manufacture and Test of a Solar Powered Minibus Commagene for Transportation of People in Adıyaman City, Turkey. *29th European Photovoltaic Solar Energy Conference and Exhibition*.

3.5. Koyuncu, T., Lüle, F., Engin, K. E., (2012). Convective and Microwave Drying Characteristics of Garden Cress Leaves Lepidium sativum L. *International Conference of Agricultural Engineering CIGR-Ageng*, 45.

3.6. Koyuncu T., Kaya, A. İ., Engin, K. E., (2015). Adıyaman Yöresinde Kullanılan Oluklu Kollektörün Veriminin Belirlenmesi. *29.Ulusal Tarımsal Mekanizasyon ve Enerji Kongresi*, 501-506.

3.7. Lüle, F., Koyuncu T., Engin, K. E., (2012). Adıyaman İlinin Tarımsal Mekanizasyon Düzeyi. *Tarımsal Mekanizasyon Ulusal Kongresi,* 27.

FOREIGN LANGUAGES

- English (Yökdil: 91.250, 2017)

HOBBIES

- Playing musical instruments
- Martial arts and sports